MODELLING OF PARALLEL HVDC-AC POWER SYSTEMS FOR DYNAMIC STUDIES AND OPTIMAL STABILIZATION

by

ALY ABDELHAMEED METWALLY

B.Sc. Ain-Shams University, Cairo 1965
M.A.Sc. University of British Columbia, Vancouver 1970

A THESIS SUBMITTED IN PARTIAL FULFILMENT OF

THE REQUIREMENTS FOR THE DEGREE OF

DOCTOR OF PHILOSOPHY

in the Department

of

Electrical Engineering

We accept this thesis as conforming to the
required standard

THE UNIVERSITY OF BRITISH COLUMBIA

September 1973

In presenting this thesis in partial fulfilment of the requirements for an advanced degree at the University of British Columbia, I agree that the Library shall make it freely available for reference and study. I further agree that permission for extensive copying of this thesis for scholarly purposes may be granted by the Head of my Department or by his representatives. It is understood that copying or publication of this thesis for financial gain shall not be allowed without my written permission.

Department of Elect. Eng.

The University of British Columbia
Vancouver 8, Canada

Date Oct. 11, 1973

Supervisor: Dr. Y.N. Yu

ABSTRACT

Due to the fast response, the hvdc lines, when properly controlled, are very useful in stabilizing power systems. In this thesis dynamic modelling and linear optimal controls for dc/ac parallel power systems are investigated. Beginning with a detailed representation of one machine-infinite bus dc/ac parallel power system several reduced order models with very good accuracy are developed. They are derived mainly through eigenvalue analysis but are compared in detail with the high order nonlinear model tests. Linear optimal control schemes, comprising excitation and/or dc reference current control signals, are designed and tested for two different one machine-infinite bus systems. After that a dynamic model for a three-terminal dc line in parallel with a delta-connected ac system is developed and again linear optimal controls are designed and tested. Two systems are studied; a two machine-infinite bus system and a three machine system. For each system two cases are investigated; two rectifiers and one inverter, or one rectifier and two inverters. It is found that in all cases the hvdc reference current control provides the most effective means in stabilizing large power systems.

TABLE OF CONTENTS

LIST OF TABLES

LIST OF ILLUSTRATIONS

ACKNOWLEDGEMENT

I am deeply grateful to Dr. Y.N. Yu, supervisor of this project, for his continued interest, inspiring guidance and unfailing patience during the research work and writing of this thesis.

Thanks are due to Mr. A. MacKenzie for draughting and Ms. Norma Duggan for typing the thesis.

The financial support from the University of British Columbia and the National Research Council of Canada is gratefully acknowledged.

I am greatly indebted to my wife Magda for her patience, sacrifices and encouragement throughout my postgraduate work.

NOMENCLATURE

A, B	linearized system matrices
$a_1 - a_4$	ac transmission line coefficients
$c_1 - c_{11}$	synchronous machine coefficients
$d_1 - d_{15}$	dc network coefficients
D, Q	common reference frame
d_j, q_j	individual machine frame
E_x	exciter voltage
$G_f + jB_f$	equivalent ac harmonic filter admittance
$G_\ell + jB_\ell$	local load admittance
H	synchronous machine inertia constant
i_d, i_q	synchronous machine terminal current components
i_{kd}, ik_q	direct and quadrature damper windings currents
i_{fd}	field current
i_{cd}, i_{cq}	shunt capacitor current components
$i_{d\ell}$, $i_{q\ell}$	local load current components
i_{df}, i_{qf}	ac harmonic filter current components
i_{dA}, i_{qA}	ac transmission line current components at sending end
i_{dB}, i_{qB}	ac transmission line current components at receiving end
I_d, I_q	dc current components
I_{ref}	dc reference current
I_R, I_I	rectifier and inverter dc currents
K_r, T_r	voltage regulator gain and time constant
K_R, T_R	rectifier firing circuit gain and time constant
K_I, T_I	inverter firing circuit gain and time constant
k	current margin
M	composite system matrix

P_m	mechanical input
P_e	energy conversion power
$P + jQ$	synchronous machine output power
P_{ac}, Q_{ac}	active and reactive powers transmitted over ac line
P_{dc}, Q_{dc}	active and reactive power input (output) to rectifier (inverter)
Q, R	weighing matrices
r_a, r_{fd}	armature and field resistances
r_{kd}, r_{kq}	direct and quadrature axis damper windings resistances
r, x_ℓ, x_c	ac transmission line parameters
R, X_ℓ, X_c	dc transmission line parameters
R_L	local load resistance
R_f, L_f, C_f	ac harmonic filter parameters
T''_{do}, T''_{qo}	direct and quadrature axis subtransient open circuit time constants
T'_{do}	direct axis transient open circuit time constant
U	optimal control vector
u_D	optimal dc control signal
u_E	optimal excitation control signal
u_X, u'_X	conventional excitation control signals
v_t	synchronous machine terminal voltage
v_d, v_q	terminal voltage dq components
v_o	infinite bus voltage
V_{ref}	synchronous machine reference voltage
V_R, V_I	rectifier and inverter dc voltages
$x_{\ell a}$	armature leakage reactance
x_{ad}, x_{aq}	direct and quadrature axis mutual reactances between stator and rotor

$x_{\ell dk}$, $x_{\ell kq}$	direct and quadrature axis damper windings reactances
$x_{\ell fd}$	field reactance
x''_d, x''_q	direct and quadrature axis subtransient reactances
x'_d	direct axis transient reactance
x_d, x_q	direct and quadrature axis synchronous reactances
x_{co}	commutation reactance
$\bar{x}_c$	shunt capacitor reactance
x, x^t	state vector and its transpose
α_R, α_I	rectifier and inverter delay angles
β	inverter's angle of advance ($= \pi - \alpha_I$)
Δ_o	deionization angle of a valve
δ	synchronous machine torque angle
δ_R	angle between terminal voltage and quadrature axis
$\Delta\omega$	speed deviation
Φ_R	power factor angle for converters
ψ_d, ψ_q	direct and quadrature axis armature flux linkages
ψ_{kd}, ψ_{kq}	direct and quadrature axis damper windings flux linkages
ψ_{fd}	field flux linkage
ω_e	synchronous speed (= 377 rad./sec.)

1. INTRODUCTION

The use of direct current (dc) goes back to the early days of electricity. The first electrical power source, the galvanic battery, delivered dc. Indeed the first electric central power station was built in New York in 1882[1] and supplied dc at 110 volts. One of the earliest dc transmission systems, the Thury system in the 1880's[2], was operated with the principle of constant current control which is very similar to modern hvdc systems. However, ac soon superseded dc in generation, transmission and utilization of electricity because of the general flexibility in voltage transformation, high voltage for transmission and low voltage for distribution, and the sturdy structure of the ac motors and their simple operation. But resurrection of hvdc has been witnessed in recent years because of the development of grid-controlled, multi-electrode, mercury-arc valves which are capable of handling large powers at very high voltages[2]. The main problem though, is still the relative costs of ac and dc equipment. The high initial cost of converting stations for dc has to be weighed against the saving in transmission. In general, the longer the transmission distance, the more favourable will be the use of hvdc. From 1950 to 1970 eight dc links had gone into commercial operation in various parts of the world[1], with transmission voltages up to 800 kV, rated powers up to 1440 MW, and distances up to 850 miles.

There are many other advantages of hvdc transmission. For underground and submarine cables dc has lower losses and the problem of charging currents is eliminated, thus increasing the current carrying capacity of cables[3]. An hvdc line may serve as an asynchronous link to

interconnect power networks of different frequencies, as witnessed in Japan[4], or networks that would be unstable if ac links were used for the interconnection, as in the case of the Eel River project[5]. The fast response of dc links can be utilized in improving the performance of the associated ac systems[6], thus suggesting a very powerful tool for stabilizing large power systems.

Considerable amount of work has been done in the field of mathematical simulation of hvdc systems. Detailed simulation of converter action on digital computers received a lot of attention[7-12]. The simulation of ac system impedance and converter transformers were also considered[13,14]. Hybrid computers[15] and dc simulators[16] were developed for the study. Representation of dc links in large ac systems for load flow studies were also reported[17-19]. For transient stability studies, simpler models were obtained by representing converters on the basis of the average value of their dc voltages[20-21].

Whereas the ac power control after a disturbance is rather slow if governors are used to control the mechanical input, or lacks continuity and smoothness if capacitor switching or dynamic resistance braking is used to control the electrical output, the power control over a dc line is quick and smooth by simply controlling the firing angles. People have started looking into the use of dc/ac parallel transmission for improving stability[22-26]. The basic control scheme is to regulate the dc power according to the system stability requirement using signals derived from the frequency differences between the interconnected systems[22], the ac voltage drops[23], a combination of frequency change and its integrals[24], and power angle magnitude or its derivative and several other schemes[25]. All these controls resulted in improving the stability

of dc/ac parallel systems including the case of short outage of dc lines. This clearly demonstrates the effectiveness of dc control in stabilizing a power system. As for the gains of all the control schemes mentioned above, they were arrived at experimentally. There is also a very recent paper[27] designing a linear optimal control for an hvdc link.

All existing hvdc links are essentially restricted to two-terminal lines mainly because of the absence of hvdc circuit breakers. Since such breakers are being developed[28-31], a sizeable number of publications is already available for multi-terminal hvdc system operation and control[32-41].

In this thesis the dynamic modelling and linear optimal control design for two-terminal as well as multi-terminal hv dc/ac parallel power systems are investigated. In Chapter 2 the dynamics of a two-terminal hv dc/ac parallel system are explained and the system components are represented mathematically in detail. This detailed model is reduced in order by applying simplifying assumptions and making approximations in Chapter 3. The validity of these assumptions and approximations is tested by eigenvalue analysis and nonlinear disturbance tests. In Chapter 4 optimum control theory is employed to design control signals for linearized models of dc/ac parallel power systems and the nonlinear system responses under disturbance are compared for different control schemes. In Chapter 5 the operation and basic control systems for a tapped three-terminal dc line superimposed on a delta connected ac network are discussed and a dynamic model for the system is constructed. Finally in Chapter 6 linear optimal control schemes are designed and tested for a two machine-infinite bus system as well as a three machine system. Both systems are studied for two modes of operation; two

rectifiers and one inverter, or one rectifier and two inverters.

2. BASIC EQUATIONS OF HVDC POWER SYSTEMS

In this chapter the basic elements of an hvdc system will be described and equations describing such a power system will be given.

2.1 The HVDC Systems

The main components of an hvdc system are the dc transmission lines, the ac power supplies, the converters and controls, the smoothing reactors, the ac harmonic filters, and the shunt capacitors. Each converter unit consists of six valves in a bridge connection for a six-pulse operation where valves are connected in pairs to each phase terminal, one with the anode and the other with the cathode as shown in Figure 2.1. The output voltage Figure 2.2, has a ripple six times the main frequency where each valve carries the full dc current for 120°. At least there are always two valves conducting in series.

From the above description it is clear that the ac current contains lots of harmonics inherent in the conversion process. Therefore filters are required to reduce the ac voltage and current ripples to an acceptable level. For a six-pulse operation the filters generally comprise branches tuned to 5th, 7th, 11th and 13th harmonics of the supply frequency. These are connected either to the primary or tertiary windings of the converter transformer[42].

The dc voltage output of a converter bridge is controlled by changing the firing angle, α, of the valves. In Figure 2.3 valve 3 will take over current from valve 1 at b instead of a. This means that the current will lag behind the voltage and reactive power must be drawn from the supply. For this reason reactive compensation via shunt capacitors is normally used. In addition, the shunt capacitor banks of the

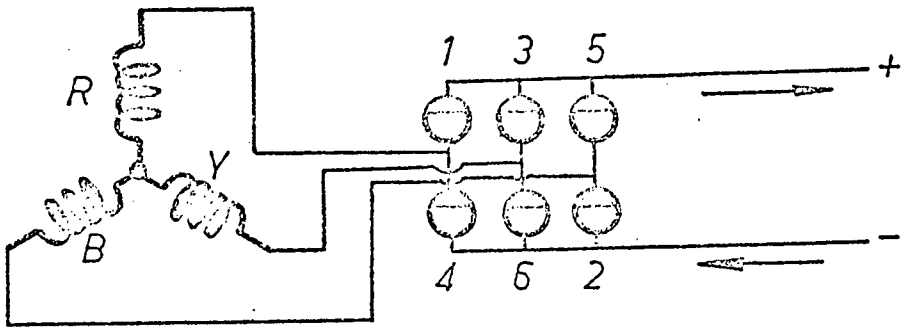

Fig. 2.1 Bridge Connection for DC Converter

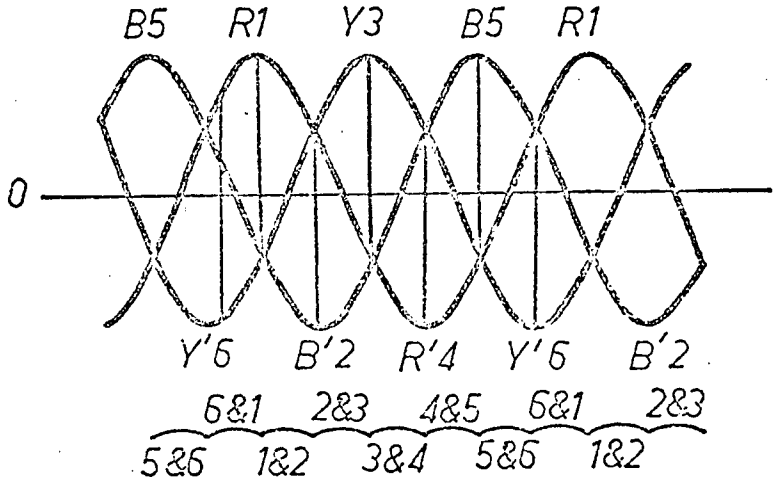

Fig. 2.2 Converter Output DC Voltage

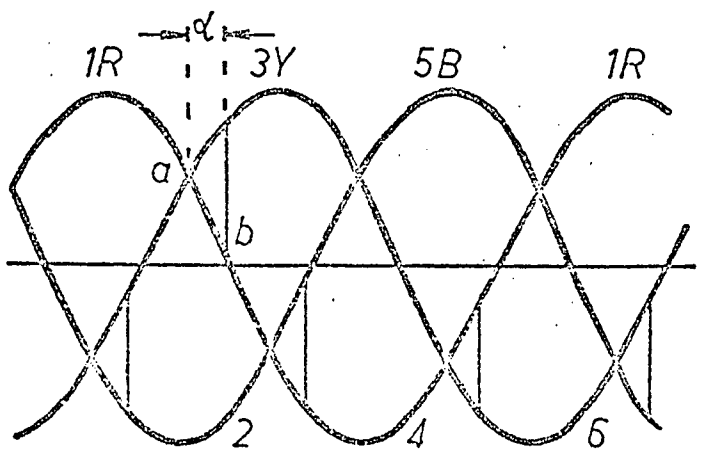

Fig. 2.3 Angle of Delay α

ac harmonic filters also supply a portion of the reactive power required.

Converter valves should be operated within their current ratings. Constant current control is thus desirable and is usually employed for rectifier bridges[7,43]. This is achieved by comparing the actual value of dc current to the desired value and adjusting the firing angle α_R accordingly. For inverter operation each valve must start firing at an angle β ($=\pi-\alpha_I$) in advance of the voltage zero such that after completion of commutation there is still an angle Δ available, greater than or equal to Δ_o, the deionization angle of the valve, to prevent commutation failure. Since voltage and current are liable to considerable changes, β must be large enough to accommodate such changes. On the other hand, the amount of reactive power required by the inverter is directly proportional to β, which means that the smaller the angle β the smaller is the reactive power required. These considerations show that a compromise has to be made between these two conflicting requirements. Such a control scheme is termed constant extinction angle control. In addition to this control a current override control is supplemented such that it allows the inverter to take over current control, at a reduced value of reference current, in case of a failure of the rectifier's current control due to low ac voltage or loss of a converter group. In such a case the rectifier will deliver voltage up to its capacity with α_R set to a minimum value of about 5°.

2.2 The Overall System

In this thesis optimal stabilizatin of parallel hvdc-ac systems is investigated. For that a dynamic modelling of the system is necessary. The model must be fairly accurate to be able to predict

the dynamic performance of the system yet not too complicated computation-wise.

Figure 2.4 shows a general layout of a parallel hvdc-ac system. The generator is connected to an infinite system through both ac and dc transmission lines. The generator is equipped with a voltage regulator and has a local resistive load R_L at the terminal. The dc line has a constant current control at the rectifier end and constant extinction angle control with current override at the inverter end. There are ac harmonic filters and compensating capacitors at the sending end.

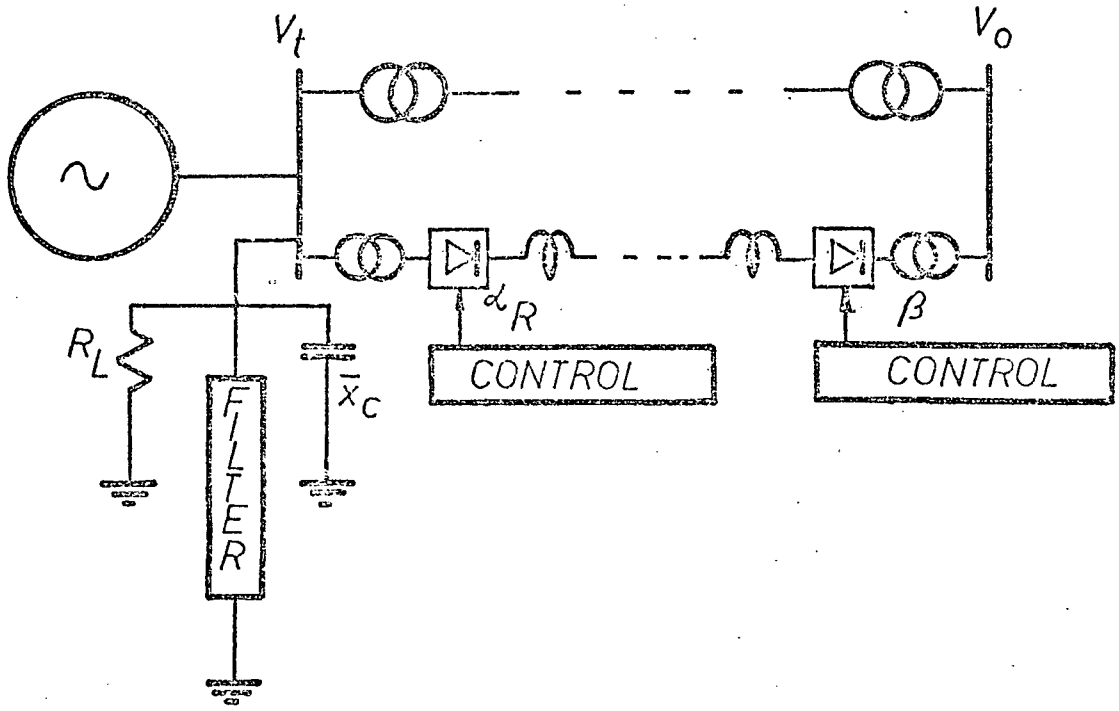

Fig. 2.4 A Typical DC/AC Parallel Power System

2.3 Synchronous Machine Equations

The flux linkages are expressed in terms of per unit reactances instead of per-unit inductances. Since $x = \omega_e L$, where $\omega_e = 377$ radians/second, ω_e will be attached to the $p\psi$ equations all the time. Also

negative reactances instead of negative currents are chosen for the generator armature circuit. Thus one has, for the flux linkages

$$\begin{bmatrix} \psi_q \\ \psi_{kq} \end{bmatrix} = \begin{bmatrix} -(x_{aq} + x_{\ell a}) & x_{aq} \\ -x_{aq} & (x_{aq} + x_{\ell kq}) \end{bmatrix} \cdot \begin{bmatrix} i_q \\ i_{kq} \end{bmatrix} \tag{2.1}$$

$$\begin{bmatrix} \psi_d \\ \psi_{kd} \\ \psi_{fd} \end{bmatrix} = \begin{bmatrix} -(x_{ad} + x_{\ell a}) & x_{ad} & x_{ad} \\ -x_{ad} & (x_{ad} + x_{\ell kd}) & x_{ad} \\ -x_{ad} & x_{ad} & (x_{ad} + x_{\ell fd}) \end{bmatrix} \begin{bmatrix} i_d \\ i_{kd} \\ i_{fd} \end{bmatrix}$$

and for the power

$$P_e = \psi_d i_q - \psi_q i_d$$

$$v_t^2 = v_d^2 + v_q^2 \tag{2.1a}$$

Then Park's equations of a synchronous machine[44] and a voltage regulator equation can be arranged in a state variable form to read

$$p\delta = \Delta\omega \tag{2.2a}$$

$$p\Delta\omega = \frac{\omega_e}{2H} (P_m - P_e)$$

$$p\psi_{fd} = \omega_e r_{fd} \left(\frac{E_x}{x_{ad}} - i_{fd}\right) \tag{2.2b}$$

$$pE_x = \frac{1}{T_r} [k_r (V_{ref} - v_t) - E_x]$$

$$p\psi_{kd} = -\omega_e r_{kd} i_{kd} \tag{2.2c}$$

$$p\psi_{kq} = -\omega_e r_{kq} i_{kq}$$

$$p\psi_d = \omega_e(v_d + r_a i_d) + (\omega_e + \Delta\omega) \psi_q \tag{2.2d}$$

$$p\psi_q = \omega_e (v_q + r_a i_q) - (\omega_e + \Delta\omega) \psi_d$$

Equations (2.2a) are the mechanical equations in state variable form, where δ is in radians, $\Delta\omega$ in rad./sec., P_m and P_e in p.u. and H in seconds. The second equation of (2.2b) describes the voltage regulator of the control loop. For simplicity only one time constant is included.

2.4 Converters and DC Control

Techniques for simulating converter action in detail are available[7-12]. For transient stability studies a simple model may be achieved by representing the converters by their average dc voltages[20,21]. This method will be used throughout this thesis. The average dc voltages for the rectifier and inverter bridges respectively are

$$V_R = \frac{3\sqrt{3}}{\pi} v_t \cos \alpha_R - \frac{3}{\pi} x_{co} I_R \tag{2.3}$$

$$V_I = \frac{3\sqrt{3}}{\pi} v_o \cos \alpha_I - \frac{3}{\pi} x_{co} I_I$$

where α_R and α_I are the firing angles of the dc control.

The constant current control for the rectifier bridge and the constant extinction angle control with current override for the inverter bridge are described as follows.

$$\cos \alpha_R = \frac{K_R}{v_t} (I_{ref} - I_R) + \cos \alpha_{Rs}$$

$$\cos \alpha_I = -\cos \Delta_o + \frac{1}{v_o} \left(\frac{2}{\sqrt{3}} x_{co} I_I + e_{cI}\right) \tag{2.4}$$

where α_{Rs} is the steady state value of α_R and e_{cI} is the current override control signal and is restricted to positive values.

$$e_{cI} = K_I (k I_{ref} - I_I) \geq 0 \tag{2.4a}$$

Equations (2.3) describe a continuous relation between the dc voltage, the firing angles, and the dc current. Since a change in the firing angle

following a commutation does not affect the average output voltage immediately, not until the end of the normal conduction period, and a change in converter current does not cause an instant change in voltage, time lags must be incorporated into the transfer functions for a transient study. Thus equations (2.3) may be rewritten

$$V_R = \frac{3\sqrt{3}}{\pi} v_t \cos \alpha_R - \frac{3}{\pi} x_{co} I'_R$$

$$V_I = \frac{3\sqrt{3}}{\pi} v_o \cos \alpha_I - \frac{3}{\pi} x_{co} I'_I \qquad (2.5)$$

where

$$pI'_R = \frac{1}{T_R} (I_R - I'_R)$$

$$p\ I'_I = \frac{1}{T_I} (I_I - I'_I) \qquad (2.6a)$$

$$p \cos \alpha_R = \frac{1}{T_R} [K_R (I_{ref} - I_R)/v_t + \cos \alpha_{Rs} - \cos \alpha_R]$$

$$p \cos \alpha_I = \frac{1}{T_I} [-\cos \alpha_I - \cos \Delta_o + (\frac{2}{\sqrt{3}} x_{co} I_I + e_{cI})/v_o] \qquad (2.6b)$$

A single time constant is incorporated into each control loop of the dc system.

2.5 Transmission Lines

Both ac and dc lines are represented by equivalent T-sections as shown in Figure 2.5. For long transmission lines more than one section can be used if more accuracy is required. The dc line is represented by

$$p\ I_R = \frac{\omega_e}{X_L} (V_R - V_c - R\ I_R) , \qquad p\ V_c = \omega_e\ X_c\ (I_R - I_I) \qquad (2.7)$$

$$p\ I_I = \frac{\omega_e}{X_L} (V_I + V_c - R\ I_I)$$

For the ac line let

$$i = i_d + j\, i_q, \quad v = v_d + j\, v_q \tag{2.8a}$$

The ac line in Park's d-q coordinates may be represented by

$$\begin{aligned}
pi_{qA} &= \frac{\omega_e}{x_\ell}\,(v_q - v_{qc} - ri_{qA}) - (\omega_e + \Delta\omega)\, i_{dA} \\
pi_{dA} &= \frac{\omega_e}{x_\ell}\,(v_d - v_{dc} - r\, i_{dA}) + (\omega_e + \Delta\omega)\, i_{qA} \\
pi_{qB} &= \frac{\omega_e}{x_\ell}\,(v_o \cos\delta - v_{qc} - ri_{qB}) - (\omega_e + \Delta\omega)\, i_{dB} \\
pi_{dB} &= \frac{\omega_e}{x_\ell}\,(v_o \sin\delta - v_{dc} - ri_{dB}) + (\omega_e + \Delta\omega)\, i_{qB} \\
pv_{qc} &= \omega_e\, x_c\, (i_{qA} + i_{qB}) - (\omega_e + \Delta\omega)\, v_{dc} \\
pv_{dc} &= \omega_e\, x_c\, (i_{dA} + i_{dB}) + (\omega_e + \Delta\omega)\, v_{qc}
\end{aligned} \tag{2.8}$$

To relate the dc current to the ac reference frame a second set of axes, d' and q', is defined such that the q' axis coincides continuously with the hypotenuse of the right triangle formed by the two components of the synchronous generator terminal voltage, v_d and v_q, as shown in Figure 2.6. The angle between the two sets of axes, δ_R, is given by

$$\delta_R = \arctan\left(\frac{v_d}{v_q}\right) \tag{2.9}$$

and the rectifier current I_R may be resolved into two components, I_d and I_q, in the ac reference frame.

$$\begin{bmatrix} I_d \\ I_q \end{bmatrix} = \frac{2\sqrt{3}}{\pi}\, I_R \begin{bmatrix} \sin\delta_R & \cos\delta_R \\ \cos\delta_R & -\sin\delta_R \end{bmatrix} \cdot \begin{bmatrix} \cos\phi_R \\ \sin\phi_R \end{bmatrix}$$

where

$$\cos\phi_R \triangleq \frac{\pi}{3\sqrt{3}}\, \frac{V_R}{v_t} \tag{2.10}$$

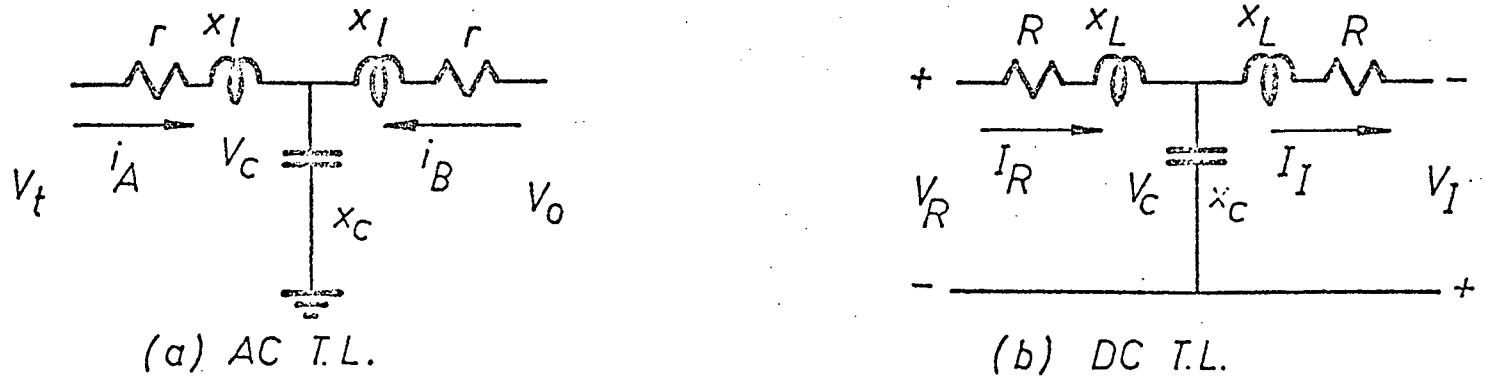

Fig. 2.5 Equivalent T-sections for Transmission Lines

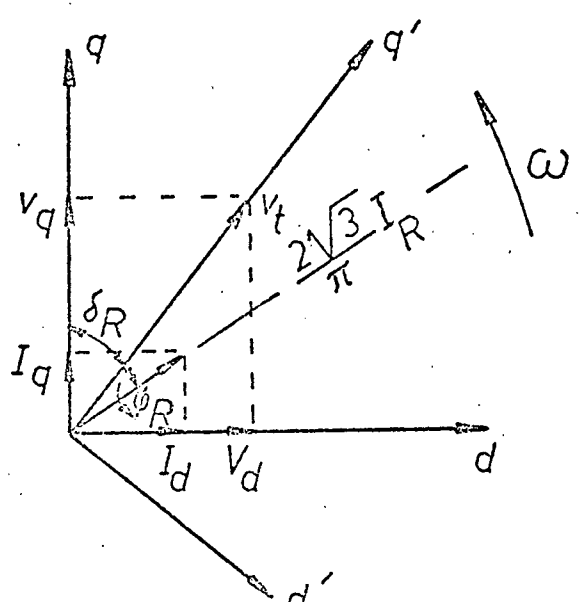

Fig. 2.6 Resolving I_R into d-q components

2.6 AC Harmonic Filters, Shunt Capacitors and Local Load

Four parallel filter branches tuned for 5th, 7th, 11th and 13th harmonics are considered. Each branch is represented by

$$p^2 i_{dfj} = \frac{1}{L_{fj}} \{pv_d - (\omega_e+\Delta\omega)v_q - R_{fj}\, pi_{dfj} + 2(\omega_e+\Delta\omega)L_{fj}\, pi_{qfj} - [\frac{1}{C_{fj}} - (\omega_e+\Delta\omega)^2 L_{fj}]i_{dfj} + [L_{fj}\, p\Delta\omega + (\omega_e+\Delta\omega)R_{fj}]\, i_{qfj}\} \quad (2.11)$$

$$p^2 i_{qfj} = \frac{1}{L_{fj}} \{pv_q + (\omega_e+\Delta\omega)v_d - 2(\omega_e+\Delta\omega)L_{fj}\, pi_{dfj} - R_{fj}\, pi_{qfj} - [L_{fj}\, p\Delta\omega + (\omega_e+\Delta\omega)R_{fj}]i_{dfj} - [\frac{1}{C_{fj}} - (\omega_e+\Delta\omega)^2 L_{fj}]\, i_{qfj}\}$$

$$j = 5, 7, 11, 13$$

Next the shunt capacitors may be represented by

$$pv_d = \omega_e \bar{x}_c\, i_{cd} + (\omega_e+\Delta\omega)\, v_q \quad (2.12)$$

$$pv_q = \omega_e \bar{x}_c\, i_{cq} - (\omega_e+\Delta\omega)\, v_d$$

where

$$i_{cd} = i_d - i_{dA} - i_{df} - i_{d\ell} - I_d \quad (2.13)$$

$$i_{cq} = i_q - i_{qA} - i_{qf} - i_{q\ell} - I_q$$

Finally the local load currents are given by

$$\begin{bmatrix} i_{d\ell} \\ i_{q\ell} \end{bmatrix} = \frac{1}{R_L} \begin{bmatrix} v_d \\ v_q \end{bmatrix} \quad (2.14)$$

2.7 State Variables

Equations (2.2), (2.6), (2.7), (2.8), (2.11) and (2.12) form a complete set of state equations for the system under study. The state variables are

$$x^t = (\delta, \Delta\omega, \psi_{fd}, E_x, \psi_{kd}, \psi_{kq}, \psi_d, \psi_q, I_R, I_I, V_c, I'_R, I'_I, \cos\alpha_R, \cos\alpha_I, i_{dA},$$

$$i_{qA}, i_{dB}, i_{qB}, v_{dc}, v_{qc}, i_{df5}, pi_{df5}, i_{qf5}, pi_{qf5}, i_{df7}, pi_{df7}, i_{qf7},$$

$$pi_{qf7}, i_{df11}, pi_{df11}, i_{qf11}, pi_{qf11}, i_{df13}, pi_{df13}, i_{qf13}, pi_{qf13}, v_d, v_q)$$

The system is of the 39th order. The auxilliary algebraic equations are given in (2.1a), (2.4a), (2.5), (2.9), (2.10), (2.13) and (2.14). The current solutions of equations (2.1) are:

$$\begin{bmatrix} i_q \\ i_{kq} \end{bmatrix} = \begin{bmatrix} -y_{kq} & y_{aq} \\ -y_{aq} & y_{q\ell} \end{bmatrix} \cdot \begin{bmatrix} \psi_q \\ \psi_{kq} \end{bmatrix}$$

$$\begin{bmatrix} i_d \\ i_{kd} \\ i_{fd} \end{bmatrix} = \begin{bmatrix} -y_{dfk} & y_{df} & y_{dk} \\ -y_{df} & y_{df\ell} & -y_{d\ell} \\ -y_{dk} & -y_{d\ell} & y_{dk\ell} \end{bmatrix} \cdot \begin{bmatrix} \psi_d \\ \psi_{kd} \\ \psi_{fd} \end{bmatrix} \qquad (2.15)$$

where

$$\begin{bmatrix} y_{kq} \\ y_{aq} \\ y_{q\ell} \end{bmatrix} = \frac{1}{\Delta_1} \begin{bmatrix} x_{aq}+x_{\ell kq} \\ x_{aq} \\ x_{aq}+x_{\ell a} \end{bmatrix}$$

$$\Delta_1 = (x_{aq}+x_{\ell a})\,(x_{aq}+x_{\ell kq}) - x_{aq}^2$$

$$\begin{bmatrix} y_{dfk} \\ y_{df} \\ y_{dk} \\ y_{df\ell} \\ y_{d\ell} \\ y_{dk\ell} \end{bmatrix} = \frac{1}{\Delta_2} \begin{bmatrix} x_{ad}\,(x_{\ell fd}+x_{\ell kd}) + x_{\ell fd}x_{\ell kd} \\ x_{ad}\,x_{\ell fd} \\ x_{ad}\,x_{\ell kd} \\ x_{ad}(x_{\ell fd}+x_{\ell a}) + x_{\ell fd}x_{\ell a} \\ x_{ad}\,x_{\ell a} \\ x_{ad}(x_{\ell kd}+x_{\ell a}) + x_{\ell kd}x_{\ell a} \end{bmatrix} \qquad (2.16)$$

$$\Delta_2 = x_{ad}x_{\ell a}(x_{\ell fd} + x_{\ell kd}) + x_{\ell fd}\ x_{\ell kd}\ (x_{ad} + x_{\ell a})$$

These equations form the base of the dynamic modelling of hvdc systems which will be developed in the next chapter.

3. DYNAMIC MODELLING AND ORDER REDUCTION

The mathematical model constructed in the previous chapter has 39 state variables which describe the system dynamics in great detail. Such complexity presents a very difficult problem in digital computation. In this chapter the order reduction of the system model is achieved through engineering approximations with the aid of eigenvalue analysis. The validity of the low order models is established through tests on the nonlinear models with disturbances.

3.1 Reduction Techniques

Numerical techniques for reducing high order systems to low order equivalents are available[45-47]. But the identity of all the parameters will be lost in the process of reduction. In this thesis the reduction will be approached by engineering approximations instead.

Again there are two approaches for the approximation. The first is called the state variable grouping technique[47], which may be called linear approximation technique, by which the nonlinear system equations are linearized first and then the system equations order is reduced in possibly several steps. At each step the state variables x are separated into two groups, x_1 and x_2, associated with large and small time constants respectively. The linearized system equations are written in a partitioned form as follows:

$$\begin{bmatrix} \dot{x}_1 \\ \dot{x}_2 \end{bmatrix} = \begin{bmatrix} A_{11} & A_{12} \\ A_{21} & A_{22} \end{bmatrix} \begin{bmatrix} x_1 \\ x_2 \end{bmatrix} \tag{3.1}$$

Neglecting the small time constants or the fast and short-lived transients by setting $\dot{x}_2$ equal to zero, x_2 is given by

$$x_2 = -A_{22}^{-1} A_{21} x_1 \tag{3.2}$$

which is then substituted back into (3.1) to give

$$\dot{x}_1 = [A_{11} - A_{12} A_{22}^{-1} A_{21}] x_1 \tag{3.3}$$

The order of the system is thus reduced by the number of state variables in x_2. According to this procedure several linear models will be obtained, but there is only one high order nonlinear model for the system.

Another approach may be called the nonlinear approximation technique by which all the time derivatives as well as speed deviation terms in the nonlinear differential equations to be eliminated are set equal to zero at each step. This is equivalent to a static representation of the system components for these equations to be eliminated. The resulting algebraic equations are then solved and substituted back into the rest of the nonlinear differential equations before linearization for linear optimal control design or eigenvalue analysis. The advantage of this approach is that for each linearized model there is one original nonlinear model. This is the approach to be followed in this chapter.

3.2 Reduced Models

In the following the models resulting from reductions will be presented. For the procedure, it is chosen that the ac harmonic filter dynamics shall be eliminated first since it consists of the largest number of equations. The next group are the ac transmission lines and machine stator windings, and so on. The details are:

STEP 1: Neglecting the ac harmonic filter dynamics of equations (2.11) the model is reduced from the 39th to the 23rd order. The resulting algebraic equations are:

$$\begin{bmatrix} i_{df} \\ i_{qf} \end{bmatrix} = \begin{bmatrix} G_f & B_f \\ -B_f & G_f \end{bmatrix} \begin{bmatrix} v_d \\ v_q \end{bmatrix} \tag{3.4}$$

where

$$\begin{bmatrix} G_f \\ B_f \end{bmatrix} = \sum_j \frac{1}{(R_{fj}^2 + x_{fj}^2)} \begin{bmatrix} R_{fj} \\ x_{fj} \end{bmatrix}$$

$$x_{fj} = \omega_e L_{fj} - \frac{1}{\omega_e c_{fj}} \qquad j = 5, 7, 11, 13 \tag{3.5}$$

STEP 2: Neglecting the ac transmission line dynamics the system's order is reduced to 17. Equations (2.8) are replaced by

$$\begin{bmatrix} i_{dA} \\ i_{qA} \\ i_{dB} \\ i_{qB} \\ v_{dc} \\ v_{qc} \end{bmatrix} = \begin{bmatrix} a_1 & -a_2 & a_3 & a_4 \\ a_2 & a_1 & -a_4 & a_3 \\ a_3 & a_4 & a_1 & -a_2 \\ -a_4 & a_3 & a_2 & a_1 \\ x_c(a_2-a_4) & x_c(a_1+a_3) & x_c(a_2-a_4) & x_c(a_1+a_3) \\ -x_c(a_1+a_3) & x_c(a_2-a_4) & -x_c(a_1+a_3) & x_c(a_2-a_4) \end{bmatrix} \begin{bmatrix} v_o \sin\delta \\ v_o \cos\delta \\ v_d \\ v_q \end{bmatrix} \tag{3.6}$$

where

$$\begin{bmatrix} a_1 \\ a_2 \\ a_3 \\ a_4 \end{bmatrix} = \frac{1}{\Delta_3} \begin{bmatrix} 2rx_c(x_\ell - x_c) \\ x_c(r^2 - x_\ell^2 + 2x_\ell x_c) \\ r[r^2 + (x_\ell - x_c)^2 + x_c^2] \\ (x_\ell - x_c)(r^2 + x_\ell^2 - 2x_\ell x_c) \end{bmatrix}$$

$$\Delta_3 = 4r^2(x_\ell - x_c)^2 + (r^2 - x_\ell^2 + 2x_\ell x_c)^2 \tag{3.7}$$

STEP 3: Neglecting the transformer voltages and voltages due to speed deviation generated in the armature windings of the synchronous

machine a 15th order model is achieved. Equations (2.2d) are replaced by

$$\begin{bmatrix} \psi_d \\ \psi_q \end{bmatrix} = \frac{1}{(1+r_a^2 y_{kq} y_{dfk})} \begin{bmatrix} r_a^2 y_{kq} y_{dk} & r_a^2 y_{kq} y_{df} & r_a y_{aq} & r_a y_{kq} & 1 \\ -r_a y_{dk} & -r_a y_{df} & r_a^2 y_{aq} y_{dfk} & -1 & r_a y_{dfk} \end{bmatrix}$$

$$\cdot [\psi_{fd} \quad \psi_{kd} \quad \psi_{kq} \quad v_d \quad v_q]^t \tag{3.8}$$

STEP 4: Representing the dc transmission line by its static impedance yields a 12th order model. Equations (2.7) become

$$\begin{aligned} I_R &= \frac{1}{2R} (V_R + V_I) \\ V_c &= \frac{1}{2} (V_R - V_I) \\ I_I &= I_R \end{aligned} \tag{3.9}$$

STEP 5: Dynamics of the shunt capacitor of equations (2.12) are neglected to give a 10th order model. The capacitor currents are thus given by

$$\begin{bmatrix} i_{cd} \\ i_{cq} \end{bmatrix} = \frac{1}{\bar{x}_c} \begin{bmatrix} -v_q \\ v_d \end{bmatrix} \tag{3.10}$$

STEP 6: The damper winding effects of equation (2.2c) are neglected. The resulting model is of the 8th order. The resulting auxilliary equations are

$$\begin{bmatrix} \psi_{kd} \\ \psi_{kq} \end{bmatrix} = \frac{1}{\Delta_4} \begin{bmatrix} x_{ad}[r_a^2 + x_{\ell a}(x_{aq}+x_{\ell a})] & r_a x_{ad} x_{\ell fd} & x_{ad} x_{\ell fd}(x_{aq}+x_{\ell a}) \\ -r_a x_{ad} x_{aq} & -x_{aq}[x_{ad} x_{\ell a} + x_{\ell fd}(x_{ad}+x_{\ell a})] & r_a x_{aq}(x_{ad}+x_{\ell fd}) \end{bmatrix}$$

$$\cdot [\psi_{fd} \quad v_d \quad v_q]^t \tag{3.11}$$

$$\Delta_4 = r_a^2 (x_{ad}+x_{\ell fd}) + (x_{aq}+x_{\ell a}) [x_{ad} x_{\ell a} + x_{\ell fd}(x_{ad} + x_{\ell a})]$$

STEP 7: The small time constants of equation (2.6a) are neglected and a 6th order model is obtained. The resulting equations are

$$I'_R = I_R$$
$$I'_I = I_I \tag{3.12}$$

STEP 8: Neglecting firing circuits dynamics of equation (2.6b) a 4th order model is obtained and the new algebraic equations are

$$I_R = I_{ref}$$
$$\cos\alpha_I = \frac{1}{v_o}\left(\frac{2}{\sqrt{3}} x_{co} I_I + e_{cI}\right) - \cos\Delta_o \tag{3.13}$$

STEP 9: Representing the voltage regulator by a static gain and neglecting the field flux decay of equation (2.2b) yields a 2nd order model with the new auxilliary equations

$$i_{fd} = \frac{E_x}{x_{ad}}$$
$$E_x = K_r (V_{ref} - v_t) \tag{3.14}$$

The steps thus chosen at this stage are, indeed, a matter of convenience, not because of the order of importance of their eigenvalues. Of course all nonlinear differential equations which are not to be eliminated are kept intact at each step.

3.3 Initial Conditions of a Parallel AC/DC Power System

For this thesis study the initial conditions assumed are the synchronous machine's terminal voltage v_t, the infinite bus voltage v_o, the power transmitted over the ac lines P_{ac}, and that over the dc line P_{dc}, and the minimum extinction angle for the inverter Δ_o. Other initial conditions, such as the reactive power over the ac line Q_{ac} and that

drawn by the rectifier Q_{dc}, and other synchronous machine initial conditions are to be determined.

Since the active and reactive powers transmitted over the ac line may be given by

$$\begin{bmatrix} P_{ac} \\ Q_{ac} \end{bmatrix} = \begin{bmatrix} i_{dA} & i_{qA} \\ -i_{qA} & i_{dA} \end{bmatrix} \begin{bmatrix} v_d \\ v_q \end{bmatrix} \tag{3.15}$$

Substituting for i_{dA} and i_{qA} from (3.6) into (3.15) and solving for $\sin\delta$ and $\cos\delta$ yields

$$\begin{bmatrix} \sin\delta \\ \cos\delta \end{bmatrix} = \frac{1}{v_o(a_1^2-a_2^2)} \begin{bmatrix} a_1 & a_2 & \frac{P_{ac}}{v_t^2} - a_3 & \frac{Q_{ac}}{v_t^2} - a_4 \\ -a_2 & a_1 & -\frac{Q_{ac}}{v_t^2} + a_4 & \frac{P_{ac}}{v_t^2} - a_3 \end{bmatrix} \cdot \begin{bmatrix} v_d \\ v_q \end{bmatrix} \tag{3.16}$$

But

$$\begin{aligned} P_{ac}^2 + Q_{ac}^2 &= v_t^2 (i_{dA}^2 + i_{qA}^2) \\ &= v_t^2\{(a_1^2+a_2^2)v_o^2 + (a_3^2+a_4^2)v_t^2 + 2v_o[(a_1a_3-a_2a_4)(v_d\sin\delta+v_q\cos\delta) + \\ &\quad (a_1a_4+a_2a_3)(v_q\sin\delta-v_d\cos\delta)]\} \end{aligned} \tag{3.17}$$

Substituting (3.16) into (3.17) and solving for Q_{ac} gives

$$Q_{ac} = a_4 v_t^2 \pm \sqrt{v_t^2[(a_1^2+a_2^2)v_o^2 - a_3^2 v_t^2 + 2a_3 P_{ac}] - P_{ac}^2} \tag{3.18}$$

To determine the dc reactive power Q_{dc} the rectifier voltage V_R has to be determined first. From (3.12) and (3.13) one has

$$\begin{aligned} I_R &= I_I = I_R' = I_I' \\ \cos\alpha_I &= -\cos\Delta_o + \frac{2}{\sqrt{3}} x_{co} \frac{I_R}{v_o} \end{aligned} \tag{3.19}$$

Substituting (3.19) into (2.5) gives

$$V_I = -\frac{3\sqrt{3}}{\pi} v_o \cos\Delta_o + \frac{3}{\pi} x_{co} I_R \tag{3.20}$$

From (3.9) and (3.20)

$$V_R = \frac{3\sqrt{3}}{\pi} v_o \cos\Delta_o + (2R - \frac{3}{\pi} x_{co}) I_R \tag{3.21}$$

But

$$P_{dc} = \frac{2}{3} V_R I_R \tag{3.22}$$

Solving (3.21) and (3.22) for V_R yields

$$V_R = \frac{1}{2}[\frac{3\sqrt{3}}{\pi} v_o \cos\Delta_o + \sqrt{(\frac{3\sqrt{3}}{\pi} v_o \cos\Delta_o)^2 + 12 P_{dc} (R - \frac{3}{2\pi} x_{co})}] \tag{3.23}$$

Since

$$\cos \Phi_R = \frac{\pi}{3\sqrt{3}} \frac{V_R}{v_t} \tag{3.24}$$

Thus

$$Q_{dc} = P_{dc} \tan \Phi_R \tag{3.25}$$

Next the synchronous machine initial conditions can be determined as follows. The active and reactive powers of the synchronous machine are given by

$$\begin{aligned} P &= P_{ac} + P_{dc} + v_t^2 (G_f + \frac{1}{RL}) \\ Q &= Q_{ac} + Q_{dc} + v_t^2 (B_f - \frac{1}{\bar{x}_c}) \end{aligned} \tag{3.26}$$

Next equations (2.15), (3.8) and (3.11) are combined to give

$$\begin{bmatrix} \psi_d \\ \psi_q \\ i_d \\ i_q \\ i_{fd} \end{bmatrix} = \begin{bmatrix} c_1 & c_2 & c_3 \\ -c_2 & c_4 & -c_5 \\ -c_6 & -c_7 & c_8 \\ c_9 & -c_6 & c_{10} \\ -c_{10} & -c_8 & c_{11} \end{bmatrix} \begin{bmatrix} v_d \\ v_q \\ \psi_{fd} \end{bmatrix} \tag{3.27}$$

where

$$\begin{bmatrix} c_1 \\ c_2 \\ c_3 \\ c_4 \\ c_5 \\ c_6 \\ c_7 \\ c_8 \\ c_9 \\ c_{10} \\ c_{11} \end{bmatrix} = \frac{1}{\Delta_4} \begin{bmatrix} r_a\,[x_{ad}\,x_{\ell a} + x_{\ell fd}\,(x_{ad} + x_{\ell a})] \\ (x_{aq} + x_{\ell a})\,[x_{ad}x_{\ell a} + x_{\ell fd}\,(x_{ad} + x_{\ell a})] \\ r_a^{\,2}\,x_{ad} \\ r_a\,(x_{ad} + x_{\ell fd})\,(x_{aq} + x_{\ell a}) \\ r_a x_{ad}\,(x_{aq} + x_{\ell a}) \\ r_a\,(x_{ad} + x_{\ell fd}) \\ (x_{ad} + x_{\ell fd})\,(x_{aq} + x_{\ell a}) \\ x_{ad}\,(x_{aq} + x_{\ell a}) \\ x_{ad}x_{\ell a} + x_{\ell fd}\;\;(x_{ad} + x_{\ell a}) \\ r_a\,x_{ad} \\ r_a^{\,2} + (x_{ad} + x_{\ell a})(x_{aq} + x_{\ell a}) \end{bmatrix} \tag{3.28}$$

and Δ_4 is defined in equation (3.11). Substituting (3.27) into $P = v_d i_d + v_q i_q$ and solving for ψ_{fd} gives

$$\psi_{fd} = \frac{P + c_6\,v_t^{\,2} + (c_7 - c_9)\,v_d v_q}{(c_8\,v_d + c_{10}\,v_q)} \tag{3.29}$$

Substituting (3.27) and (3.29) into

$$Q = v_q i_d - v_d i_q \tag{3.30}$$

and solving for v_q gives

$$v_q = \frac{[r_a P + (x_{aq} + x_{\ell a})\,Q + v_t^{\,2}]}{[(x_{aq} + x_{\ell a})P - r_a Q]}\;\; v_d \tag{3.31}$$

Substituting (3.31) into (2.1a) gives

$$v_d = \frac{v_t\,[(x_{aq} + x_{\ell a})\,P - r_a Q]}{\sqrt{[r_a^2 + (x_{aq}+x_{\ell a})^2]\,(P^2+Q^2) + 2v_t^2[r_a P + (x_{aq}+x_{\ell a})Q] + v_t^4}} \qquad (3.32)$$

Thus v_d can be calculated from (3.32), v_q from (3.31) and ψ_{fd} from (3.29).

Finally the torque angle δ can be determined from (3.6) to read

$$\delta = \arctan \frac{(a_2a_4-a_1a_3)v_d - (a_1a_4+a_2a_3)v_q + a_1\,i_{dA} + a_2\,i_{qA}}{(a_1a_4+a_2a_3)v_d + (a_2a_4-a_1a_3)v_q - a_2\,i_{dA} + a_1\,i_{qA}} \qquad (3.33)$$

where the ac transmission line currents i_{dA} and i_{qA} are determined from (2.13) after i_d and i_q, i_{df} and i_{qf}, I_R, I_d and I_q, and i_{cd} and i_{cq} are determined from (3.27), (3.4), (3.22), (2.10) and (3.10) respectively.

The rectifier and inverter firing angles are determined from (2.5) and (3.13) respectively.

3.4 System Data

The system studied has the following data, all in per unit except for angles in degrees and inertia constant and time constants in seconds. Most data are taken from reference 20. The rest are assumed.

Synchronous machine and voltage regulator

r_a	0.005	r_{fd}	0.00055	r_{kd}	0.02	r_{kq}	0.04
$x_{\ell a}$	0.1	$x_{\ell fd}$	0.1	$x_{\ell kd}$	0.1	$x_{\ell kq}$	0.2
x_{ad}	1.0	x_{aq}	0.7	H	3 sec.	k_r	20.0 T_r 2.0 sec.

AC and DC transmission lines

r	0.0784	x_ℓ	0.52	x_c	5.556
R	0.2792	X_L	18.112	X_c	20.28 x_{co} 0.432

AC harmonic filters, local load, and shunt capacitor

r_{f5}	0.065	r_{f7}	0.0892	r_{f11}	0.062	r_{f13}	0.0704
L_{f5}	0.00862	L_{f7}	0.00862	L_{f11}	0.00332	L_{f13}	0.00332
c_{f5}	0.0000325	c_{f7}	0.00001695	c_{f11}	0.000017625	c_{f13}	0.000012575
R_L	6.05	$\bar{x}_c$	212.0				

DC Controllers

K_R	30	T_R	0.002778 sec.	K_I	30	T_I	0.002778 sec.	k	0.9

Operating point

v_t	1.1	v_o	1.0	P_{ac}	0.4	P_{dc}	0.4
Δ_o	5°	δ	51.05°	ψ_{fd}	1.165	ψ_{kd}	1.0057
ψ_d	0.947	ψ_{kq}	-0.497	ψ_q	-0.568	v_d	0.565
v_q	0.944	E_x	1.59	V_{ref}	1.18	P	1.0
Q	0.15	P_m	1.004	i_d	0.584	i_q	0.71
i_{fd}	1.59	i_{dA}	0.19	i_{qA}	0.31	i_{dB}	-0.34
i_{qB}	-0.18	v_{dc}	0.71	v_{qc}	0.82	Q_{ac}	0.0073
I_R	0.363	I_d	0.331	I_q	0.225	V_R	1.65
V_c	1.55	V_I	-1.45	α_R	8.25°	α_I	141.7°
Q_{dc}	0.185	$i_{d\ell}$	0.09	$i_{q\ell}$	0.16	i_{cd}	-0.004
i_{cq}	0.003	i_{df5}	-0.012	i_{qf5}	0.007	i_{df7}	-0.006
i_{qf7}	0.004	i_{df11}	-0.006	i_{qf11}	0.004	i_{df13}	-0.0045
i_{qf13}	0.003						

3.5 Eigenvalue Analysis

Both state variable grouping technique and nonlinear approximation technique described in section 3.1 are employed to calculate the eigenvalues for the different system models developed in section 3.2. The results are tabulated in Tables I and II respectively. There is not much difference in high order models for the two methods. But the difference becomes evident when the model order becomes low. This is because of two different ways of making approximations. For example the ac harmonic filters equations (2.11) are replaced by (3.4) in nonlinear approximation and the filter currents are given in terms of v_d and v_q only. On the other hand when the same equations (2.11) are linearized and then solved the resulting currents are in terms of $\Delta\omega$, ψ_{fd}, ψ_{kd}, ..., I_R, $\cos\alpha_R$, ..., v_d and v_q due to the presence of pv_d, pv_q and $p\Delta\omega$ terms in the equations. The nonlinear approximation approach seems to be giving more accurate results. It is especially clear for the second order model. While the nonlinear approximation technique gives a pair of imaginary eigenvalues, which is expected since damping is neglected in the synchronous machine equations, the state variable grouping technique yields a conjugate pair of eigenvalues with positive real parts indicating an unstable system which contradicts the results from higher order models analysis.

The eigenvalues for the 39th order model are plotted in the complex plane in Fig. 3.1. It is noticed that a majority of the eigenvalues are clustered in the region between -10 and -200 of the real axis. The dominant eigenvalues are found to be these corresponding to δ, $\Delta\omega$, ψ_{fd} and E_x equations. The largest eigenvalues correspond to v_d, v_q, v_{dc} and v_{qc} equations. Based on this information the following

2nd Order	0.126±j6.76									
4th Order	-0.052±j7.1	-0.336±j1.11								
6th Order	-0.052±j7.1	-0.336±j1.11	-362,-35156							
8th Order	-0.052±j7.1	-0.336±j1.11	-362,-35156	-360,-360						
10th Order	-0.15±j7.14	-0.33±j1.1	-363,-30532	-360,-360	-41.9,-26.1					
12th Order	-0.15±j7.14	-0.33±j1.1	-363,-39685	-360,-360	-41.9,-26.1	-18250±j59136				
15th Order	-0.15±j7.14	-0.33±j1.1	-365	-360,-360	-41.9,-26.1	-6623±j64990	-185±j761			
							-20.5±j327			
17th Order	-0.15±j7.14	-0.33±j1.1	-365	-360,-360	-41.8,-26.2	-4415±j10930	-122±j785	-847±j1892		
							-15.5±j325			
23rd Order	-0.164±j7.14	-0.33±j1.1	-365	-360,-360	-41.9,-26.3	-1039±j5524	-143±j809	-73±j1993	-2620±j4267	
							-14.8±j326		-59:1 ±j1216	
									-50±j376	
39th Order	-0.164±j7.14	-0.33±j1.1	-365	-360,-360	-41.9,-26.3	-6577±j15988	-143±j811	-76.7±j1977	-34339,-7018	-8.95±j1490
							-14.8±j326		-61±j1198	-9.5±j2245
									-50±j376	-18±j2191
										-23.7±j2947
										-55±j4358
										-73±j5118
										-92±j3568
										-123±j4335

Table I Eigenvalues by state variable grouping technique

2nd Order	0.0±j6.76									
4th Order	-0.083±j7.1	-0.34±j1.11								
6th Order	-0.083±j7.1	-0.34±j1.11	-362,-35156							
8th Order	-0.083±j7.1	-0.34±j1.11	-362,-35156	-360,-360						
10th Order	-0.18±j7.13	-0.33±j1.1	-362,-30531	-360,-360	-41.9,-26.15					
12th Order	-0.18±j7.13	-0.33±j1.1	-362,-31455	-360,-360	-41.9,-26.15	-166910±j495377				
15th Order	-0.18±j7.13	-0.33±j1.1	-364	-360,-360	-41.9,-26.15	-49562±j488820	-185±j760			
							-20.5±j327			
17th Order	-0.17±j7.13	-0.33±j1.1	-364.5	-360,-360	-41.8,-26.2	-37936±j72148	-123±j783	-1116±j1963		
							-15.5±j325			
23rd Order	-0.164±j7.13	-0.33±j1.1	-365	-360,-360	-41.9,-26.3	-6572±j13689	-143±j806	-64.3±j2004	-36945,-5154	
							-14.9±j326		-55±j1227	
									-50±j376	
39th Order	-0.164±j714	-0.33±j1.1	-365	-360,-360	-41.9,-26.3	-6577±j15988	-143±j811	-76.7±j1977	-34339,-7018	-8.95±j1490
							-14.8±j326		-61±j1198	-9.5±j2245
									-50±j376	-18±j2191
										-23.7±j2947
										-55±j4358
										-73±j5118
										-92±j3568
										-123±j4335

Table II Eigenvalues by nonlinear elimination technique

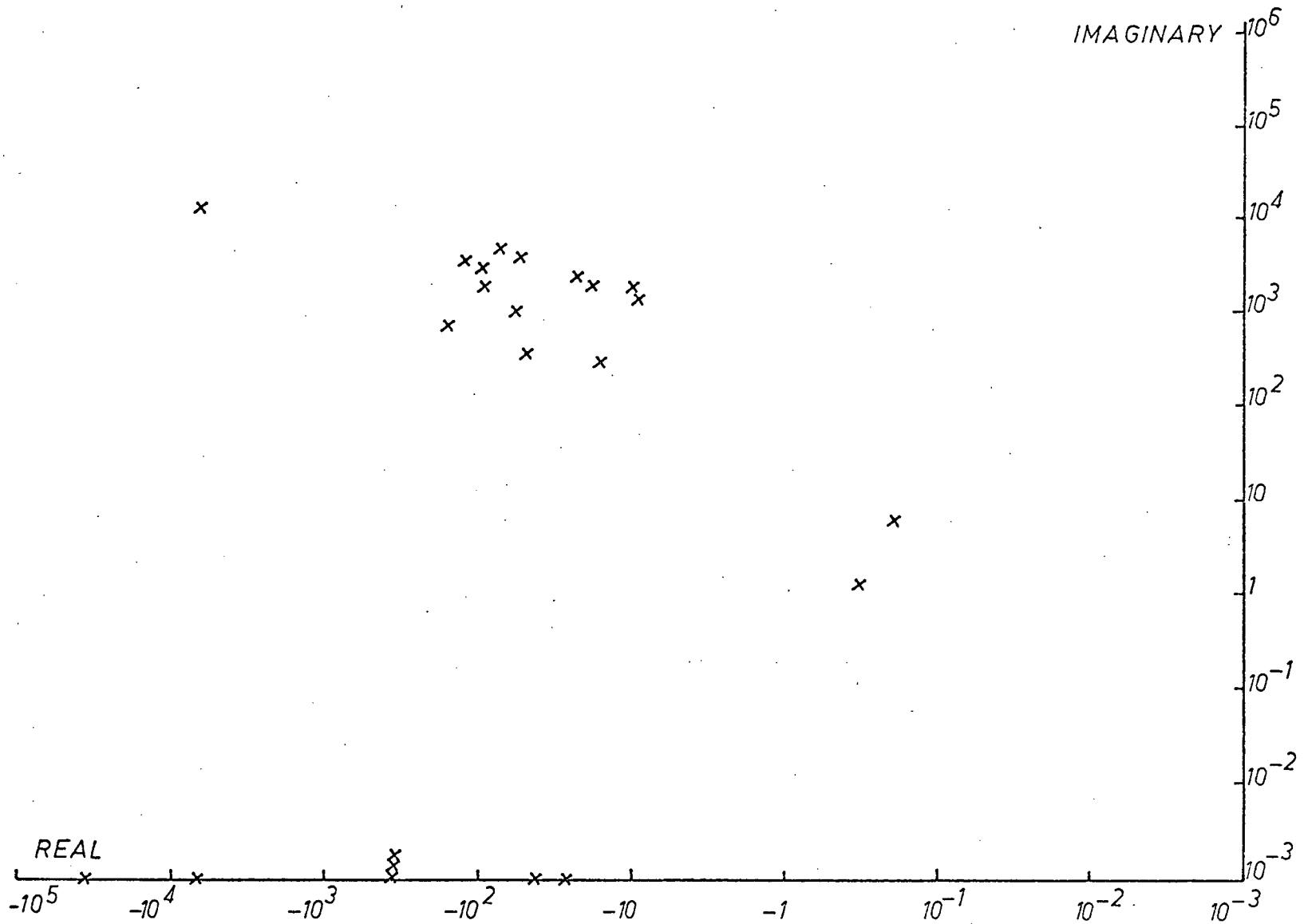

Fig. 3.1 EIGENVALUES FOR 39th ORDER MODEL

classification of system models is suggested:

1. A fourth order model comprising δ, $\Delta\omega$, ψ_{fd} and E_x as state variables is the simplest model one can have for system dynamic studies.
2. A sixth order model including $\cos\alpha_R$ and $\cos\alpha_I$ in addition to the 4th order states is fairly accurate and can be used for control design including an hvdc system.
3. If one wants more accurate results the 5th harmonic filter may be included resulting in a tenth order model.
4. The thirty-ninth order model is accurate but impractical in digital computation.

3.6 Nonlinear Tests with System Disturbances

To compare the four suggested models nonlinear system response tests subjected to different types of disturbances are compared. Figs. 3.2 and 3.3 show the change in rotor angle δ and speed deviation $\Delta\omega$ with time for a 25% step change in the dc reference current. For this disturbance it is seen from Fig. 3.2 that results are very close but the 6th order model gives the closest response to that of the 39th order model. Figures 3.4 and 3.5 show the system's response with a 25% step reduction in mechanical torque input. The 6th and 10th order models give identical response closer to that of the 39th order model than the 4th order model. Figures 3.6 and 3.7 show the system response to a three phase ground fault at the middle of one ac line for 6 cycles followed by isolating the faulted line at both ends and a successful reclosure after 0.4 second after the fault is removed. In this case only the responses of the 39th and 6th order models are plotted. It is noticed that even for such a severe disturbance the 6th order model results are still

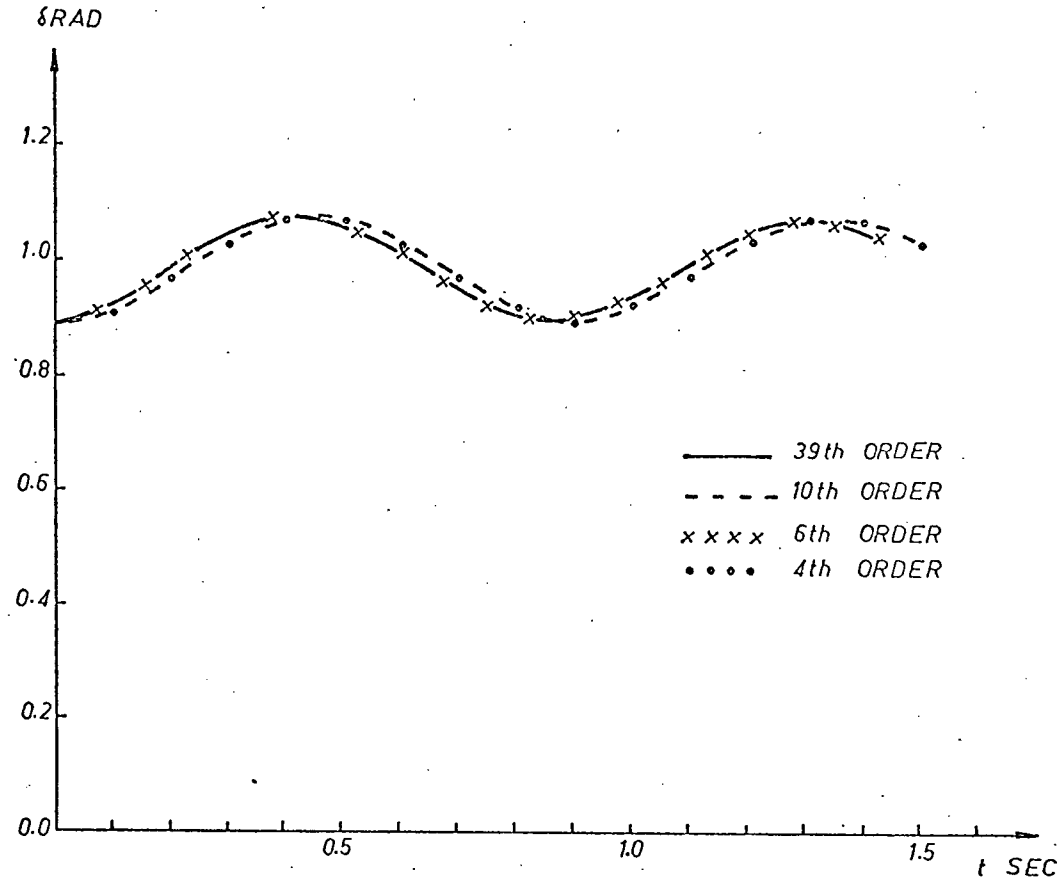

Fig. 3.2 STEP CHANGE IN I_{ref}

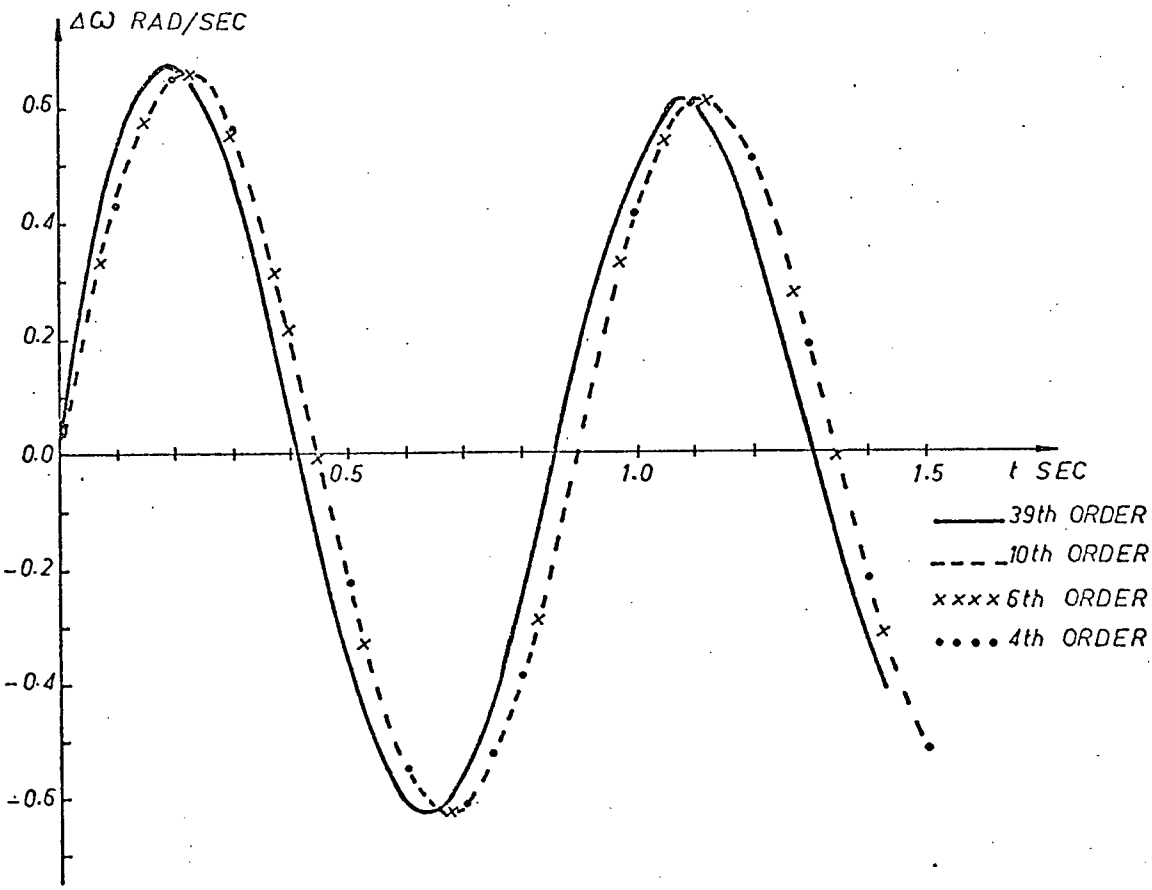

Fig. 3.3 STEP CHANGE IN I_{ref}

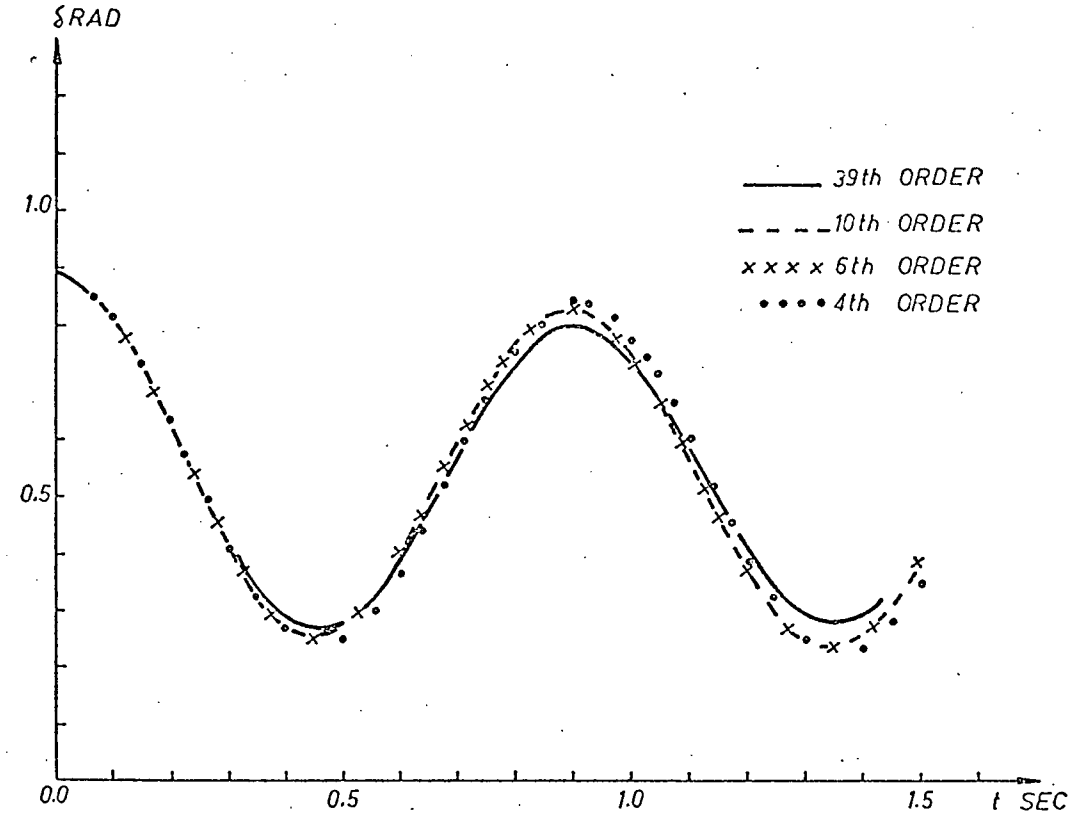

Fig. 3.4 STEP CHANGE IN P_m

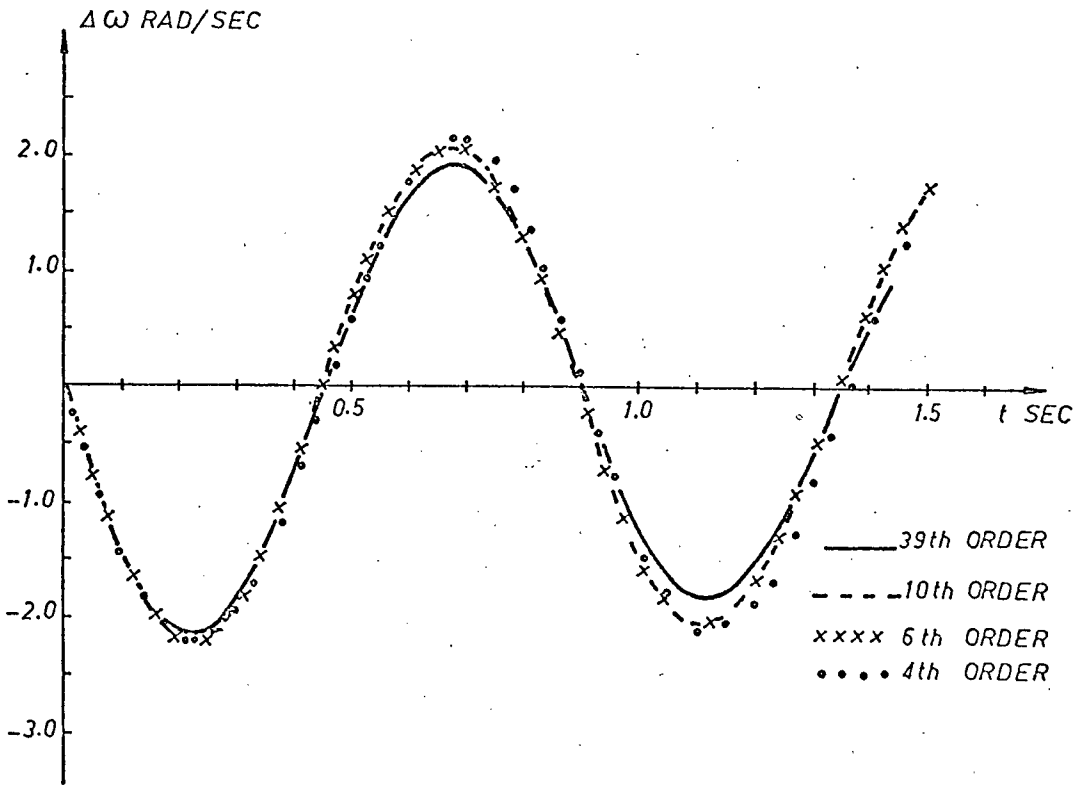

Fig. 3.5 STEP CHANGE IN P_m

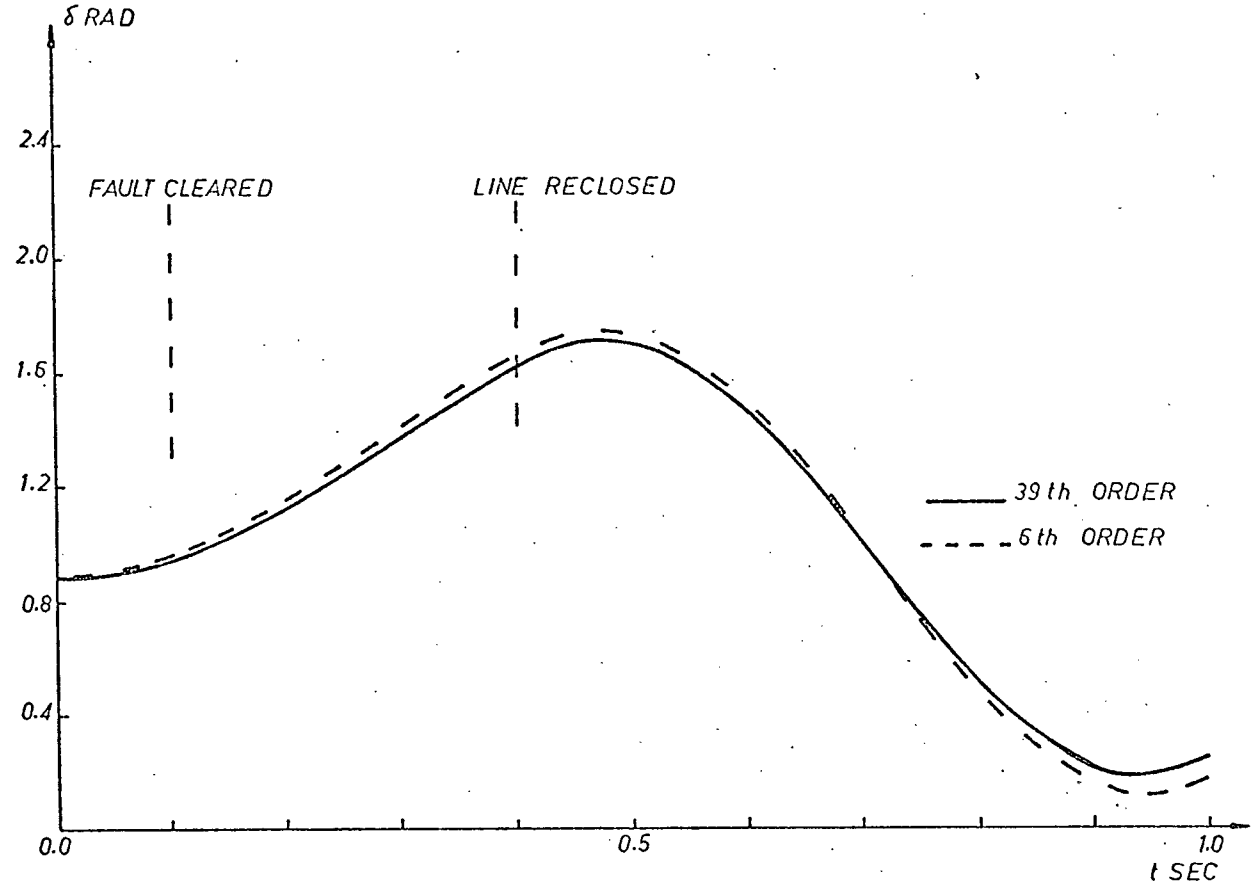

Fig. 3.6 THREE PHASE FAULT ON AC LINE

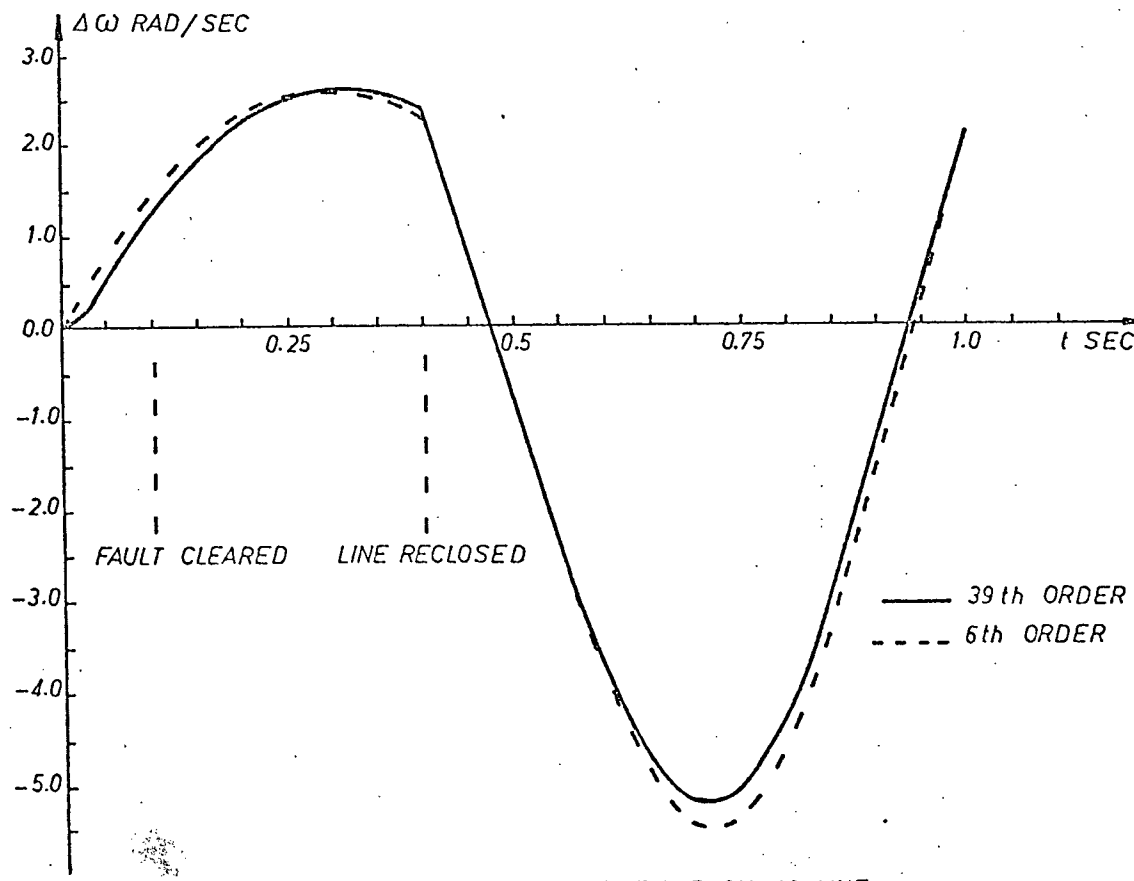

Fig. 3.7 THREE PHASE FAULT ON AC LINE

close to those of the 39th order model. From these test results, supported also by eigenvalue analysis, it is decided that from now on in the succeeding chapters only the 6th order model will be used for the control design.

4. STABILIZATION OF DC/AC PARALLEL SYSTEMS BY LINEAR OPTIMAL CONTROL SIGNALS

In this chapter linear optimal control theory is employed to stabilize dc/ac parallel power systems. Two systems are investigated; the first is to stabilize an existing system, and the second is to stabilize an expanded system by adding a parallel dc link to the existing ac line in order to increase the transmission capacity of the system. Several control schemes are designed and the disturbance test results on nonlinear system models are compared. For all designs the sixth order system model, i.e. $\Delta\dot{\delta}$, $\Delta\dot{\omega}$, $\Delta\dot{\psi}_{fd}$, $\Delta\dot{E}_x$, $\Delta\dot{\cos\alpha}_R$ and $\Delta\dot{\cos\alpha}_I$, is employed.

4.1 Linear Optimal Regulator Problem

The system's linearized equations are written as

$$\dot{x} = Ax + BU \tag{4.1}$$

It is required to find an optimal control U that minimizes the quadratic cost function

$$J = \frac{1}{2} \int_0^\infty (x^t Qx + U^t RU)\, dt \tag{4.2}$$

subject to (4.1), where Q and R are positive definite matrices. The required optimal control is given by[48]

$$U = -R^{-1} B^t Kx \tag{4.3}$$

where the Riccati matrix K is obtained from the solution of the nonlinear algebraic matrix equation

$$KA + A^t K - KBR^{-1} B^t K + Q = 0 \tag{4.4}$$

Several computation techniques for the solution are available utilizing the properties of the state and costate composite system matrix M[49,50],

$$M = \begin{bmatrix} A & -BR^{-1}B^{t} \\ -Q & -A^{t} \end{bmatrix} \tag{4.5}$$

the matrix K may be computed from

$$K = X_{II}\, X_{I}^{-1} \tag{4.6}$$

where

$$X = \begin{bmatrix} X_{I} & X_{III} \\ XII & XIV \end{bmatrix} \tag{4.7}$$

is the eigenvector matrix of M and the eigenvectors X_I and X_{II} correspond to the stable eigenvalues of M or the eigenvalues of the controlled system.

4.2 Control Signals for an Existing System

The system considered here is the same as described in Chapter 3, which was shown in Figure 2.3. Three different stabilization schemes are investigated; the first with an optimal excitation control u_E on the synchronous machine alone without any stabilization signal on dc, the second with optimal current control u_D on dc but without excitation stabilization on the synchronous machine, and the third with both u_E and u_D controls designed together. The control signals designed for the system's linearized model are tested on the original nonlinear system and the system's response to the disturbances and also the system's eigenvalues are compared.

For the data given in Chapter 3 the linearized state equations for the system are

$$\begin{bmatrix} \Delta\dot{\delta} \\ \Delta\dot{\omega} \\ \Delta\dot{\psi}_{fd} \\ \Delta\dot{E}_x \\ \Delta\dot{\cos\alpha}_R \\ \Delta\dot{\cos\alpha}_I \end{bmatrix} = \begin{bmatrix} 0.0 & 1.0 & 0.0 & 0.0 & 0.0 & 0.0 \\ -52.1 & 0.0 & -112.6 & 0.0 & -92.1 & -46.7 \\ -0.14 & 0.0 & -0.46 & 0.21 & -0.2 & -0.2 \\ -0.24 & 0.0 & -6.92 & -0.5 & -1.11 & 0.92 \\ -278.2 & 0.0 & -8042.0 & 0.0 & -14197.0 & -10672.0 \\ 5.09 & 0.0 & 147.1 & 0.0 & 259.7 & -164.8 \end{bmatrix} \begin{bmatrix} \Delta\delta \\ \Delta\omega \\ \Delta\psi_{fd} \\ \Delta E_x \\ \Delta\cos\alpha_R \\ \Delta\cos\alpha_I \end{bmatrix}$$

$$+ BU \qquad (4.8)$$

The B matrices for the three controls are given by

$$u_E: B = [0 \quad 0 \quad 0 \quad k_r/T_r \quad 0 \quad 0]^t$$

$$u_D: B = [0 \quad 0 \quad 0 \quad 0 \quad k_R/T_R\, v_t \quad 0]^t \qquad (4.9)$$

$$u_E \text{ and } u_D: B = \begin{bmatrix} 0 & 0 & 0 & k_r/T_r & 0 & 0 \\ 0 & 0 & 0 & 0 & K_R/T_R\, v_t & 0 \end{bmatrix}^t$$

In all three cases the matrices Q and R of equation (4.2) are taken as unit matrices. The system's eigenvalues for all cases are listed in Table III and the corresponding control laws are given in (4.10).

Table III Eigenvalues of the existing power system for various controls

Control Used	Eigenvalues		
no control	$-0.084 \pm j7.093$	$-0.339 \pm j1.108$	-365, -13997
u_E	$-0.728 \pm j7.154$	-0.403, -9.915	-365, -13997
u_D	-1.512, -43.89	$-0.349 \pm j1.13$	-348, -17097
u_E and u_D	-1.56, -43.89	-0.383, -9.87	-348, -17097

$$\begin{bmatrix} u_E \\ u_D \\ u_E \\ u_D \end{bmatrix} = \left[\begin{array}{cccccc} -5.79 & -0.36 & -7.32 & -1.09 & -0.002 & -0.025 \\ 0.415 & 1.004 & -0.17 & -0.0004 & -0.319 & -0.082 \\ -0.159 & -0.0017 & -0.495 & -0.961 & 0.8\times10^{-5} & -0.0045 \\ 0.402 & 1.005 & -0.532 & 0.008 & -0.319 & -0.082 \end{array}\right]$$

$$[\Delta\delta \quad \Delta\omega \quad \Delta\psi_{fd} \quad \Delta E_x \quad \Delta\cos\alpha_R \quad \Delta\cos\alpha_I]^t \qquad (4.10)$$

It is noticed in Table III that the dominant pair of eigenvalues in all three cases have been shifted to the left of the complex plane indicating the stabilizing effect of these controls. The damping ratio for the dominant eigenvalues is improved in the case of u_E control. For the other cases the dominant pair is decoupled into two real eigenvalues. For u_E and u_D controls all the eigenvalues are real indicating a non-oscillatory system.

4.3 Nonlinear Tests

The system disturbance considered in all cases is a three phase to ground fault at the middle of one circuit of the ac transmission line for 0.1 sec. The faulted line is then isolated by disconnecting it from both ends followed by a successful reclosure at 0.5 sec. after the fault is completely removed. The system's response is summarized in Figures 4.1 to 4.6. It is noticed from these figures that the excitation control signal u_E by itself does not improve the system's stability effectively despite the fact that the control effort reaches maximum all the time as shown in Fig. 4.6. The limits set for the control signals are $\pm$0.12 p.u. for u_E and $\pm$0.3 p.u. for u_D. The limits for u_E were chosen as $\pm$0.12 p.u. after several other values were tried. It is shown in Figure 4.7 that the higher the u_E limits, the higher will be the overshoot in machine

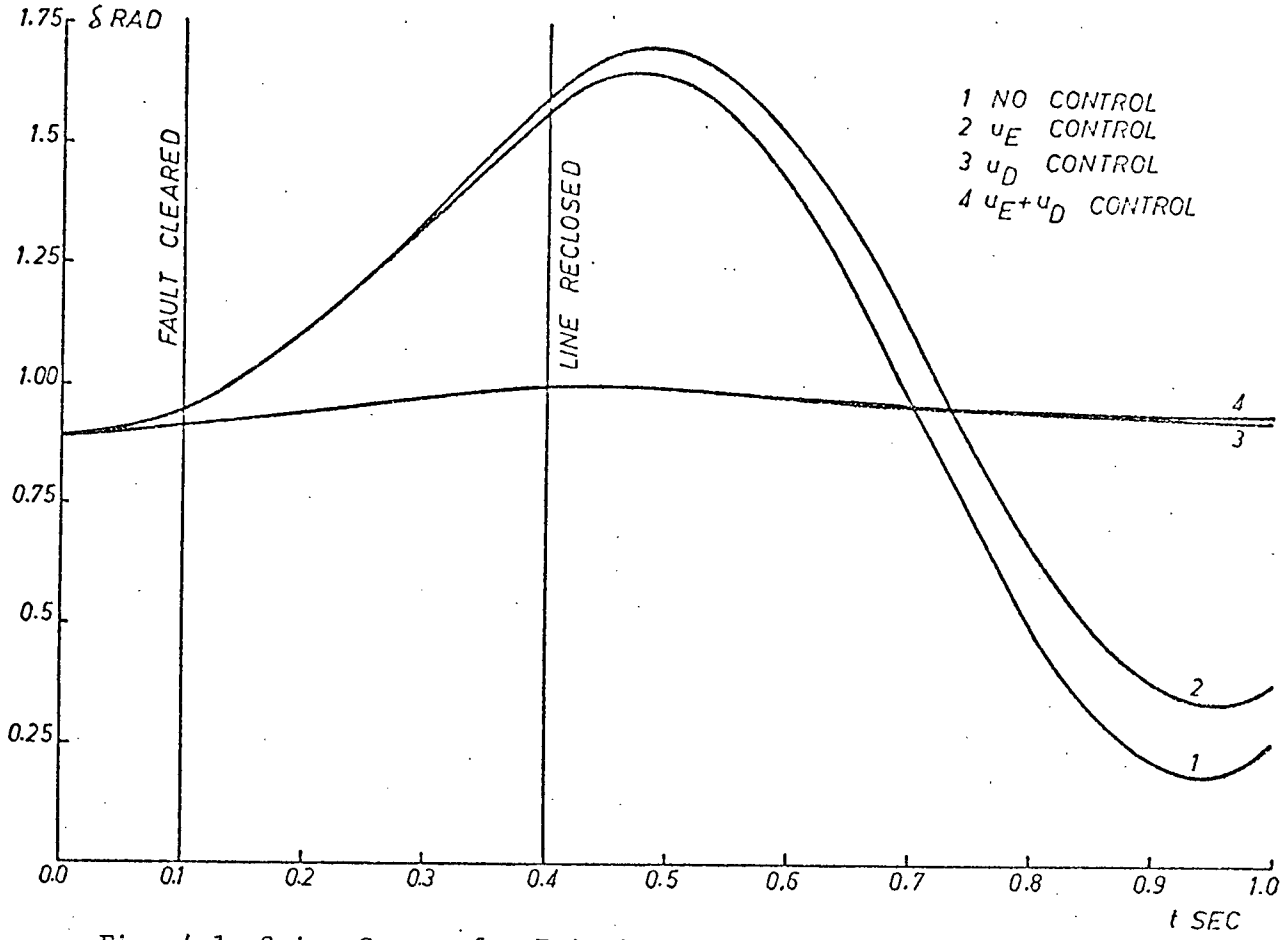

Fig. 4.1 Swing Curves for Existing System

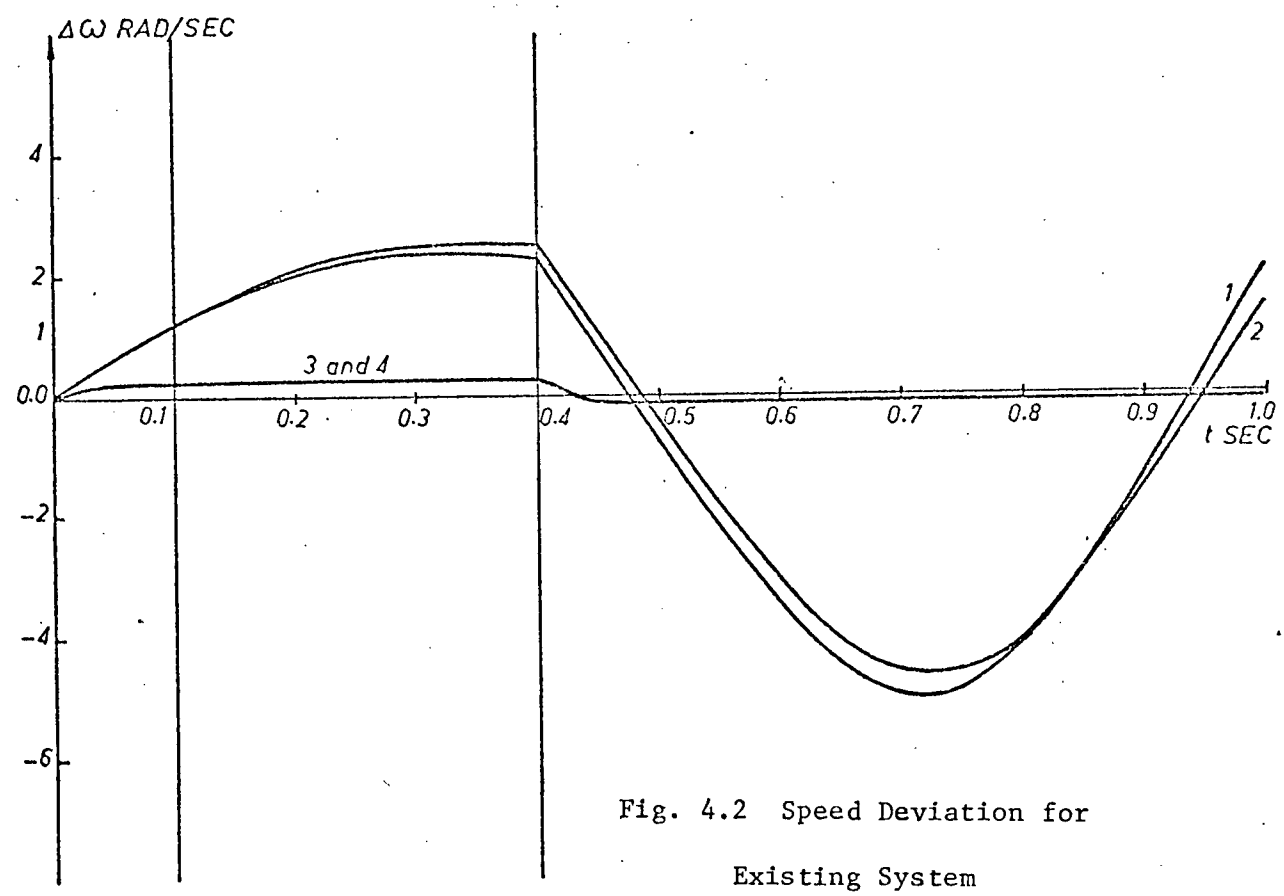

Fig. 4.2 Speed Deviation for Existing System

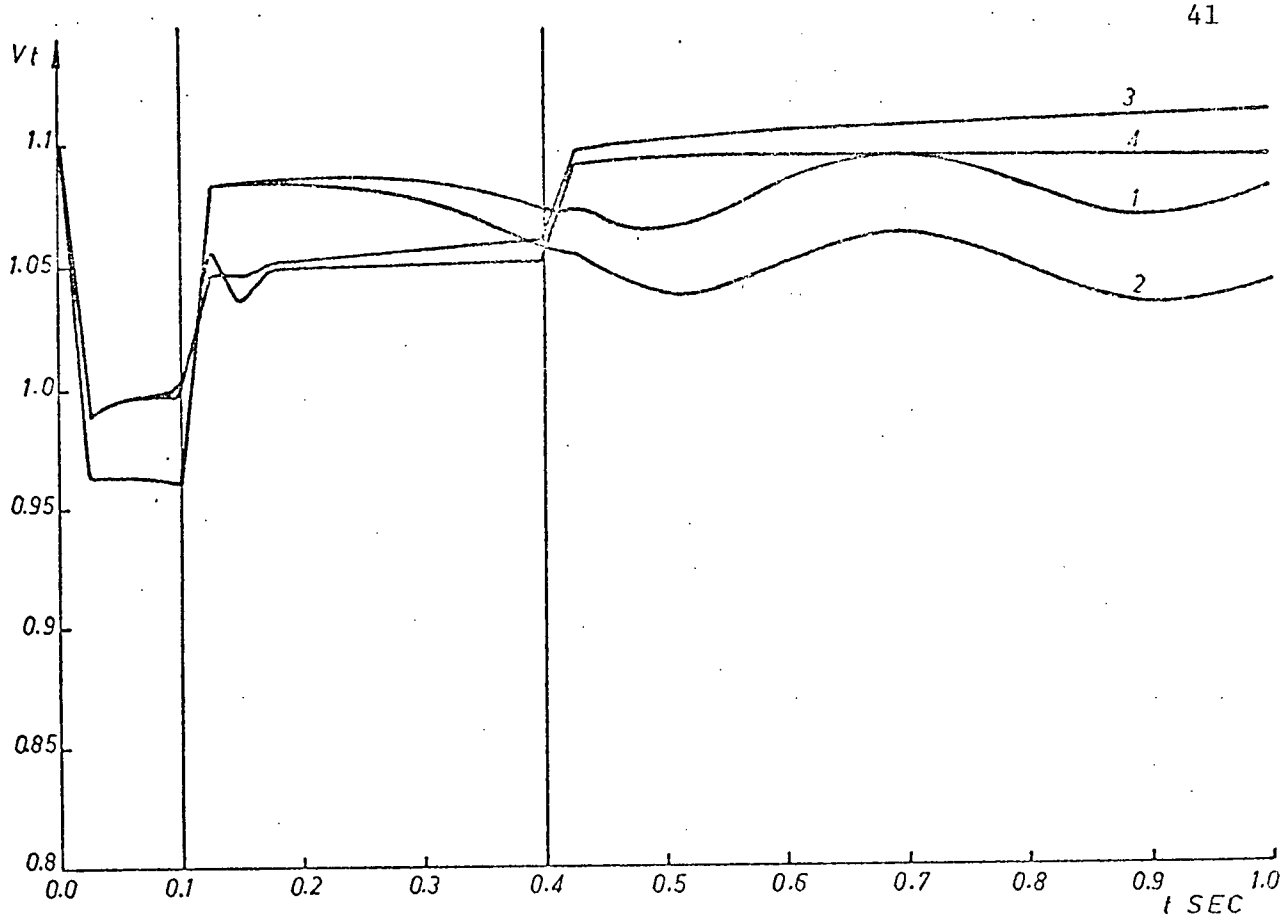

Fig. 4.3 Terminal Voltage Variations for Existing System

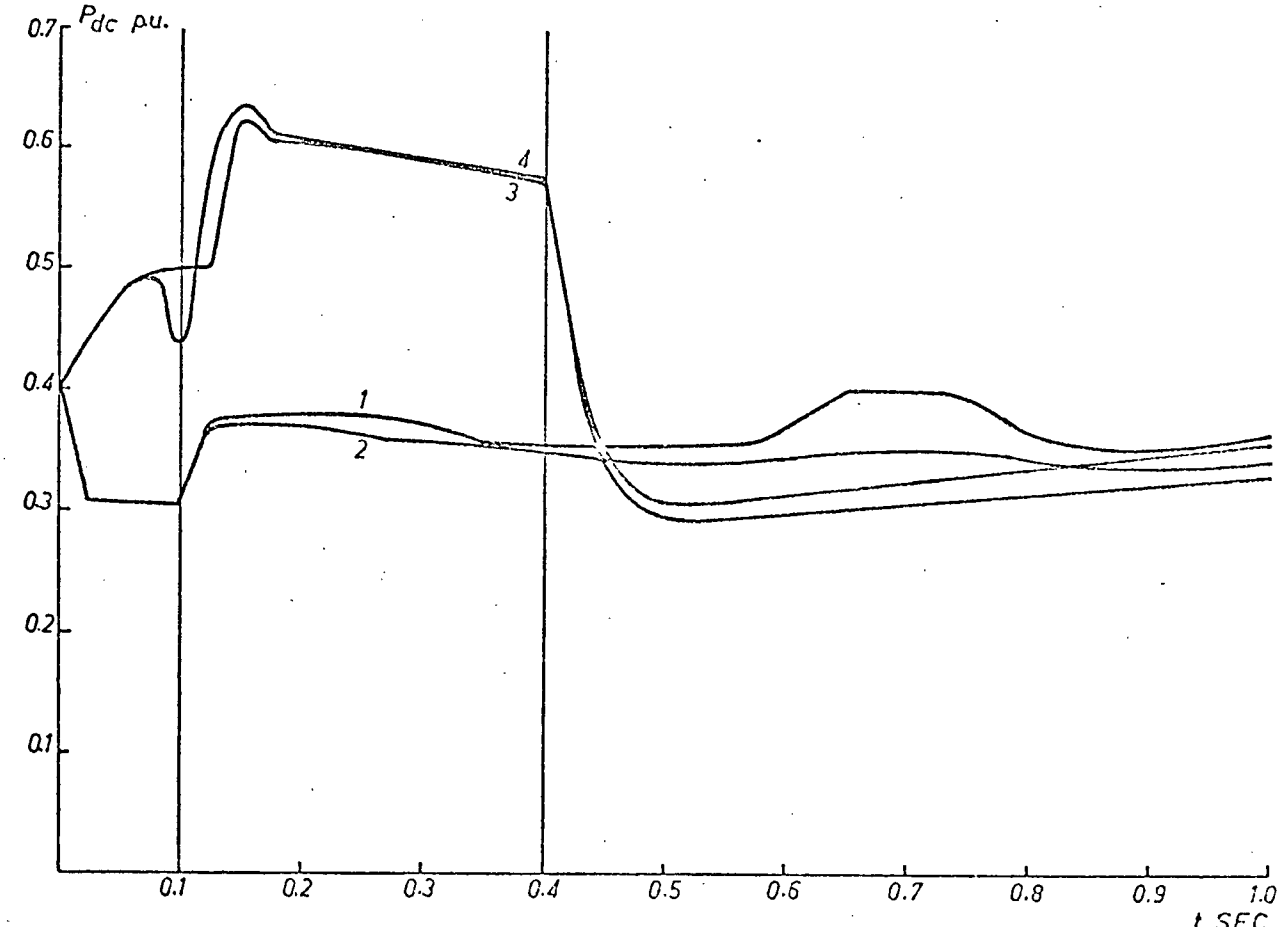

Fig. 4.4 Variation of DC Power for Existing System

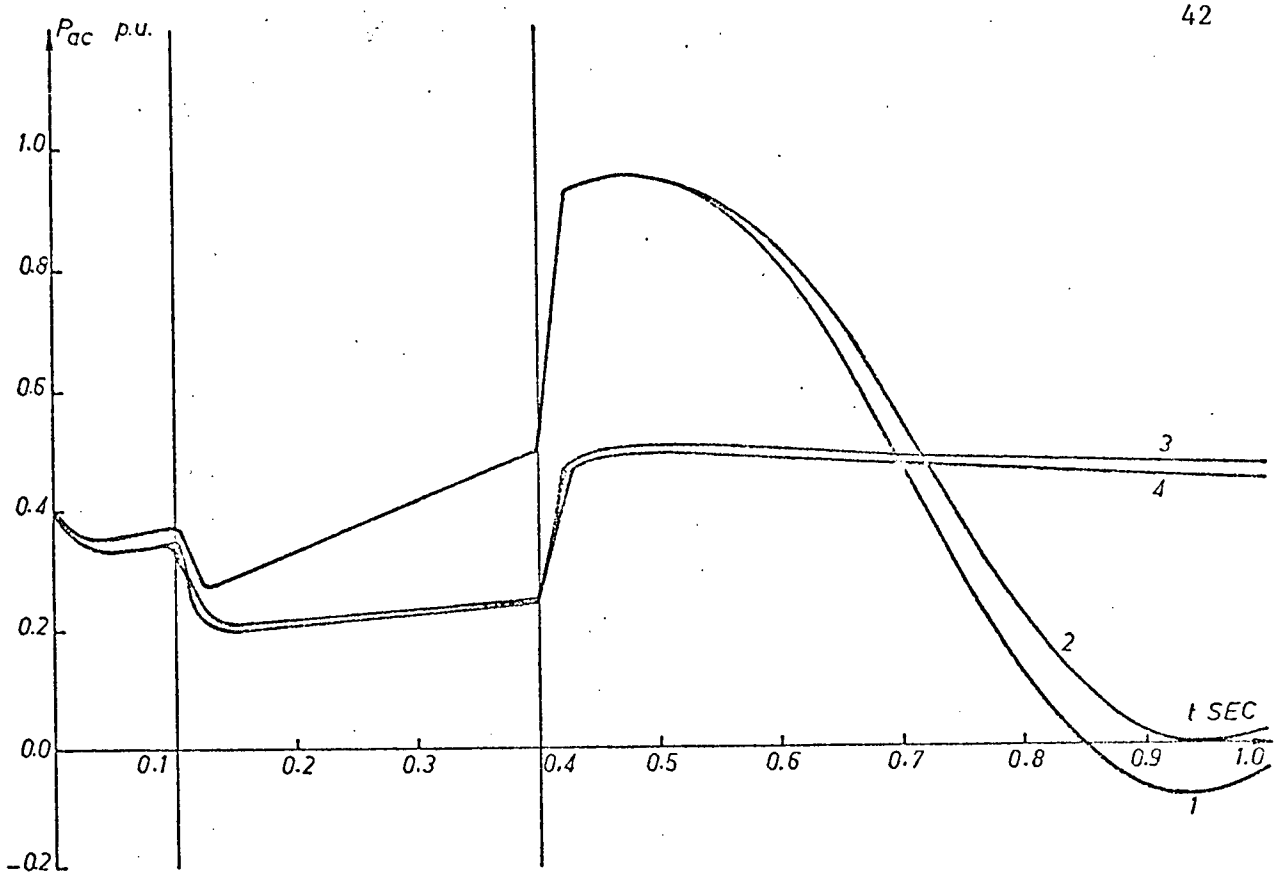

Fig. 4.5 Variation of AC Power for Existing System

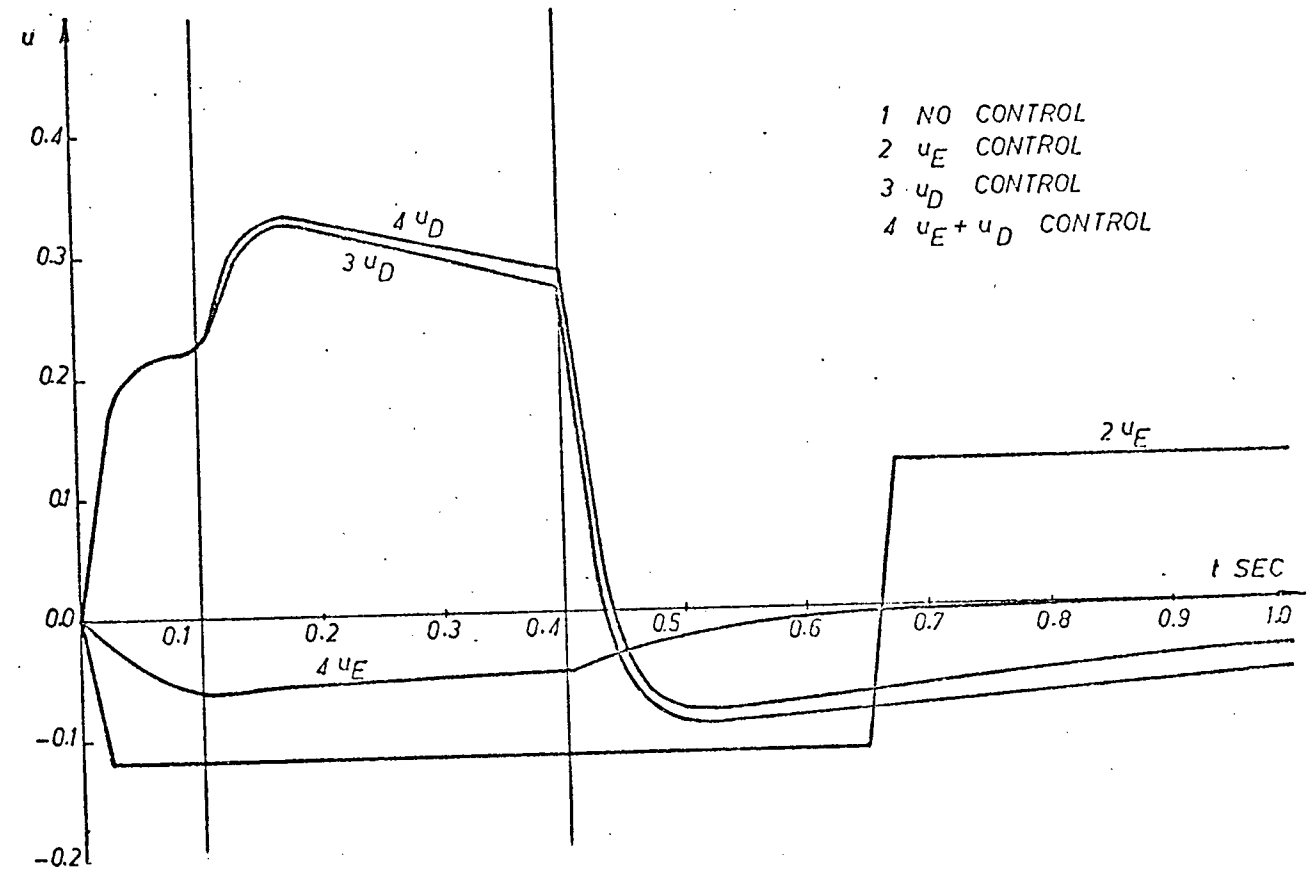

Fig. 4.6 Control Effort for Existing System

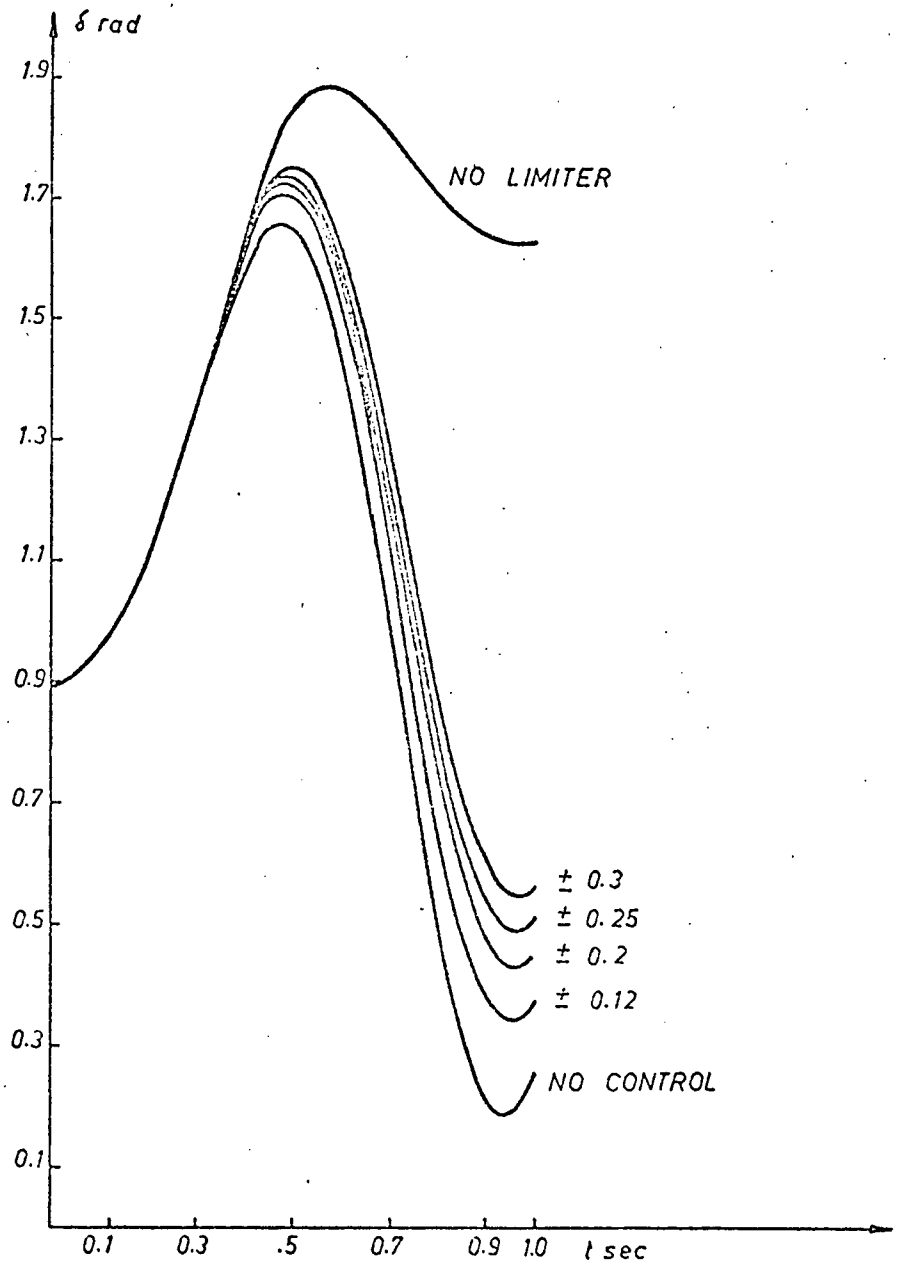

Fig. 4.7 Swing Curves with Varying Limits on u_E

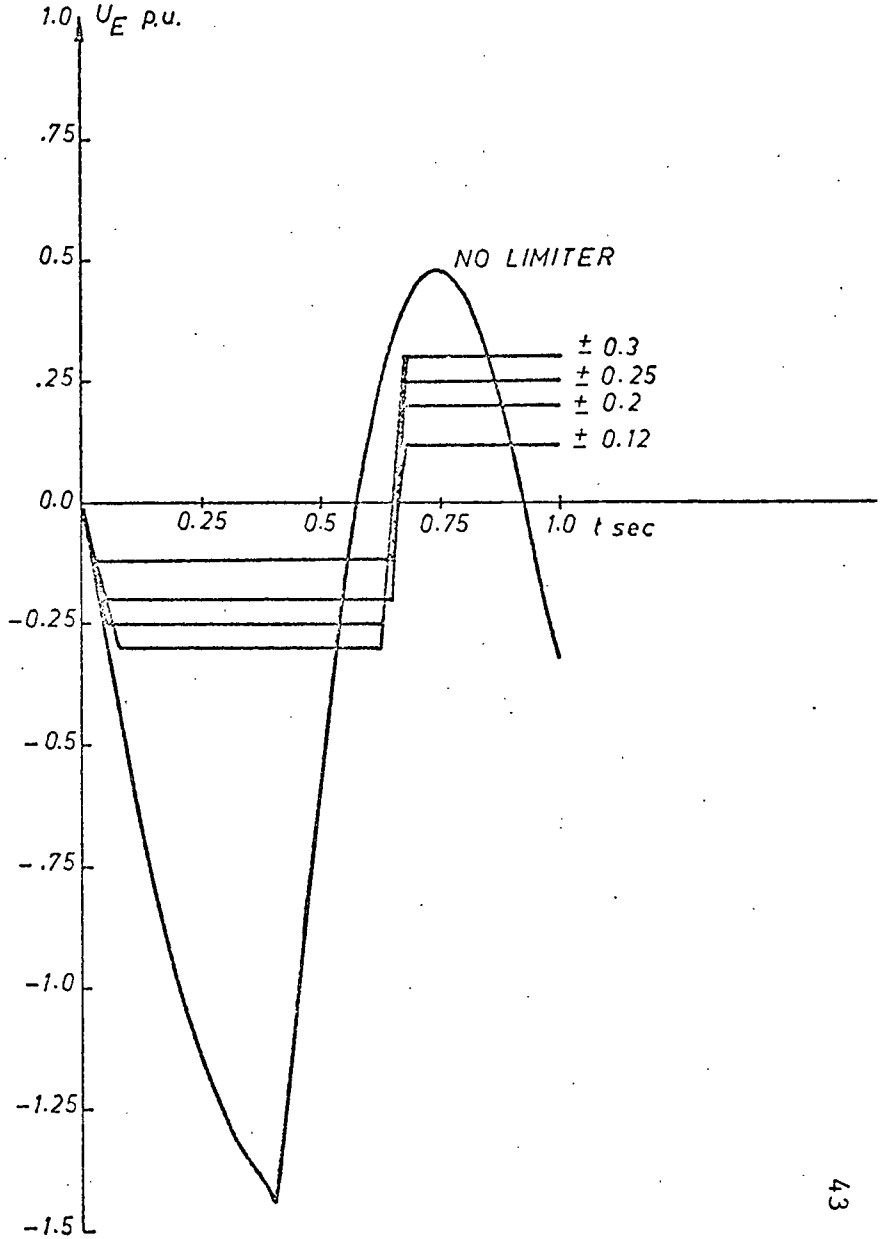

Fig. 4.8 Excitation Control Effort with Varying Limits on u_E

swing. The machine goes unstable when u_E is not restricted. Figure 4.8 shows the control efforts for different cases. The dc control limits are so chosen that it will not overload the dc line or operate it under very light load. It is found that the stabilization is very effective either with the dc control signal u_D alone or combined with the excitation control signal u_E. The angular deviation is very small, and the dc line picks up the load originally carried by the faulty line very quickly. It is also noted that the system's responses with u_D control alone or with u_E and u_D controls are very close except that the terminal voltage changes are smaller in the later case.

4.4 A Fourth Order Model Study

Due to the presence of two large eigenvalues on the sixth order model corresponding to the dc firing circuits dynamics the step size in numerical integration is very small thus requiring longer computation time. It was thought that it would be interesting to find out if these two small time constants associated with the firing circuits can be neglected in order to save the computation time. The resulting system's linearized equations of the fourth order become

$$\begin{bmatrix} \Delta\dot{\delta} \\ \Delta\dot{\omega} \\ \Delta\dot{\psi}_{fd} \\ \Delta\dot{E}_x \end{bmatrix} = \begin{bmatrix} 0.0 & 1.0 & 0.0 & 0.0 \\ -50.3 & 0.0 & -60.4 & 0.0 \\ -0.135 & 0.0 & -0.345 & 0.207 \\ -0.217 & 0.0 & -6.3 & -0.5 \end{bmatrix} \cdot \begin{bmatrix} \Delta\delta \\ \Delta\omega \\ \Delta\psi_{fd} \\ \Delta E_x \end{bmatrix} + BU \qquad (4.11)$$

The matrix B is given by

u_E: $B = [0.0 \quad 0.0 \quad 0.0 \quad 10.0]^t$

u_D: $B = [0.0 \quad -52.5 \quad -0.163 \quad 0.108]^t$

u_E and u_D: $B = \begin{bmatrix} 0.0 & 0.0 & 0.0 & 10.0 \\ 0.0 & -52.5 & -0.163 & 0.108 \end{bmatrix}^t$ (4.12)

The system's eigenvalues are listed in Table IV and the corresponding control laws are given in (4.13)

Table IV Eigenvalues for a fourth order model

control used	eigenvalues	
no control	$-0.084 \pm j7.093$	$-0.339 \pm j1.108$
u_E	$-0.728 \pm j7.154$	$-0.388, -9.915$
u_D	$-1.39, -51.49$	$-0.349 \pm j1.13$
u_E and u_D	$-1.42, -51.49$	$-0.35, -9.87$

$$\begin{bmatrix} u_E \\ u_D \\ u_E \\ u_D \end{bmatrix} = \begin{bmatrix} -5.78 & -0.359 & -7.24 & -1.09 \\ 0.444 & 1.005 & -0.023 & -0.02 \\ -0.109 & -0.002 & -0.286 & -0.957 \\ 0.43 & 1.006 & -0.45 & 0.004 \end{bmatrix} \cdot \begin{bmatrix} \Delta\delta \\ \Delta\omega \\ \Delta\psi_{fd} \\ \Delta E_x \end{bmatrix} \quad (4.13)$$

The same nonlinear test with system disturbance is applied to this model and the corresponding swing curves are plotted in Figure 4.9. It is found that there is considerable deviation between the fourth and sixth order models and some accuracy is sacrificed by neglecting the two small time constants for faster computation. It is decided that the dc firing circuit dynamics will be retained from now on in the dc system studies for the rest of this thesis.

4.5 Expanded System

The system investigated in this section had an ac system consisting of a synchronous generator transmitting power to an infinite system over a double circuit ac transmission line, Figure 4.10. The

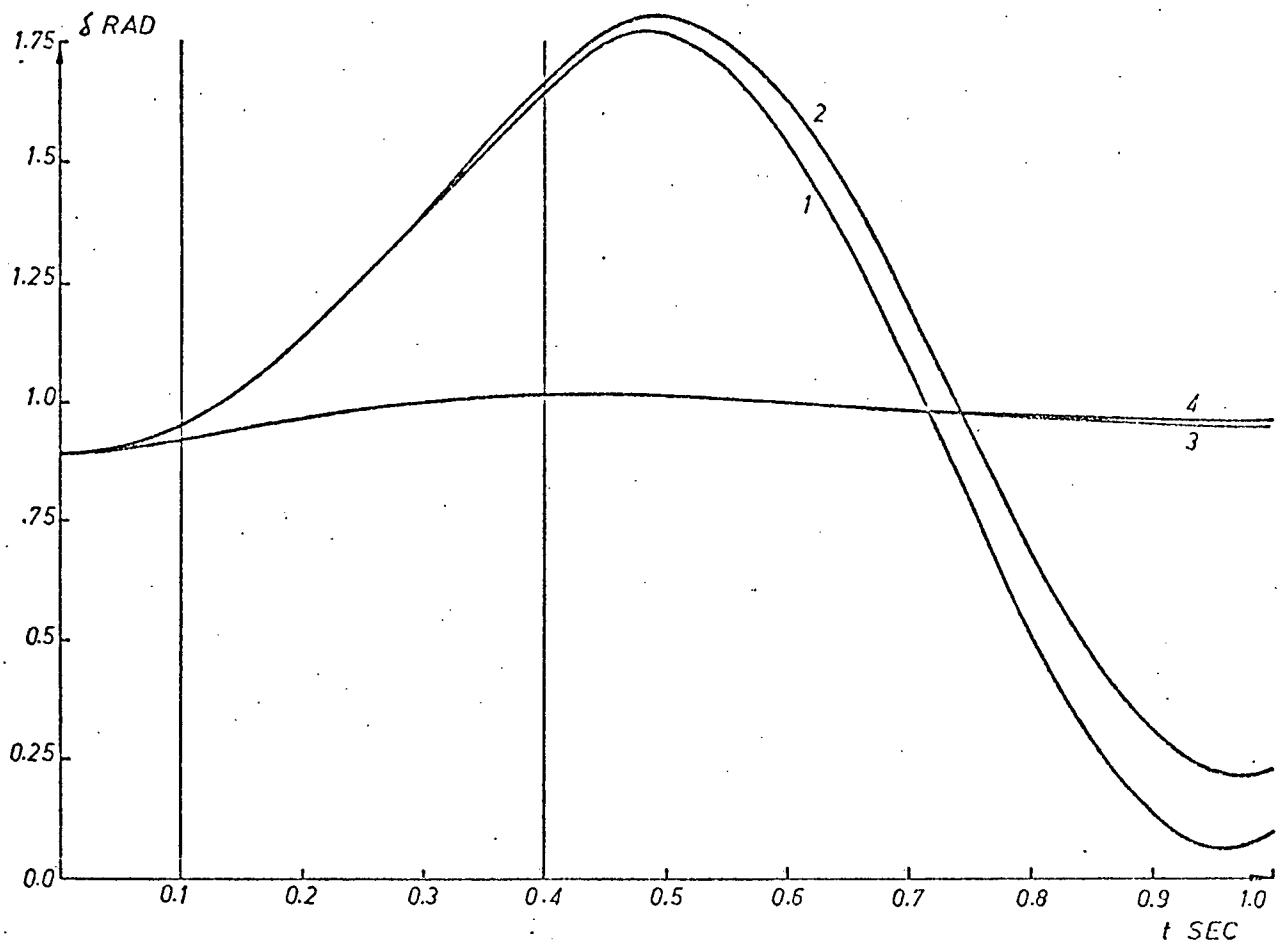

Fig. 4.9 Swing Curves for a 4th Order Model

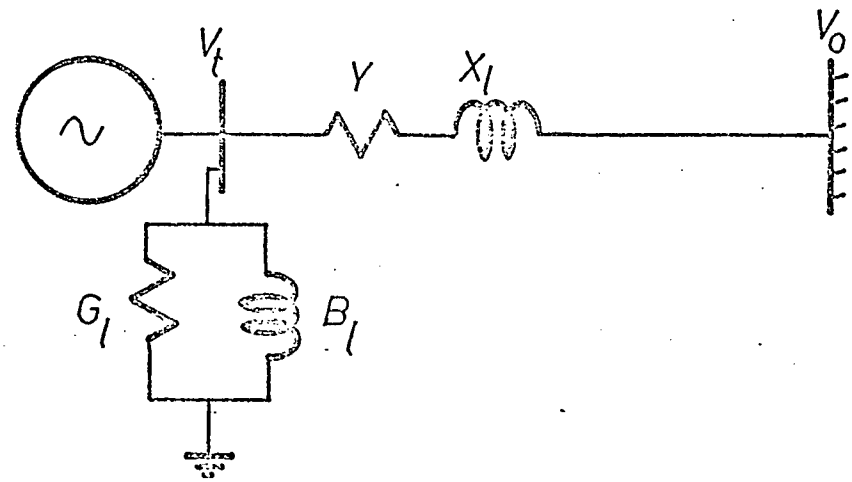

Fig. 4.10 AC System to be Expanded

generator is equipped with a voltage regulator and also has a local load at the terminal bus. This system is expanded by adding a dc link in parallel after the generating capacity is doubled. The system was unstable at the outset and a conventional excitation control signal is designed.

The ac system's per unit data was as follows:

Synchronous machine and voltage regulator:

x_d	0.973	x_q	0.55	T'_{do}	7.76 sec.	K_r	130
x'_d	0.19	$x_{\ell a}$	0.04	H	4.63 sec.	T_r	0.05 sec.

AC transmission line and local load:

r	-0.034	x_ℓ	0.997	G_ℓ	0.249	B_ℓ	0.262

Operating point:

v_t	1.05	Q	0.02	δ	65.2°	i_d	0.4
v_o	1.02	ψ_{fd}	1.22	v_d	0.45	i_q	0.81
P	0.952	E_x	1.34	v_q	0.95		

From the data given the linearized fourth order system's model, equations (2.2a) and (2.2b) were

$$\begin{bmatrix} \Delta\dot{\delta} \\ \Delta\dot{\omega} \\ \Delta\dot{\psi}_{fd} \\ \Delta\dot{E}_x \end{bmatrix} = \begin{bmatrix} 0.0 & 1.0 & 0.0 & 0.0 \\ -22.4 & 0.0 & -39.7 & 0.0 \\ -0.1 & 0.0 & -0.2 & 0.15 \\ 223.6 & 0.0 & 1794.2 & -20.0 \end{bmatrix} \begin{bmatrix} \Delta\delta \\ \Delta\omega \\ \Delta\psi_{fd} \\ \Delta E_x \end{bmatrix} \tag{4.14}$$

The system's eigenvalues were

$$0.18 \pm j5.16, \qquad -10.3 \pm j13.3$$

which indicates an unstable system. A conventional excitation control

signal u_x is designed[51],

$$u_x = \frac{k_e S}{1 + T_e S} \Delta\omega = \frac{0.04 S}{1 + 0.5S} \Delta\omega \qquad (4.15)$$

and is added to the system resulting in

$$\begin{bmatrix} \Delta\dot{\delta} \\ \Delta\dot{\omega} \\ \Delta\dot{\psi}_{fd} \\ \Delta\dot{E}_x \\ \dot{u}_x \end{bmatrix} = \begin{bmatrix} 0.0 & 1.0 & 0.0 & 0.0 & 0.0 \\ -22.4 & 0.0 & -39.7 & 0.0 & 0.0 \\ -0.1 & 0.0 & -0.2 & 0.15 & 0.0 \\ 223.6 & 0.0 & 1794.2 & -20.0 & 2600.0 \\ -1.8 & 0.0 & -3.2 & 0.0 & -2.0 \end{bmatrix} \begin{bmatrix} \Delta\delta \\ \Delta\omega \\ \Delta\psi_{fd} \\ \Delta E_x \\ u_x \end{bmatrix} \qquad (4.16)$$

The corresponding eigenvalues become

$$-2.5 \pm j3.5, \quad -4.6, \quad -6.3 \pm j11.9$$

Thus the system is stabilized.

Next the system is expanded by doubling its capacity. With the base MVA of the synchronous machine doubled, the p.u. ac line and local load data become

r -0.068 x_ℓ 1.994 G_ℓ 0.1245 B_ℓ 0.131

The new dc line and harmonic filters' data are

R 0.066 x_{co} 0.2 G_f 0.22×10^{-3} B_f -0.14

It happened that the reactive power can be sufficiently provided by the harmonic filters and no special condenser for power factor correction is needed. The system's new operating point is given as

v_t 1.05 v_o 1.02 P 0.9765 Q 0.0622

P_{ac} 0.504 Q_{ac} 0.187 P_{dc} 0.335 Q_{dc} 0.135

δ 81.15° Δ_o 15° v_d 0.449 v_q 0.949

ψ_{fd} 1.233 E_x 1.388 V_{ref} 1.061 V_R 1.61

V_I -1.57 $\cos\alpha_R$ 0.962 $\cos\alpha_I$ -0.868 I_R 0.312

For the given data the system's linearized equations are

$$\begin{bmatrix} \Delta\dot{\delta} \\ \Delta\dot{\omega} \\ \Delta\dot{\psi}_{fd} \\ \Delta\dot{E}_x \\ \Delta\dot{\cos\alpha}_R \\ \Delta\dot{\cos\alpha}_I \\ \dot{u}_x \end{bmatrix} = \begin{bmatrix} 0.0 & 1.0 & 0.0 & 0.0 & 0.0 & 0.0 & 0.0 \\ 0.388 & 0.0 & -119.4 & 0.0 & -173.3 & -120.3 & 0.0 \\ -0.04 & 0.0 & -0.38 & 0.15 & -0.35 & -0.33 & 0.0 \\ 183.0 & 0.0 & -1860.0 & -20.0 & -443.8 & 134.0 & 2600.0 \\ 2171.1 & 0.0 & -22068.0 & 0.0 & -40020.0 & -32172.4 & 0.0 \\ -17.7 & 0.0 & 179.5 & 0.0 & 318.2 & -105.4 & 0.0 \\ 0.03 & 0.0 & -9.55 & 0.0 & -13.9 & -9.62 & -2.0 \end{bmatrix}$$

$$\cdot [\Delta\delta \quad \Delta\omega \quad \Delta\psi_{fd} \quad \Delta E_x \quad \Delta\cos\alpha_R \quad \Delta\cos\alpha_I \quad u_x]^t \qquad (4.17)$$

and the corresponding eigenvalues are

$-0.87 \pm j2.4, \quad -4.76, \quad -7.85 \pm j11, \quad -363.6, \quad -39762.6$

The system is still stable. However, because of the new situation, the excitation control signal u_x originally designed for the ac system is modified to become

$$u'_x = \frac{0.09\ S}{1 + S}\ \Delta\omega \qquad (4.18)$$

and the system's eigenvalues for this case are

$-1.94 \pm j2.04, \quad -2.06, \quad -7.63 \pm j10.8, \quad -363.6, \quad -39762.6$

The system is more stable with the new adjustment.

In addition to the above two cases where the system is stabilized by excitation control signals u_x and u'_x respectively, three new controls are designed and compared with old schemes

1. No modification of the excitation control u_x and no optimal control signals.
2. With only the modified excitation control signal u'_x.
3. An optimal dc current control u_D is designed with excitation control removed.
4. A dc control u_D is designed in conjunction with u_x.
5. A dc control u_D is designed in conjunction with the modified excitation control u'_x.

The system's eigenvalues for the last three cases are listed in Table V.

Table V Eigenvalues for expanded system

Control	Eigenvalues
u_D	$-0.93, \quad -38.5 \qquad -10.75 \pm j13.1 \qquad -379, \quad -41071.2$
u_x and u_D	$-1.06 \pm j1.5 \qquad -55.35 \pm j66.7 \quad -0.8 \quad -384.5, \quad -41071.2$
u'_x and u_D	$-0.85 \pm j1.01 \qquad -58.4 \pm j71 \quad -0.667 \quad -385.2, \quad -41071.2$

The control laws for different cases are given by

$$\begin{array}{l} u_D \\ \text{ux and } u_D \\ u'_x \text{ and } u_D \end{array} \begin{bmatrix} u_D \\ \hline u_D \\ \hline u_D \end{bmatrix} = \left[\begin{array}{ccccccc} 2.05 & 1.13 & -13.2 & -0.045 & -0.133 & -0.27 & 0.0 \\ \hline 1.37 & 0.92 & -7.73 & 0.75 & -0.14 & 0.88 & 19.75 \\ \hline 1.52 & 0.99 & -9.3 & 0.76 & -0.14 & 0.9 & 18.8 \end{array}\right]$$

$$[\Delta\delta \quad \Delta\omega \quad \Delta\psi_{fd} \quad \Delta E_x \quad \Delta\cos\alpha_R \quad \Delta\cos\alpha_I \quad u_x \text{ or } u'_x]^t \qquad (4.19)$$

The nonlinear test of section 4.3 with the same disturbance is applied to this system but with a fault duration reduced to 0.05 sec. and line reclosure at 0.25 sec. after the fault occurrence. The nonlinear system response is summarized in Figures 4.11 to 4.16. Figure 4.11 indicates that in the first two cases, where u_x and u'_x respectively are applied, the system is unstable despite the fact that the corresponding

eigenvalues are stable. This clearly demonstrates the necessity of nonlinear tests and that eigenvalue analysis, although necessary, is not sufficient. Although the dc control signal u_D is more effective than the excitation controls, it is not sufficient by itself to maintain stability. The system's response with combined excitation and dc controls is much better and the two responses with u_x or u'_x controls are very close whether the excitation control signal is modified or not. The terminal voltage variations, Figure 4.13, are more pronounced in cases 1 and 2 and the voltage oscillation continues after the line is restored whereas the terminal voltage approaches its steady state value asymptotically after 0.35 sec. in cases 3,4 and 5. Figures 4.14 and 4.15 show the variation of transmitted power over the dc and ac lines respectively. In cases 1 and 2 the dc link is operating under constant current control and the dc power is nearly constant about, the original value, 0.335 p.u. while the ac power is changing widely after line reclosure. In cases 4 and 5 the dc line picks up the power lost by the ac line and returns to rated value when the line is reclosed. In the mean time the ac line is transmitting the rated power. A similar behaviour is noted in case 3 up to a point where the ac power starts to drop again and the dc line picks up the difference. The dc control effort in cases 4 and 5 is smaller than case 3 as shown in Figure 4.16. The control stays at limit values, $\pm$ 0.25, for about 0.3 sec. then decreases rapidly and approaches zero asymptotically.

It is concluded from the above discussion that a combined dc and excitation control scheme is the best for the dc/ac parallel system with slightly better results for u_D and u'_x than u_D and u_x controls.

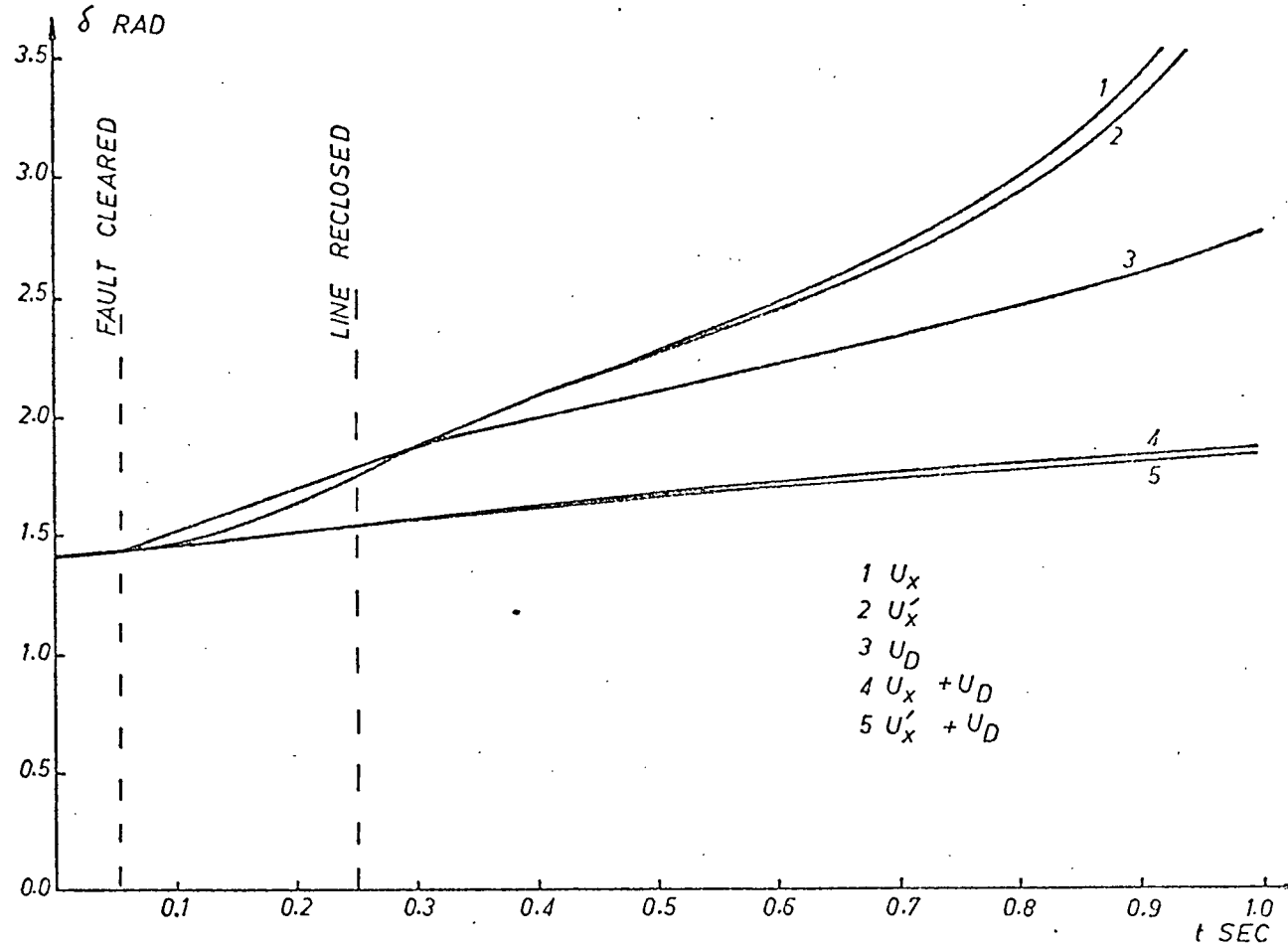

Fig. 4.11 Swing Curves for Expanded System

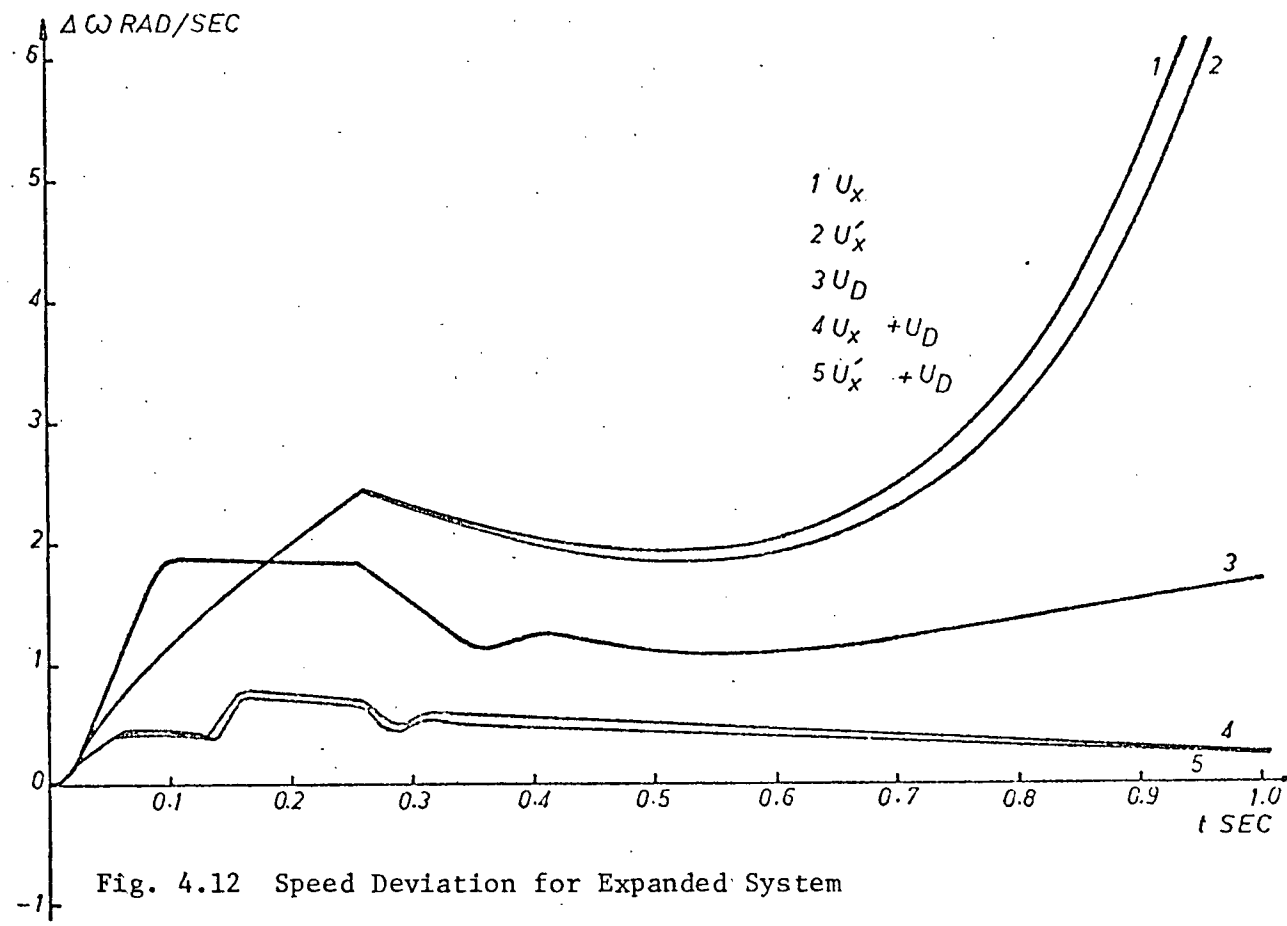

Fig. 4.12 Speed Deviation for Expanded System

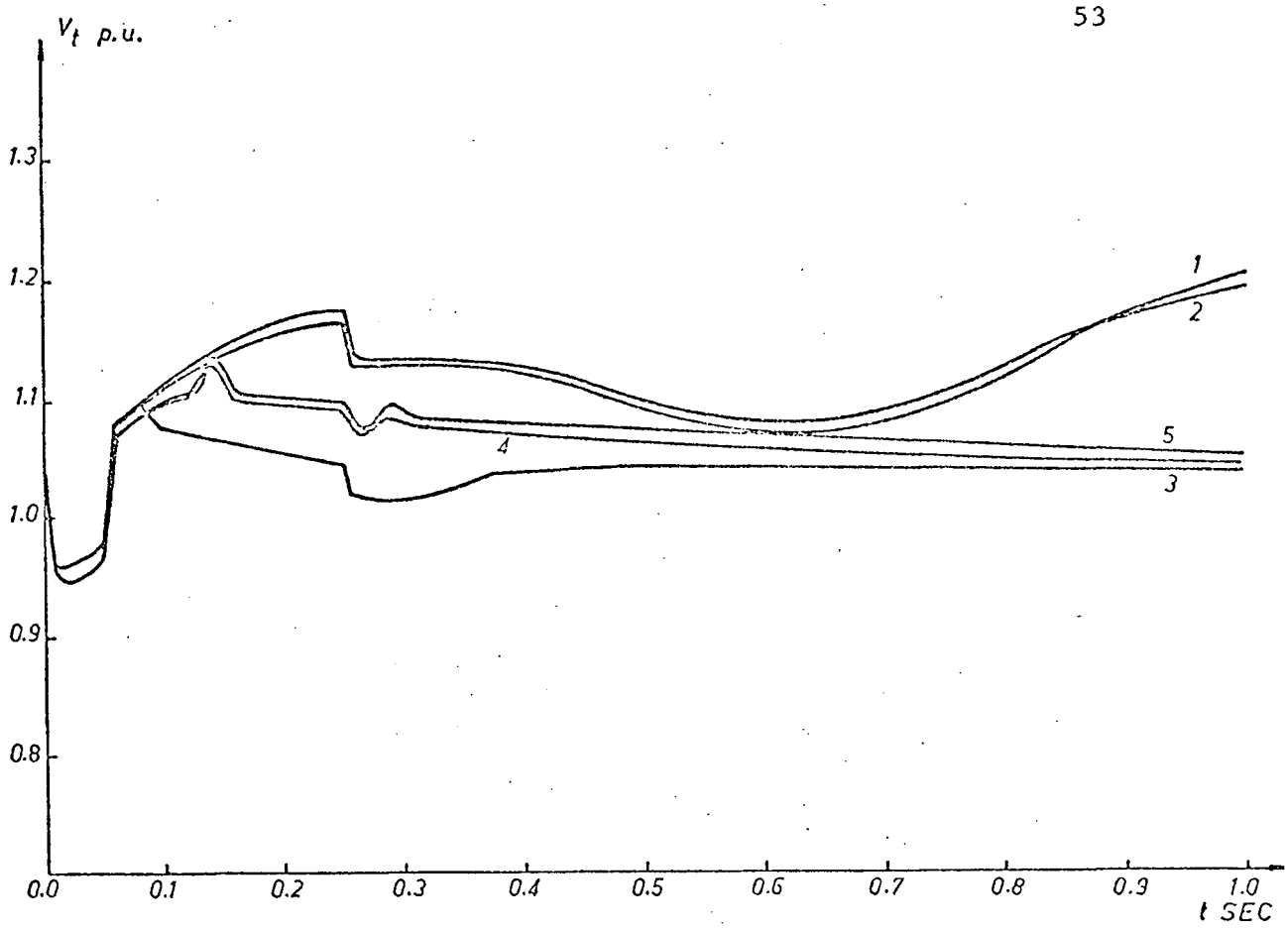

Fig. 4.13 Terminal Voltage Variations for Expanded System

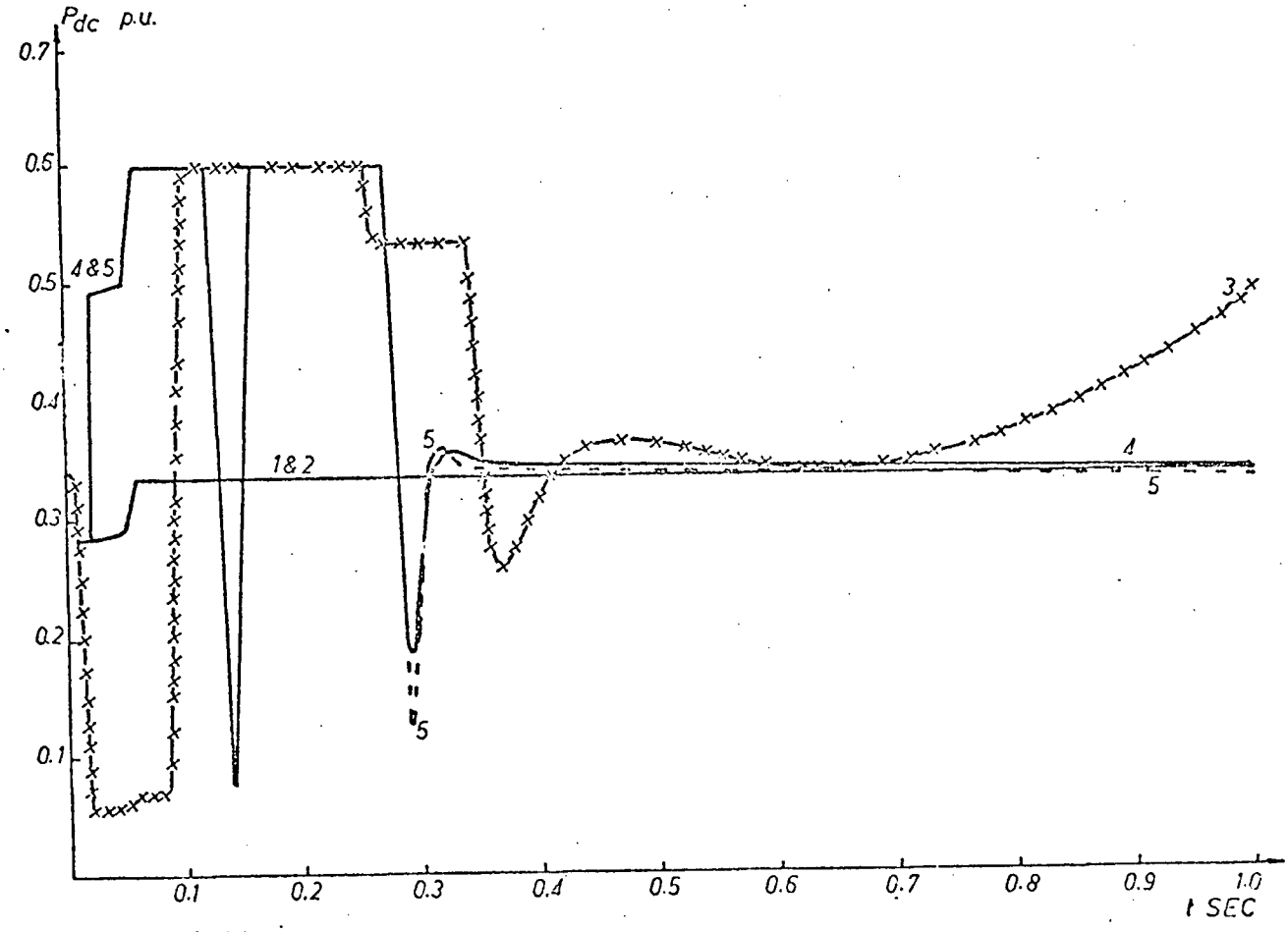

Fig. 4.14 Variation of DC Power for Expanded System

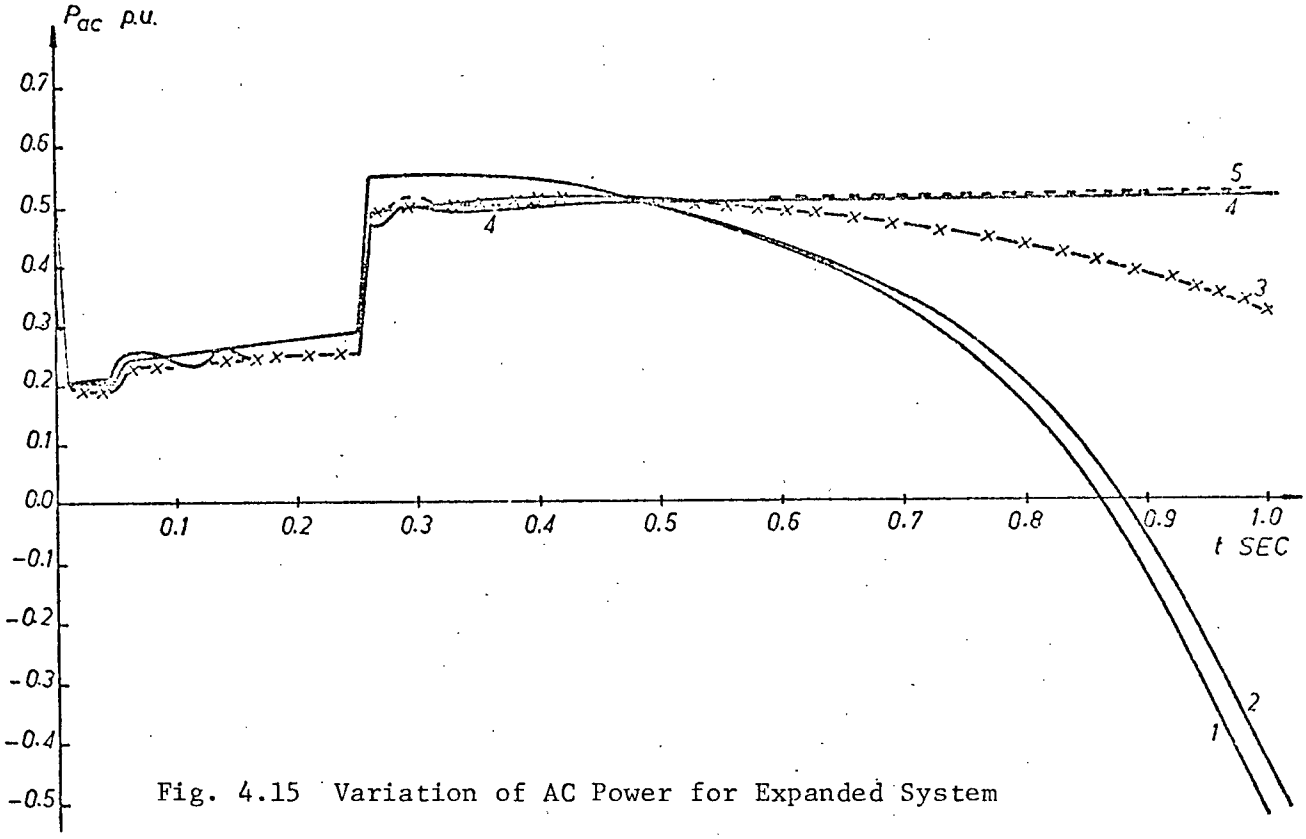

Fig. 4.15 Variation of AC Power for Expanded System

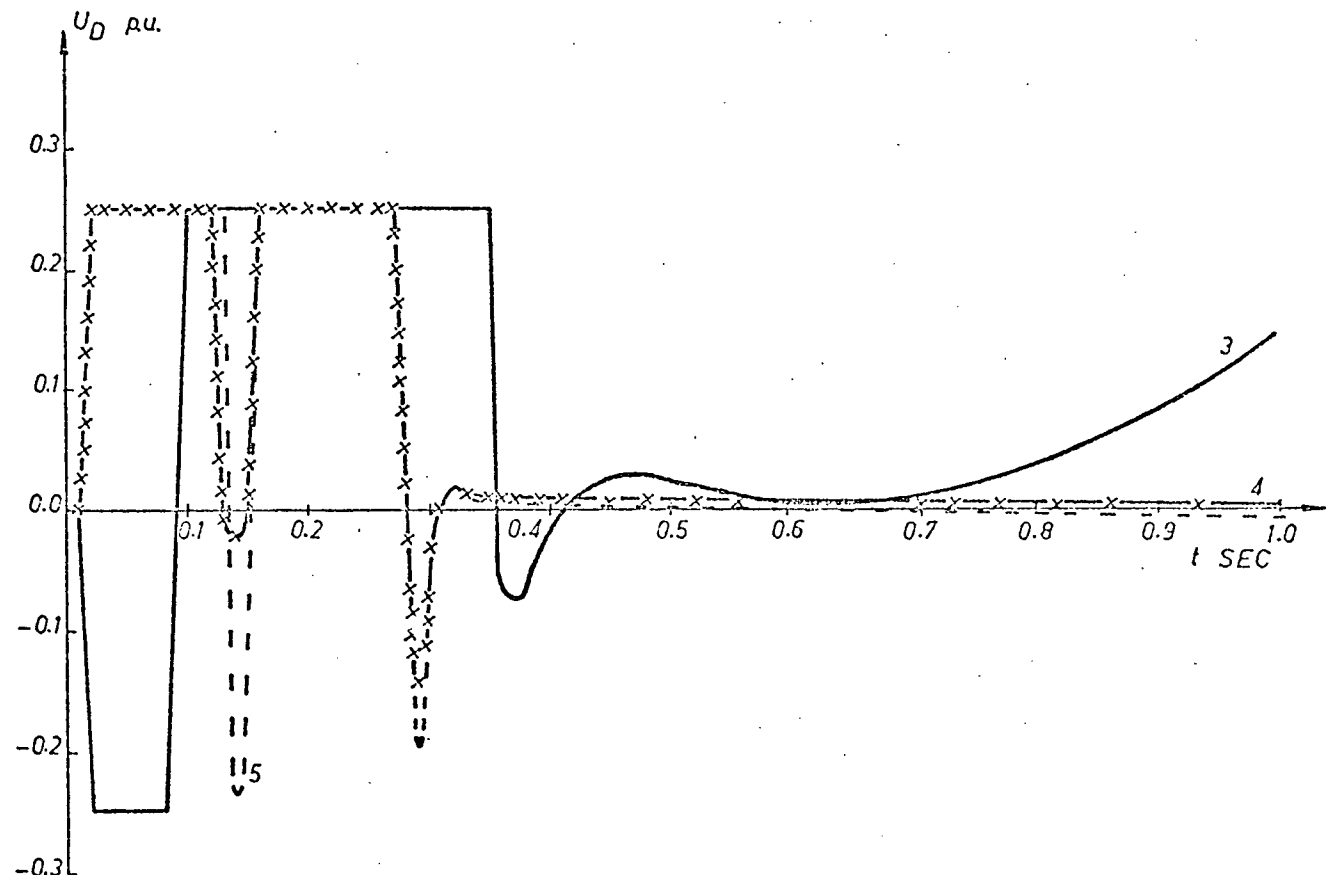

Fig. 4.16 Control Effort for Expanded System

5. MULTITERMINAL HVDC SYSTEMS

All hvdc systems designed so far have been restricted to the two-terminal operation in which power is transmitted over an hvdc link from system A to system B. However, hvdc need not be so limited and can be readily extended to the multi-terminal operation. In this and the next Chapter the operation and control of a three terminal dc link in conjunction with a delta connected ac system are studied. Two operation modes are considered; two rectifiers and one inverter or one rectifier and two inverters. The ac system is either a two-machine infinite system or a three-machine system. The equations describing system dynamics and the determination of the operating point are given in this chapter.

5.1 Operation and Control of Multiterminal DC Lines

As partly explained in Chapter 2 the normal operation mode of a two-terminal dc line is to control the currents of both the rectifier and inverter with identical current orders but giving the inverter a current margin signal of a polarity opposite to the current order. The inverter is normally operating on constant extinction angle control which maintains a minimum safe angle of advance and a maximum dc line voltage while the line current is regulated by the delay angle α_R. The current control will be taken over by the inverter only if the rectifier is unable to provide the ordered current at its minimum delay angle.

The same principles of operation can be adopted without change for a tapped dc line with two rectifiers and one inverter. The inverter current order is the algebraic sum of the two rectifiers' current orders plus the current margin. However, the same policy can not be applied

to the case of one rectifier and two inverters. If both inverters were on constant extinction angle control there would only be one ratio of power flow between the two receiving stations. For this reason one of the inverters and the rectifier are given specific current orders while the second inverter regulates the dc line voltage[37]. The difference between these two current orders minus the current margin is applied to the second inverter's current override control. Changing the current order of the first inverter without changing the rectifier's current order would result in current transfer between the two inverters. An alternative control policy was also proposed[40] where constant extinction angle control is applied at more than one inverter. It is argued that the first control method has the disadvantage that reactive power compensation must be provided for constant current operation at all but one of the converter stations whereas the second method improves this situation. In the second method the desired power flow can be achieved by adjusting the ac voltages at the inverter stations by means of tap changer control. In this chapter the first control method is adopted.

5.2 System Equations

The system to be studied is given in Figure 5.1, consisting of a tapped dc line superimposed on a delta connected ac network. Bus number 3 is an infinite system which will be replaced by a small generator for later studies. There are in general three converter stations where converter station 1 is always operated as a rectifier and that of station 2 always as an inverter. As for converter station 3 it is operated either as a rectifier or as an inverter depending on which cases are studied. The system is modelled in general as follows; the

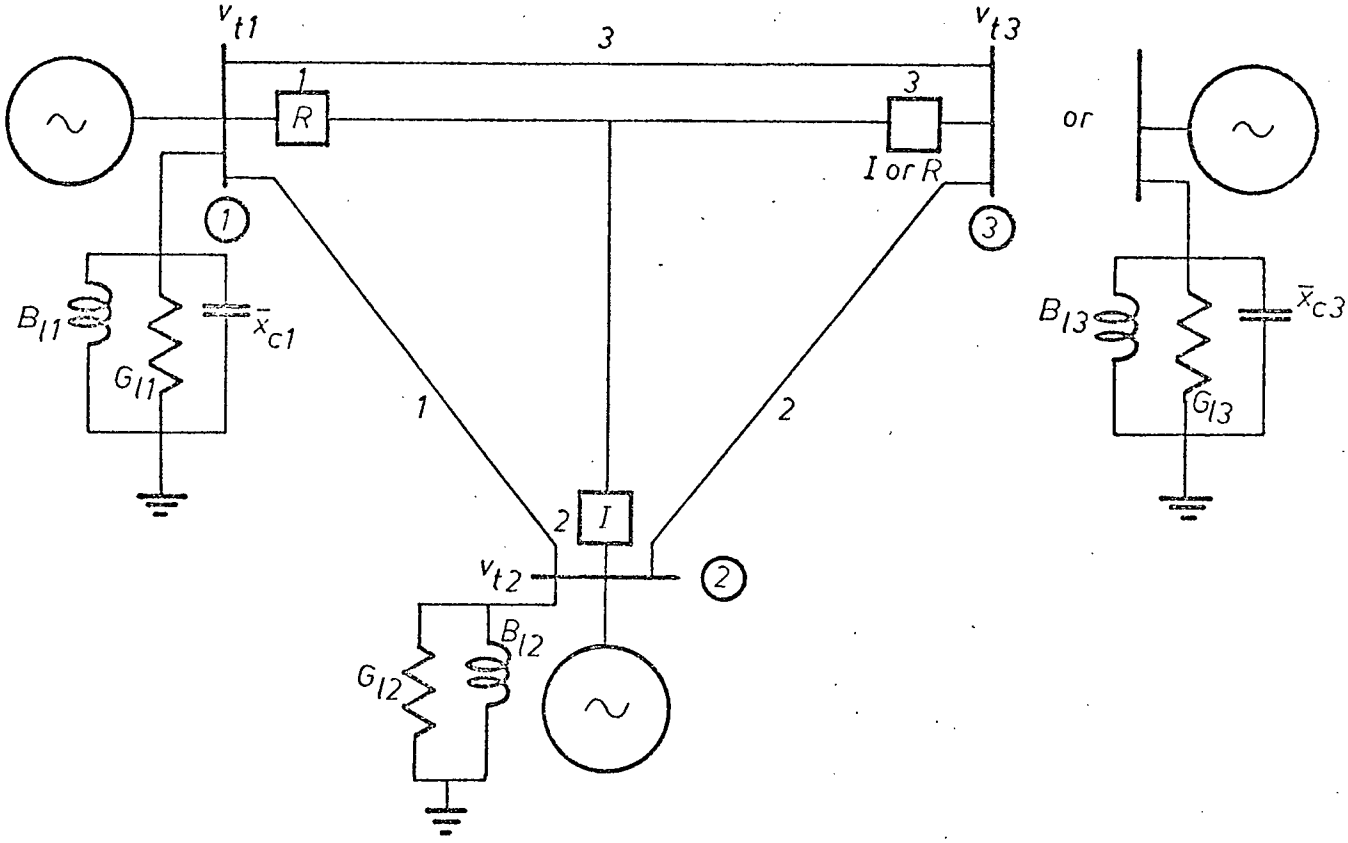

Fig 5.1 THREE-TERMINAL DC/AC POWER SYSTEM

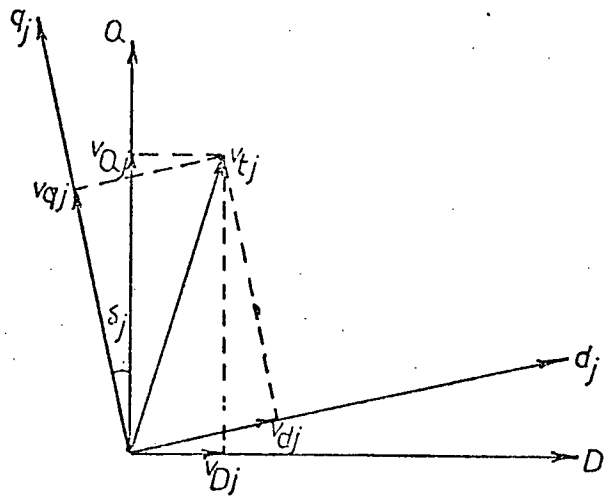

Fig. 5.2 TRANSFORMATION BETWEEN COMMON AND INDIVIDUAL MACHINE FRAMES

synchronous machines are represented by third order models with single time lag voltage regulators. Converter controls are also represented by single time lags. The transmission network is represented by static impedances and the ac harmonic filters are not considered but the condensers supplying the required reactive power are included. The system state equations are given by

$$p\delta_j = \Delta\omega_j \ , \quad p\Delta\omega_j = \frac{\omega_e}{2H_j} \ (P_{mj} - P_{ej})$$

$$p\psi_{fdj} = \omega_e \ r_{fdj} \ (\frac{E_{xj}}{x_{adj}} - i_{fdj})$$

$$pE_{xj} = \frac{1}{T_{rj}} \ [K_{rj} \ (V_{refj} - v_{tj}) - E_{xj}] \qquad (5.1)$$

$$p\cos\alpha_{Rj} = \frac{K_{Rj}}{T_{Rj} v_{tj}} \ (I_{refj} - I_{Rj})$$

$$p\cos\alpha_{Ij} = \frac{1}{T_{Ij}} \ [-\cos\alpha_{Ij} - \cos\Delta_{oj} + \frac{1}{v_{tj}} \ (\frac{2}{\sqrt{3}} \ x_{coj} \ I_{Ij} + e_{cIj})]$$

where

$$e_{cIj} = K_{Ij} \ (k_j \ I_{refj} - I_{Ij})$$

$$k_j = 1 \text{ for constant current control} \qquad (5.2)$$

$$< 1 \text{ for constant extinction angle control}$$

where the subscript j indicates the unit number.

For a multi-machine power system study a common reference frame (D,Q) must be chosen[53]. This frame is rotating at the synchronous speed. The individual machine angle δ_j is defined as the angle between the quadrature axis q_j of the individual machine with respect to the quadrature axis Q of the common frame. The transformation between the D,Q and the individual d_j, q_j frames is given by

$$\begin{bmatrix} F_{Dj} \\ F_{Qj} \end{bmatrix} = \begin{bmatrix} \cos\delta_j & -\sin\delta_j \\ \sin\delta_j & \cos\delta_j \end{bmatrix} \cdot \begin{bmatrix} f_{dj} \\ f_{qj} \end{bmatrix} \tag{5.3}$$

$$\begin{bmatrix} f_{dj} \\ f_{qj} \end{bmatrix} = \begin{bmatrix} \cos\delta_j & \sin\delta_j \\ -\sin\delta_j & \cos\delta_j \end{bmatrix} \cdot \begin{bmatrix} F_{Dj} \\ F_{Qj} \end{bmatrix}$$

where f_j can be either voltage or current.

The synchronous machine quantities referred to individual dq frames are given by

$$P_{ej} = \psi_{dj}\ i_{qj} - \psi_{qj}\ i_{dj}$$

$$v_{tj}^2 = v_{dj}^2 + v_{qj}^2$$

$$\begin{bmatrix} \psi_{dj} \\ \psi_{qj} \\ i_{dj} \\ i_{qj} \\ i_{fdj} \end{bmatrix} = \begin{bmatrix} c_{1j} & c_{2j} & c_{3j} \\ -c_{2j} & c_{4j} & -c_{5j} \\ -c_{6j} & -c_{7j} & c_{8j} \\ c_{9j} & -c_{6j} & c_{10j} \\ -c_{10j} & -c_{8j} & c_{11j} \end{bmatrix} \cdot \begin{bmatrix} v_{dj} \\ v_{qj} \\ \psi_{fdj} \end{bmatrix} \tag{5.4}$$

where coefficients c_{1j} to c_{11j} are given in equation (3.28).

Next, the local loads and capacitor currents are given by

$$\begin{bmatrix} i_{d\ell j} \\ i_{q\ell j} \end{bmatrix} = \begin{bmatrix} G_{\ell j} & -B_{\ell j} \\ B_{\ell j} & G_{\ell j} \end{bmatrix} \cdot \begin{bmatrix} v_{dj} \\ v_{qj} \end{bmatrix} \tag{5.5}$$

$$\begin{bmatrix} i_{cdj} \\ i_{cqj} \end{bmatrix} = \frac{1}{x_{cj}} \begin{bmatrix} -v_{qj} \\ v_{dj} \end{bmatrix} \tag{5.6}$$

and the currents transmitted over line ℓ connecting busses j and k are

given in DQ coordinates by

$$\begin{bmatrix} i_{Dj\ell} \\ i_{Qj\ell} \\ i_{Dk\ell} \\ i_{Qk\ell} \end{bmatrix} = \begin{bmatrix} a_{1\ell} & a_{2\ell} & a_{3\ell} & -a_{4\ell} \\ -a_{2\ell} & a_{1\ell} & a_{4\ell} & a_{3\ell} \\ a_{3\ell} & -a_{4\ell} & a_{1\ell} & -a_{2\ell} \\ a_{4\ell} & a_{3\ell} & -a_{2\ell} & a_{1\ell} \end{bmatrix} \cdot \begin{bmatrix} v_{Dj} \\ v_{Qj} \\ v_{Dk} \\ v_{Qk} \end{bmatrix} \qquad (5.7)$$

where a_1 to a_4 are the transmission line coefficients given in equation (3.7).

Substituting (5.3) into (5.7) yields

$$\begin{bmatrix} i_{dj\ell} \\ i_{qj\ell} \\ i_{dk\ell} \\ i_{qk\ell} \end{bmatrix} = \begin{bmatrix} a_{1\ell} & a_{2\ell} & (a_{3\ell}\cos\delta_{jk} + a_{4\ell}\sin\delta_{jk}) & (a_{3\ell}\sin\delta_{jk} - a_{4\ell}\cos\delta_{jk}) \\ -a_{2\ell} & a_{1\ell} & -(a_{3\ell}\sin\delta_{jk} - a_{4\ell}\cos\delta_{jk}) & (a_{3\ell}\cos\delta_{jk} + a_{4\ell}\sin\delta_{jk}) \\ (a_{3\ell}\cos\delta_{jk} - a_{4\ell}\sin\delta_{jk}) & -(a_{3\ell}\sin\delta_{jk} + a_{4\ell}\cos\delta_{jk}) & a_{1\ell} & a_{2\ell} \\ (a_{3\ell}\sin\delta_{jk} + a_{4\ell}\cos\delta_{jk}) & (a_{3\ell}\cos\delta_{jk} - a_{4\ell}\sin\delta_{jk}) & -a_{2\ell} & a_{1\ell} \end{bmatrix}$$

$$\cdot [v_{dj} \quad v_{qj} \quad v_{dk} \quad v_{qk}]^t \qquad (5.8)$$

The dc voltages and currents are determined from

$$\sum_{j=1}^{r} I_{Rj} = \sum_{k=1}^{v} I_{Iv}$$

$$V_{Rj} = \frac{3\sqrt{3}}{\pi} v_{tj} \cos\alpha_{Rj} - \frac{3}{\pi} x_{coj} I_{Rj} \qquad j = 1, 2, \ldots, r$$

$$V_{Ij} = \frac{3\sqrt{3}}{\pi} v_{tj} \cos\alpha_{Ij} - \frac{3}{\pi} x_{coj} I_{Ij} \qquad j = 1, 2, \ldots, v$$

$$V_{Rj} = V_b + 2R_j I_{Rj} \qquad j = 1, 2, \ldots, r$$

$$V_{Ij} = -V_b + 2R_j I_{Ij} \qquad j = 1, 2, \ldots, v \tag{5.9}$$

The formulation is rather in general where r is the number of rectifiers, v is the number of inverters, and V_b is the voltage at the tapping point.

For the three-terminal system with rectifier stations 1 and 3, and inverter station 2, the solution of (5.9) becomes

$$\begin{bmatrix} V_{R1} \\ V_{I2} \\ V_{R3} \\ I_{R1} \\ I_{I2} \\ I_{R3} \end{bmatrix} = \begin{bmatrix} d_1 & -d_2 & d_3 \\ -d_4 & d_5 & -d_6 \\ d_7 & -d_8 & d_9 \\ d_{10} & d_{11} & -d_{12} \\ d_{11} & d_{13} & d_{14} \\ -d_{12} & d_{14} & d_{15} \end{bmatrix} \cdot \begin{bmatrix} v_{t1} & \cos\alpha_{R1} \\ v_{t2} & \cos\alpha_{I2} \\ v_{t3} & \cos\alpha_{R3} \end{bmatrix} \tag{5.10}$$

On the other hand for rectifier station 1 and inverter stations 2 and 3, the solution becomes

$$\begin{bmatrix} V_{R1} \\ V_{I2} \\ V_{I3} \\ I_{R1} \\ I_{I2} \\ I_{I3} \end{bmatrix} = \begin{bmatrix} d_1 & -d_2 & -d_3 \\ -d_4 & d_5 & d_6 \\ -d_7 & d_8 & d_9 \\ d_{10} & d_{11} & d_{12} \\ d_{11} & d_{13} & -d_{14} \\ d_{12} & -d_{14} & d_{15} \end{bmatrix} \begin{bmatrix} v_{t1} & \cos\alpha_{R1} \\ v_{t2} & \cos\alpha_{I2} \\ v_{t3} & \cos\alpha_{I3} \end{bmatrix} \tag{5.11}$$

where

$$\begin{bmatrix} d_1 \\ d_2 \\ d_3 \\ d_4 \\ d_5 \\ d_6 \\ d_7 \\ d_8 \\ d_9 \\ d_{10} \\ d_{11} \\ d_{12} \\ d_{13} \\ d_{14} \\ d_{15} \end{bmatrix} = \frac{3\sqrt{3}}{R_E} \begin{bmatrix} R_{E2}\ R_{E3} + 2R_1\ (R_{E2} + R_{E3}) \\ 3/\pi\ x_{co1}\ R_{E3} \\ 3/\pi\ x_{co1}\ R_{E2} \\ 3/\pi\ x_{co2}\ R_{E3} \\ R_{E1}\ R_{E3} + 2R_2\ (R_{E1} + R_{E3}) \\ 3/\pi\ x_{co2}\ R_{E1} \\ 3/\pi\ x_{co3}\ R_{E2} \\ 3/\pi\ x_{co3}\ R_{E1} \\ R_{E1}\ R_{E2} + 2R_3\ (R_{E1} + R_{E2}) \\ R_{E2} + R_{E3} \\ R_{E3} \\ R_{E2} \\ R_{E1} + R_{E3} \\ R_{E1} \\ R_{E1} + R_{E2} \end{bmatrix} \qquad (5.12)$$

and $R_{Ej} = 2R_j + \frac{3}{\pi}\ x_{coj} \qquad j = 1, 2, 3$

$$R_E = R_{E1}\ (R_{E2} + R_{E3}) + R_{E2}\ R_{E3}$$

Finally the current components referred to individual machine frame are given by

$$\begin{bmatrix} I_{dj} \\ I_{qj} \end{bmatrix} = \frac{2\sqrt{3}}{\pi}\ I_{dcj} \begin{bmatrix} \sin\delta_{Rj} & \cos\delta_{Rj} \\ \cos\delta_{Rj} & -\sin\delta_{Rj} \end{bmatrix} \cdot \begin{bmatrix} \cos\phi_{Rj} \\ \sin\phi_{Rj} \end{bmatrix} \quad j = 1, 2, 3 \qquad (5.13)$$

where $\delta_{Rj} = \arctan (v_{dj}/v_{qj})$

$$\cos\phi_{Rj} = \frac{\pi}{3\sqrt{3}} \frac{V_{dcj}}{v_{tj}}$$

$$\sin\phi_{Rj} = \pm \sqrt{1 - \cos^2\phi_{Rj}}$$

Of $\sin \Phi_{Rj}$ the positive sign is used for rectifiers and the negative sign for inverters. The terminal voltage components v_{dj} and v_{qj} are determined from

$$\begin{aligned} i_{dj} &= i_{d\ell j} + i_{cdj} + \sum_{\ell} i_{dj\ell} + I_{dj} \\ i_{qj} &= i_{q\ell j} + i_{cqj} + \sum_{\ell} i_{qj\ell} + I_{qj} \end{aligned} \tag{5.14}$$

5.3 Initial Conditions

Given the terminal voltages v_{tj}, j = 1, 2, 3, the generator output powers P_1 and P_2, the dc power P_{dc1} and the minimum extinction angles Δ_{oj} for inverters the system's operating point is determined as follows:

For one rectifier and two inverters operation equation (5.1) gives

$$\cos\alpha_{I2} = -\cos\Delta_{o2} + \frac{2}{\sqrt{3}} \frac{x_{co2}}{v_{t2}} I_{I2} \tag{5.15}$$

$$\cos\alpha_{I3} = -\cos\Delta_{o3} + \frac{2}{\sqrt{3}} \frac{x_{co3}}{v_{t3}} I_{I3} \tag{5.16}$$

For two rectifiers and one inverter operation, where the rectifier's current ratio is given as x, equation (5.16) is replaced by

$$I_{R1} = x\, I_{R3} \tag{5.17}$$

Let the dc power be given as

$$P_{dc1} = \frac{2}{3} V_{R1} I_{R1} \tag{5.18}$$

Then the dc voltages, currents and firing angles can be determined by substituting equations (5.15), (5.16) or (5.17) and (5.18) into (5.10) or (5.11). Substituting the results into (5.13) the dc current components I_{dj} and I_{qj} are given in terms of v_{dj} and v_{qj}.

Choosing the common reference frame (D,Q) to coincide with (d_3,q_3) the angle δ_3 is equal to zero. From the given powers P_1 and P_2 one has

$$\psi_{fdj} = \frac{P_j + c_{6j} v_{tj}^2 + (c_{7j}-c_{9j}) v_{dj} v_{qj}}{(c_{8j} v_{dj} + c_{10j} v_{qj})} \qquad j = 1, 2 \qquad (5.19)$$

Since v_{dj} can be expressed in terms of v_{qj} and the terminal voltages v_{tj}, substituting (5.4), (5.5), (5.6), (5.8), (5.13) and (5.19) into (5.15) v_{qj}, j = 1, 2, 3, δ_1, δ_2 and ψ_{fd3} can be solved.

5.4 Numerical Example

The system studied is basically the same for all four cases. The only differences are the operating points and loading conditions.

Synchronous machines 1 and 2 are identical of the same capacity, synchronous machine 3 is a smaller machine which has a capacity of only one third of either of the two. The machines have the following per unit data

x''_d = (0.09, 0.09, 0.54) p.u. $\quad x_d$ = (1.28, 1.28, 4.5) p.u.

x''_q = (0.13, 0.13, 0.6) p.u. $\quad x_q$ = (0.8, 0.8, 3.8) p.u.

x'_d = (0.18, 0.18, 0.69) p.u. $\quad x_{\ell a}$ = (0.1, 0.1, 0.35) p.u.

T'_{do} = (2.5, 2.5, 2.3) sec. $\quad T''_{do}$=(0.018, 0.018, 0.0192) sec

T''_{qo} = (0.011, 0.011, 0.0117) sec. H = (4.0, 4.0, 1.33) sec.

r_a = (0.0097, 0.0097, 0.1008) p.u.

The ac transmission lines have the following constants

$r = (0.0364, 0.03185, 0.0455)$ p.u. $\quad x_\ell = (0.905, 0.79, 1.13)$ p.u.

$x_c = (16.05, 18.35, 12.85)$ p.u.

All dc lines are assumed of equal length and have the same parameters

$R = 0.0432$ p.u. and $X_c = 64.2$ p.u.

The commutation reactances are $x_{co} = (0.3, 0.3, 0.21)$ p.u.

The voltage regulators are assumed identical and also the converter control parameters are assumed similar:

$K_r = 20$, $T_r = 2$ sec., $K_R = 30$, $T_R = 0.002778$ sec., $k = 0.9$

The local loads and shunt capacitors for two rectifiers - one inverter case are given by

$G_\ell = (0.145, 1.9, 0.17)$p.u. $\quad B_\ell = -(0.09, 0.04, 0.02)$ p.u.

$\frac{1}{x_c} = (0.088, 0.0, 0.0795)$

The operating conditions for the two rectifiers and one inverter system are given by

$v_t = (1.03, 1.0, 1.02)$ p.u. $\quad P = (0.96, 0.975, 0.325)$ p.u.

$Q = (0.213, 0.323, 0.033)$ p.u. $\quad P_{dc} = (0.197, -0.371, 0.186)$ p.u.

$Q_{dc} = (0.093, -0.178, 0.083)$ p.u. $\quad P_{ac} = (0.393, -0.173, -0.212)$ p.u.

$Q_{ac} = (0.114, -0.011, 0.011)$ p.u. $\quad \delta = (0.21, -0.515, 0.0)$ rad.

$\delta_R = (0.553, 0.55, 0.799)$ rad. $\quad \psi_{fd} = (1.121, 1.119, 1.026)$ p.u.

$\psi_d = (0.883, 0.859, 0.731)$ p.u. $\quad \psi_q = -(0.548, 0.53, 0.756)$ p.u.

$v_d = (0.541, 0.522, 0.731)$ p.u. $\quad v_q = (0.876, 0.853, 0.711)$ p.u.

$E_x = (1.735, 1.864, 1.861)$ p.u. $\quad V_{ref} = (1.117, 1.093, 1.113)$ p.u.

$P_m = (0.969, 0.985, 0.335)$ p.u. $\quad \cos\alpha = (0.936, -0.837, 0.933)$

$V_{dc} = (1.54, -1.49, 1.54)$ p.u. $\quad I_{dc} = (0.192, 0.373, 0.181)$

For the one rectifier and two inverters system the local loads and shunt capacitors are given by

$$G_\ell = (0.145, 1.55, 0.5) \text{ p.u.} \qquad B_\ell = -(0.09, 0.7, 0.2) \text{ p.u.}$$

$$\frac{1}{\bar{x}_c} = (0.13, 0.0, 0.0) \text{ p.u.}$$

and the other operating conditions are

$v_t = (1.04, 1.01, 1.0)$ p.u. $\quad P = (0.96, 0.975, 0.322)$ p.u.

$Q = (0.134, 0.678, 0.08)$ p.u. $\quad P_{dc} = (0.371, -0.184, -0.177)$ p.u.

$Q_{dc} = (0.141, -0.069, -0.061)$ p.u. $\quad P_{ac} = (0.292, -0.136, -0.139)$ p.u.

$Q_{ac} = (0.046, -0.002, -0.033)$ p.u. $\quad \delta = (0.124, -0.492, 0.0)$ rad.

$\delta_R = (0.569, 0.457, 0.738)$ rad. $\quad \psi_{fd} = (1.109, 1.227, 1.076)$ p.u.

$\psi_d = (0.883, 0.912, 0.759)$ p.u. $\quad \psi_q = -(0.566, 0.456, 0.7)$ p.u.

$v_d = (0.561, 0.446, 0.672)$ p.u. $\quad v_q = (0.876, 0.906, 0.74)$ p.u.

$E_x = (1.659, 2.229, 2.002)$ p.u. $\quad V_{ref} = (1.123, 1.121, 1.1)$ p.u.

$P_m = (0.968, 0.988, 0.333)$ p.u. $\quad \cos\alpha = (0.9925, -0.9054, -0.9248)$

$V_{dc} = (1.608, -1.563, -1.564)$ p.u. $\quad I_{dc} = (0.346, 0.1765, 0.1695)$ p.u.

6. LINEAR OPTIMAL CONTROL FOR MULTITERMINAL DC/AC SYSTEMS

In this chapter linear optimal control signals are designed for the three-terminal system described in Chapter 5. Two systems are investigated; a two-machine infinite system, and a three-machine system. For each system two modes of operation are studied; two rectifiers and one inverter, and one rectifier and two inverters. Four control schemes are tested for each case. Firstly, optimal excitation control signals, u_E's, are applied to all machines. Secondly, optimal dc current control signals, u_D's, are applied to converters regulating dc current. Thirdly, an excitation control signal is applied to the machine connected to the converter station operating on constant extinction angle control and dc current control signals are applied to the rest of the converter stations. Finally all excitation and dc current control signals are applied simultaneously.

In designing the linear optimal regulator a performance function of the quadratic form must be chosen. Moussa and Yu[52] developed a method for determining the Q matrix with the dominant eigenvalue shift of the closed loop system. This technique was also applied to multimachine stabilization studies[53]. It was found from their results that weights must be given to $\Delta\omega$ and $\Delta\delta$ in order to obtain a very stable system. a limited number of diagonal matrices are tested with varying emphasis on the deviation of rotor angles δ, that of speed $\Delta\omega$, and the field flux linkages ψ_{fd}. The reason for giving weight on ψ_{fd} is mainly because of the dc lines involved and it was not necessary for ac lines alone. As for the weighing matrix R it is always taken as a unit matrix.

6.1 Two Machine-Infinite Bus System with Two Rectifiers and One Inverter

Converter stations 1 and 3 are operated as rectifiers while converter station 2 is operated as an inverter in this case. For the data given in Chapter 5 the linearized state equations for the system are given in eqn. (6.1).

The diagonal matrices Q and the nonzero elements of matrices B for different control schemes are given by

u_{E1}, u_{E2} : $Q = \text{diag}\{10, 100, 1, 1, 1, 10, 100, 1, 1, 1, 1\}$

$b_{4,1} = 10.0, \quad b_{9,2} = 10.0$

u_{D1}, u_{D3} : $Q = \text{diag}\{10, 1, 100, 1, 1, 10, 1, 100, 1, 1, 1\}$

$b_{5,1} = 10485.44, \quad b_{11,2} = 10588.23$ (6.2)

u_{D1}, u_{E2}, u_{D3} : $Q = \text{diag}\{10, 1, 100, 1, 1, 10, 1, 100, 1, 1, 1\}$

$b_{5,1} = 10485.44, \quad b_{9,2} = 10.0, \quad b_{11,3} = 10588.23$

$u_{E1}, u_{D1}, u_{E2}, u_{D3}$: $Q = \text{diag}\{10, 1, 10, 1, 1, 10, 1, 10, 1, 1, 1\}$

$b_{4,1} = 10.0, \quad b_{5,2} = 10485.44, \quad b_{9,3} = 10.0, \quad b_{11,4} = 10588.23$

and the corresponding control laws are given in eqn. (6.3). The system's eigenvalues are listed in Table VI.

A three-phase ground fault at the middle of one circuit of ac line 1 is used as a disturbance for the nonlinear tests to compare the different control schemes designed. The fault duration is 0.07 sec. followed by isolating the faulted line from both ends. The system responses are shown in Figures 6.1 to 6.7 for the following cases

case 0: no optimal control whatsoever.

case 1: optimal excitation controls for both machines.

case 2: optimal dc controls for rectifier stations 1 and 3.

$$
\begin{bmatrix}
\Delta\dot{\delta}_1 \\
\Delta\dot{\omega}_1 \\
\Delta\dot{\psi}_{fd1} \\
\Delta\dot{E}_{x1} \\
\Delta\dot{\cos\alpha}_{R1} \\
\Delta\dot{\delta}_2 \\
\Delta\dot{\omega}_2 \\
\Delta\dot{\psi}_{fd2} \\
\Delta\dot{E}_{x2} \\
\Delta\dot{\cos\alpha}_{I2} \\
\Delta\dot{\cos\alpha}_{R3}
\end{bmatrix}
=
\begin{bmatrix}
0.0 & 1.0 & 0.0 & 0.0 & 0.0 & 0.0 & 0.0 & 0.0 & 0.0 & 0.0 & 0.0 \\
-26.0 & 0.0 & -114.0 & 0.0 & -123.4 & 7.225 & 0.0 & -0.72 & 0.0 & -38.8 & 63.6 \\
-0.35 & 0.0 & -1.5 & 0.45 & -1.26 & 0.142 & 0.0 & 0.145 & 0.0 & -0.393 & 0.82 \\
0.405 & 0.0 & -6.58 & -0.5 & -0.434 & -0.369 & 0.0 & -0.87 & 0.0 & -0.145 & -0.769 \\
501.6 & 0.0 & -18991.0 & 0.0 & -33213.0 & 177.0 & 0.0 & 5075.5 & 0.0 & -11125.0 & 16942.0 \\
0.0 & 0.0 & 0.0 & 0.0 & 0.0 & 0.0 & 1.0 & 0.0 & 0.0 & 0.0 & 0.0 \\
20.98 & 0.0 & 22.42 & 0.0 & 17.07 & -53.9 & 0.0 & -151.4 & 0.0 & 43.89 & 68.0 \\
0.11 & 0.0 & 0.388 & 0.0 & 0.409 & -0.372 & 0.0 & -1.902 & 0.447 & 0.988 & 0.81 \\
0.617 & 0.0 & -0.834 & 0.0 & -1.26 & -1.099 & 0.0 & -6.55 & -0.5 & -2.89 & -0.501 \\
16.43 & 0.0 & 72.54 & 0.0 & 133.0 & -34.8 & 0.0 & -228.0 & 0.0 & -78.9 & -6.43 \\
1657.4 & 0.0 & 12689.0 & 0.0 & 21752.4 & 2339.4 & 0.0 & 11649.4 & 0.0 & -13772.0 & -35626.0
\end{bmatrix}
$$

$$
\cdot[\Delta\delta_1 \quad \Delta\omega_1 \quad \Delta\psi_{fd1} \quad \Delta E_{x1} \quad \Delta\cos\alpha_{R1} \quad \Delta\delta_2 \quad \Delta\omega_2 \quad \Delta\psi_{fd2} \quad \Delta E_{x2} \quad \Delta\cos\alpha_{I2} \quad \Delta\cos\alpha_{R3}]^t + BU \qquad (6.1)
$$

$$
\begin{bmatrix} u_{E1} \\ u_{E2} \\ \hline u_{D1} \\ u_{D3} \\ \hline u_{D1} \\ u_{E2} \\ u_{D3} \\ \hline u_{E1} \\ u_{D1} \\ u_{E2} \\ u_{D3} \end{bmatrix} = \begin{bmatrix} -38.4 & 6.37 & -60.4 & -2.48 & -0.023 & 21.4 & -1.01 & -3.53 & -0.057 & 0.285 & -0.003 \\ 5.66 & 3.38 & -3.53 & -0.057 & -0.004 & -40.6 & 6.84 & -88.4 & -2.93 & -1.04 & 0.015 \\ \hline 3.1 & 1.01 & -0.98 & 0.75 & -0.22 & -1.69 & -0.22 & -5.0 & 0.75 & -0.101 & -0.108 \\ -0.39 & -0.35 & 0.49 & 0.79 & -0.11 & -2.58 & -0.97 & -1.02 & 0.67 & 0.15 & -0.195 \\ \hline 2.63 & 1.05 & -3.3 & 0.41 & -0.22 & -1.09 & -0.26 & -2.41 & -0.04 & -0.086 & -0.108 \\ 0.51 & 0.02 & -1.42 & 0.51 & -0.4×10^{-4} & -0.77 & 0.12 & -9.81 & -1.32 & -0.004 & -0.3×10^{-5} \\ -0.76 & -0.31 & -1.4 & 0.53 & -0.109 & -2.11 & -0.998 & 0.93 & -0.003 & 0.16 & -0.195 \\ \hline -0.06 & 0.03 & -2.16 & -1.04 & -0.8×10^{-5} & -0.005 & -0.003 & -0.04 & -0.005 & -0.002 & 0.1×10^{-4} \\ 2.4 & 1.02 & -1.3 & -0.009 & -0.22 & -0.85 & -0.27 & -1.12 & -0.013 & -0.087 & -0.108 \\ 0.16 & 0.016 & -0.25 & -0.005 & -0.1×10^{-4} & -0.6 & 0.034 & -3.83 & -1.11 & 0.004 & 0.1×10^{-4} \\ -0.93 & -0.33 & 0.037 & 0.012 & -0.11 & -1.94 & -1.01 & 2.06 & 0.01 & 0.16 & -0.19 \end{bmatrix}
$$

$$
\cdot [\Delta\delta_1 \quad \Delta\omega_1 \quad \Delta\psi_{fd1} \quad \Delta E_{x1} \quad \Delta\cos\alpha_{R1} \quad \Delta\delta_2 \quad \Delta\omega_2 \quad \Delta\psi_{fd2} \quad \Delta E_{x2} \quad \Delta\cos\alpha_{I2} \quad \Delta\cos\alpha_{R3}]^t \qquad (6.3)
$$

Table VI Eigenvalues for 2 Machine-Infinite Bus, 2 Rectifiers System

Control used	Eigenvalues
no control	-53657.4, -15084.8, -177.3, -0.605±j1.35, -0.342±j4.77, -0.293±j6.81, -0.261±j1.83
u_{E1} , u_{E2}	-53657.4, -15084.8, -177.3, -15.74,-13.5, -7.45±j12.9, -6.16±j10.74, -0.35, -0.32
u_{D1} , u_{D3}	-54675, -18423, -162.1, -39.8, -22.95,-3.36, -3.16, -1.17±j2.1, -0.5±j1.58
u_{D1} , u_{E2} , u_{D3}	-54675, -18423, -162, -39.83,-22.96 -6.98, -5.95, -4.39, -3.37, -0.717 ± j1.7
u_{E1} , u_{D1} , u_{E2} , u_{D3}	-54675, -18423, -162, -39.44,-22.8, -9.6, -9.2, -3.76, -3.4, -2.39, -1.81

case 3: case 2 plus excitation control for the machine connected to inverter station 2.

case 4: case 1 plus case 2.

Figures 6.1 and 6.2 show that machine 1 loses stability but machine 2 remains stable when there is no optimal control signals, case 0. Next when excitation control signals are applied to both machines the stability of machine 1 is getting worse and machine 2 that was originally stable goes out of step, case 1. Still next where optimal dc controls are applied to rectifiers 1 and 3 the system is stable, case 2. Finally the system is stable and the responses are very close for both cases 3 and 4. The angle and speed deviations are less in case 2 than cases 3 and 4.

The changes in terminal voltages are shown in Figures 6.3 and 6.4. It is noted that at ac bus 1 the deviations are small for cases 2 and 3 with larger changes for cases 4, 0, and 1 respectively. For machine 2 the terminal voltage deviations, Figure 6.4, are smallest for case 4 followed by cases 2, 1, 3 and 0 respectively.

Figures 6.5 (a, b, c) show the changes in power transmitted over the dc transmission network. Consider case 0 first. The dc power drops for the first 0.07 sec. during the fault because of ac terminal voltages drops, and then returns to rated values. After 0.69 sec. the power carried by dc line 1 drops sharply for 0.1 sec., between approximately 0.69 and 0.79 sec., then continues to drop at a slower rate because of the deterioration of v_{t1} while the power carried by line 3 increases in a similar fashion because of drops in v_{t2} with v_{t3} remaining constant. But the total dc power is decreased. Consider case 1 next. The same pattern is noticed but with sharper drops in P_{dc1}

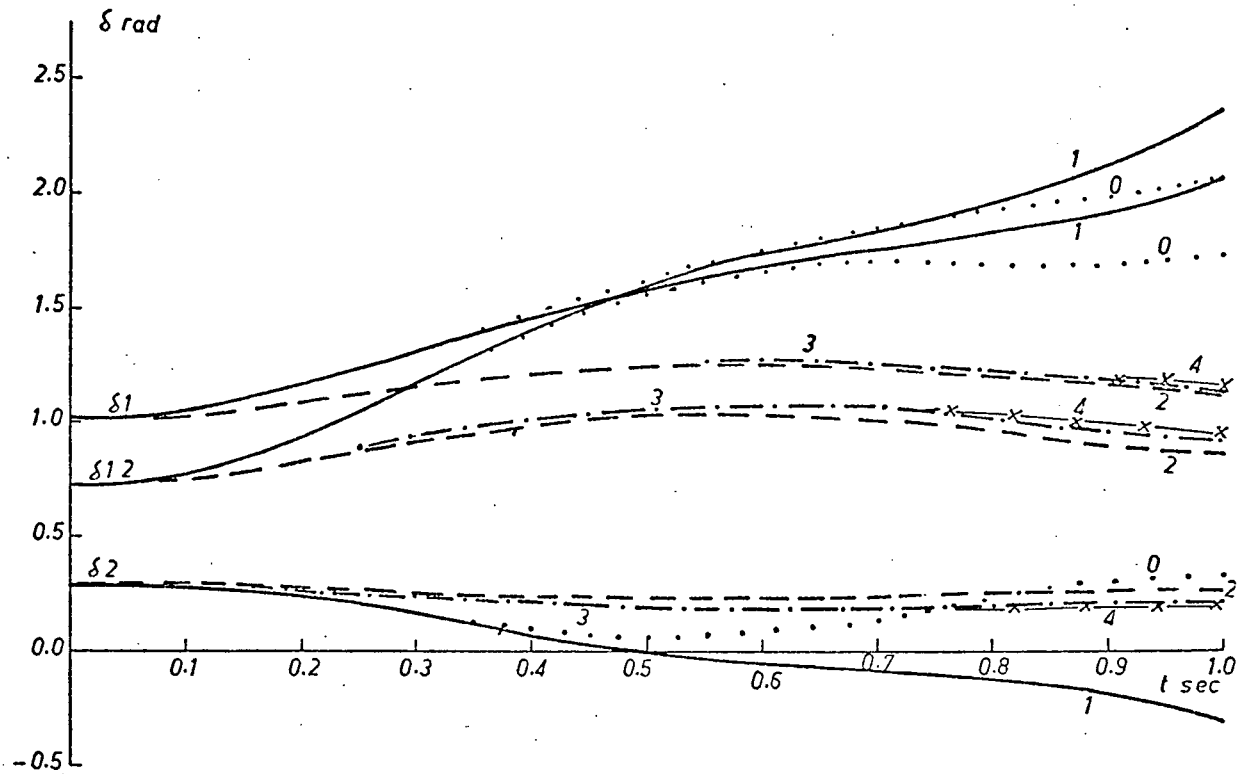

Fig. 6.1 Swing Curves for 2 Machine, 2 Rectifier System

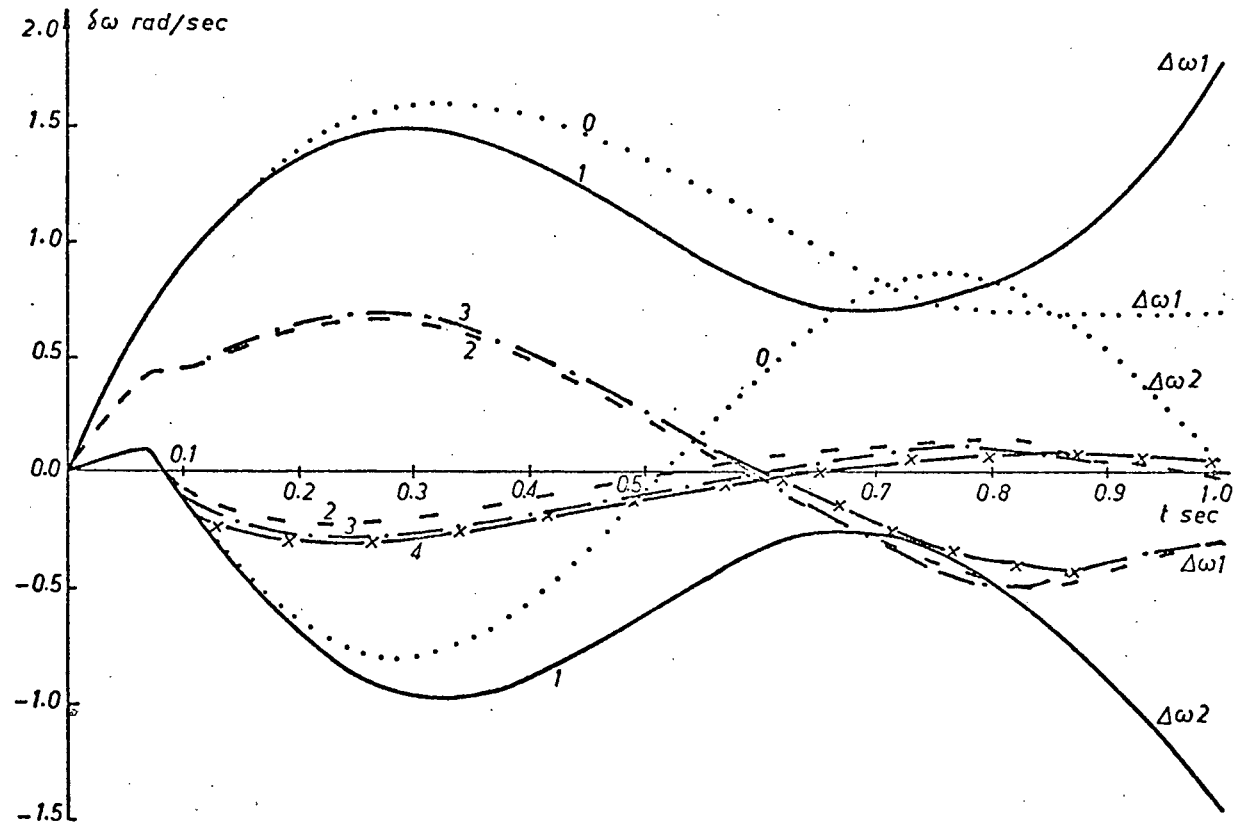

Fig. 6.2 Speed Deviation for 2 Machine, 2 Rectifier System

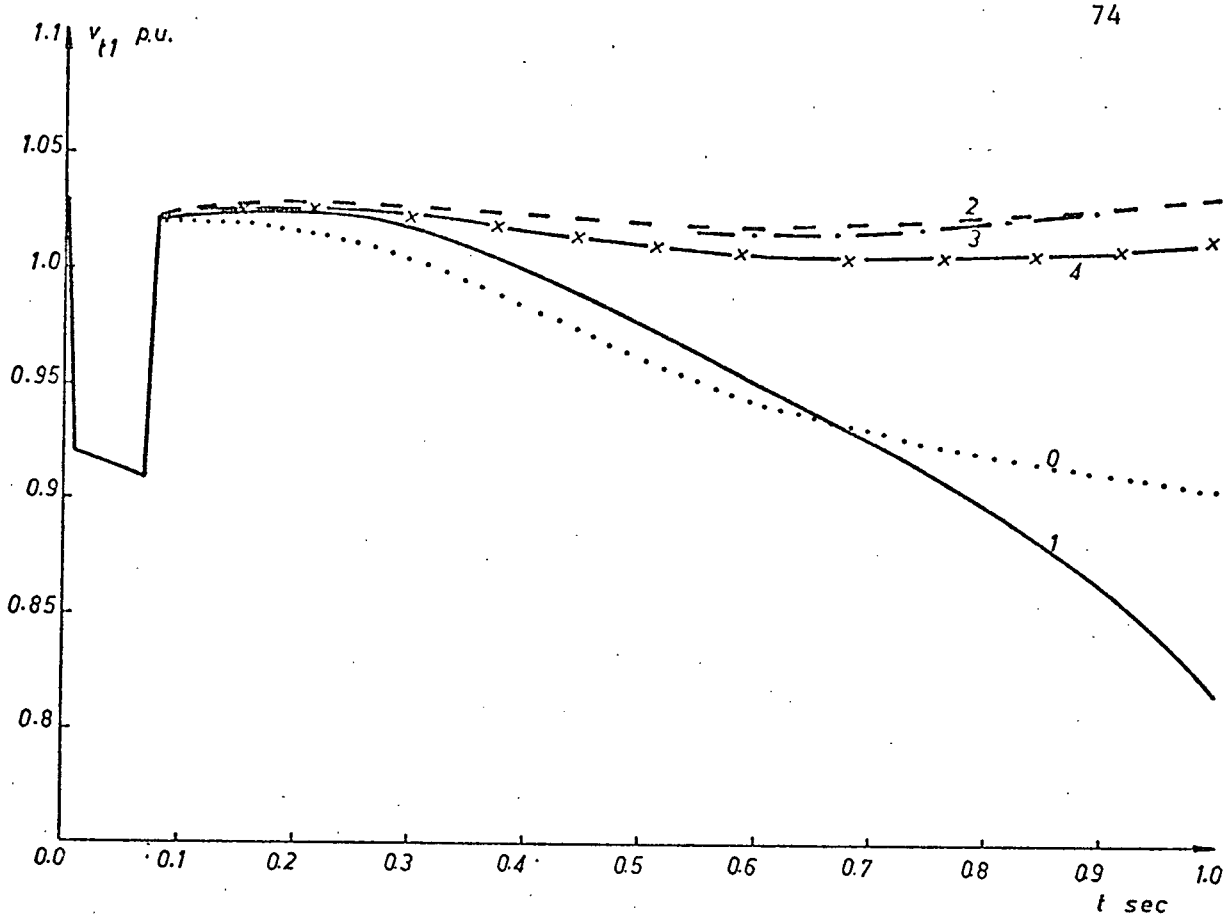

Fig. 6.3 Terminal Voltage Variations at Bus 1 for 2 Machine, 2 Rectifier System

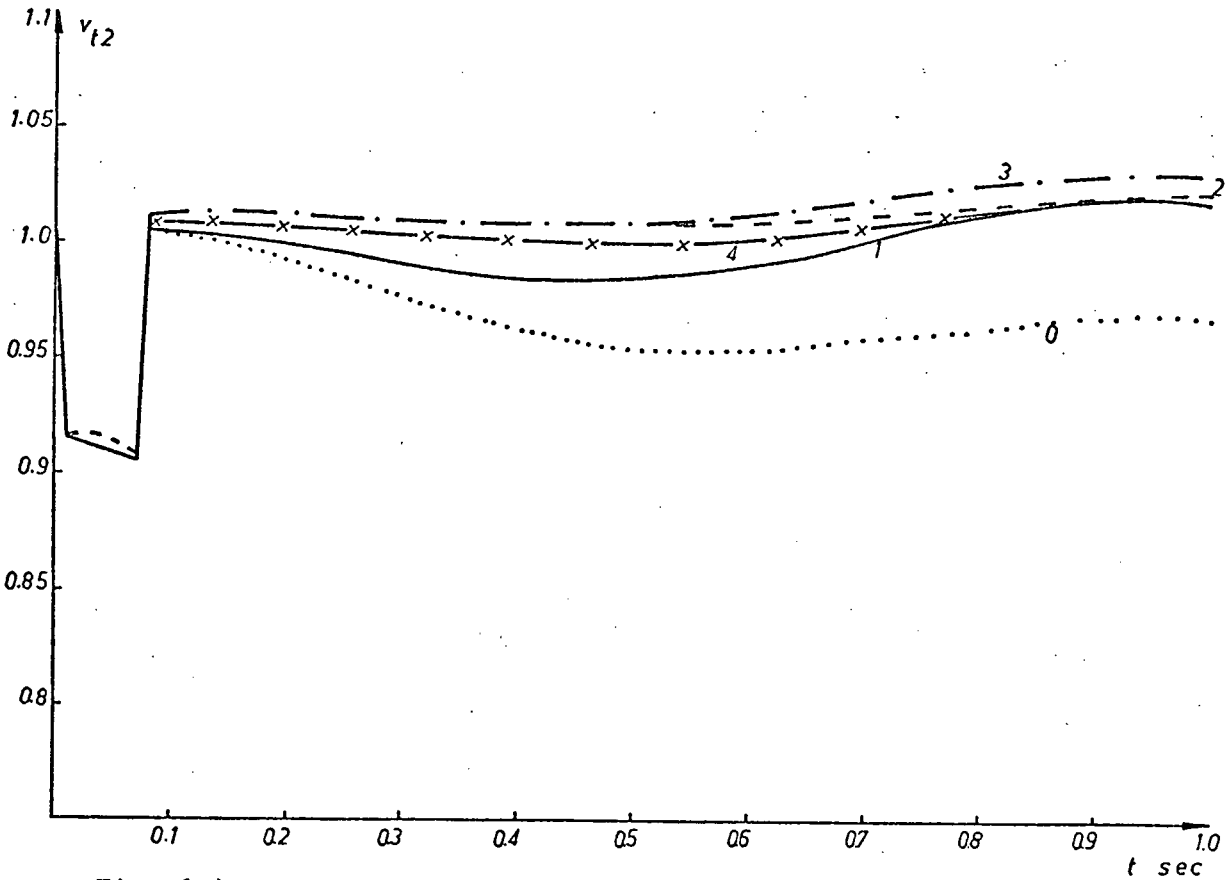

Fig. 6.4 Terminal Voltage Variations at Bus 2 for 2 Machine, 2 Rectifier System

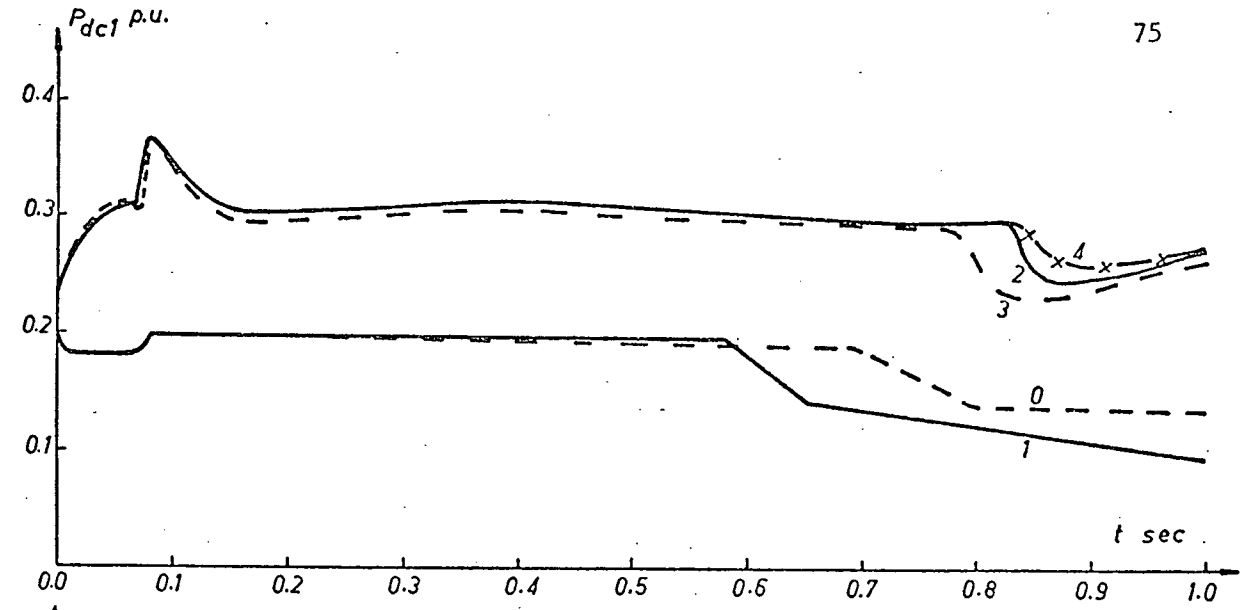

(a)

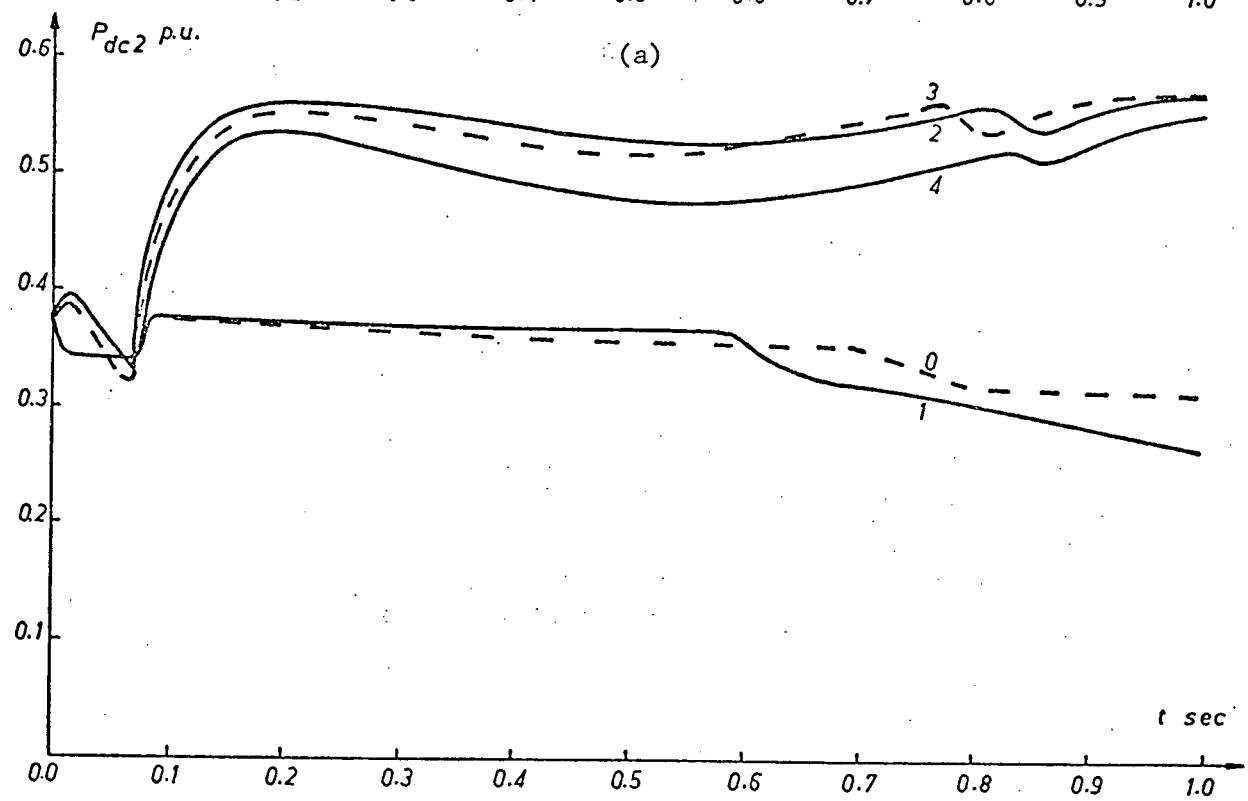

(b)

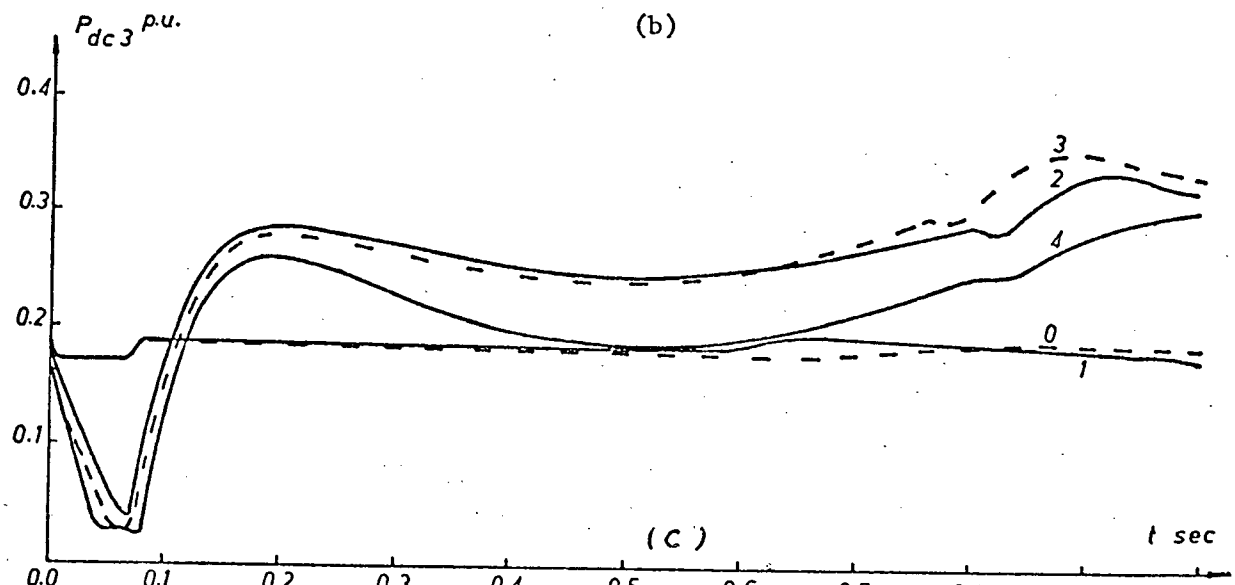

Fig. 6.5 DC Power Variations for 2 Machine 2 Rectifier System

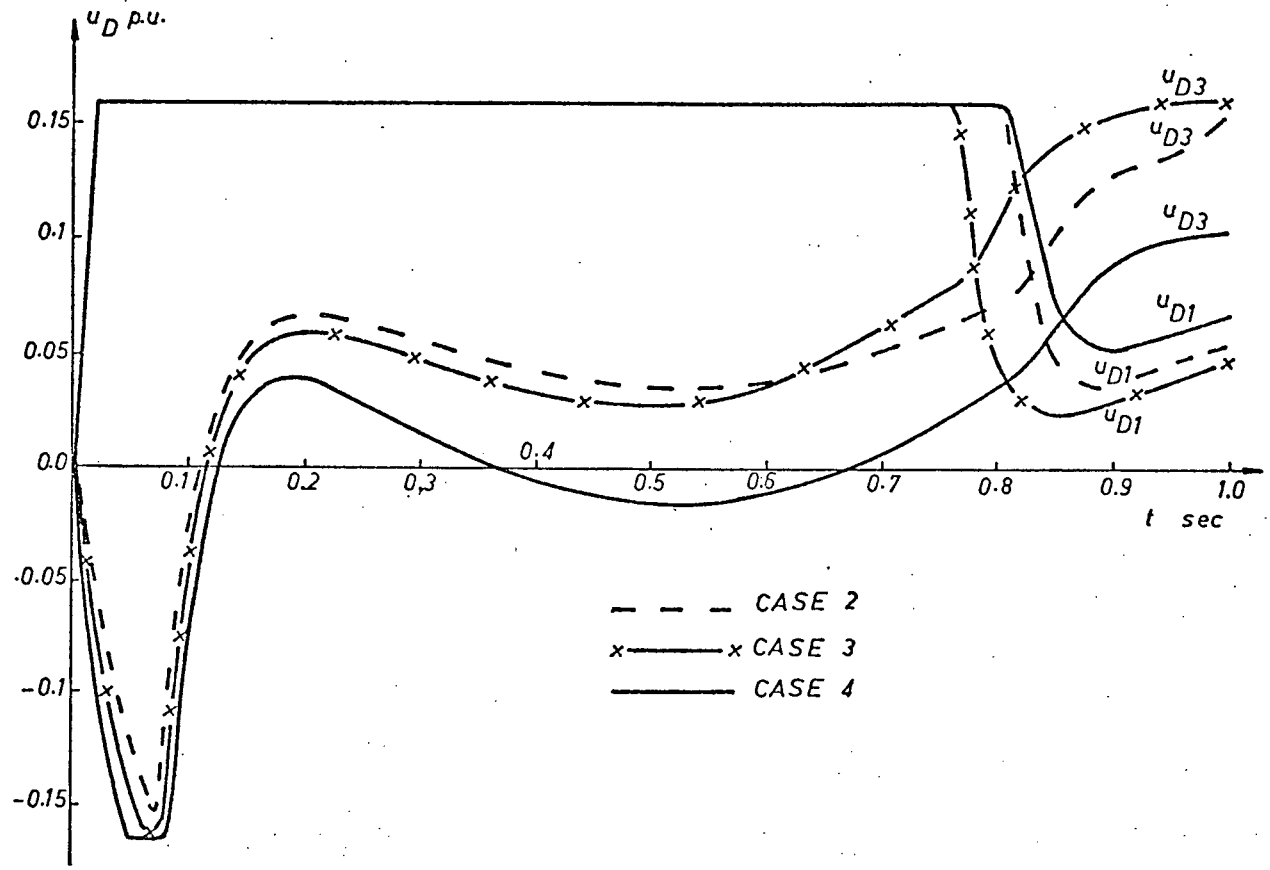

Fig. 6.6 DC Control Effort for 2 Machine, 2 Rectifier System

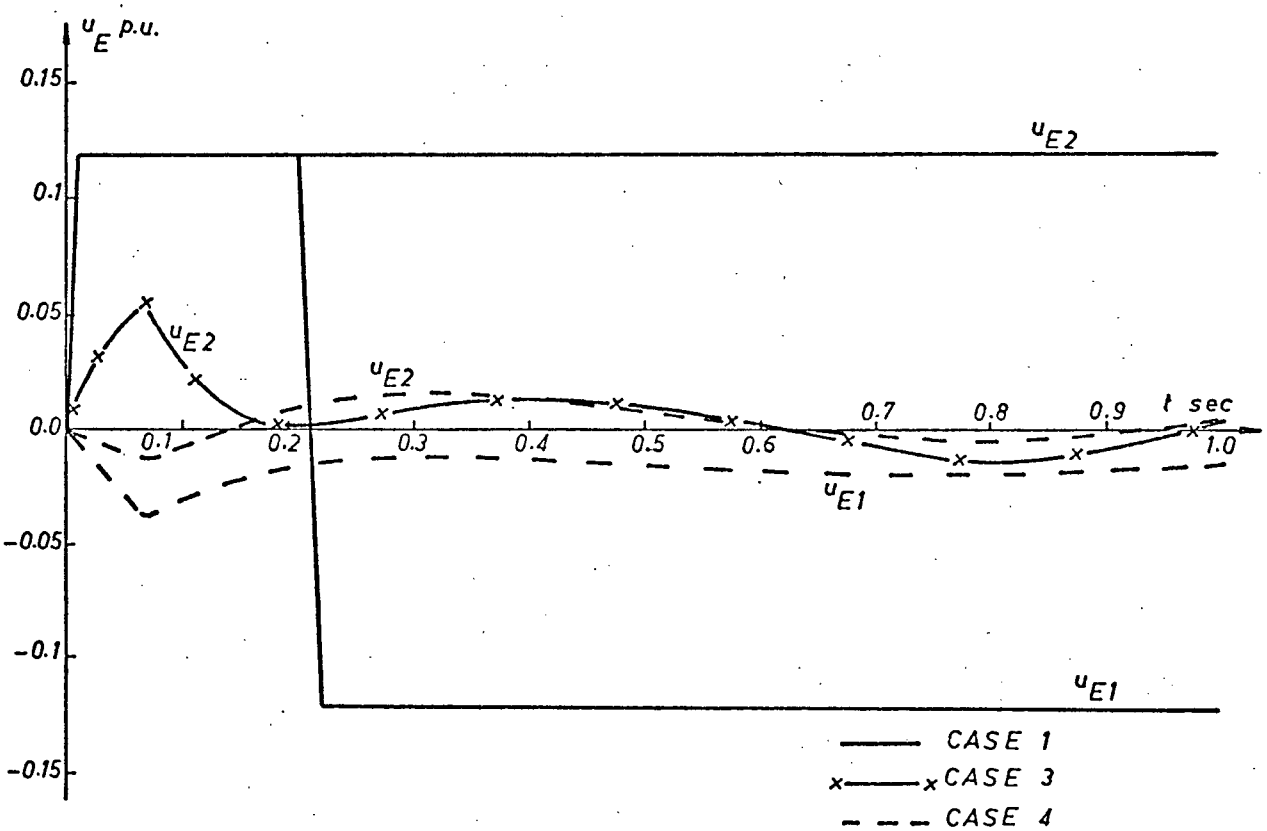

Fig. 6.7 Excitation Control Effort for 2 Machine, 2 Rectifier System

because of larger drops in v_{t1}. For cases 2, 3 and 4 the dc reference currents are modified by optimal control signals and therefore the total power transmitted over the dc network is significantly increased to absorb some power from the ac system, which may cause large acceleration of the synchronous machines, and consequently resulting in a more stable system.

The control efforts are shown in Figures 6.6 and 6.7. It is interesting to notice that the dc control effort at rectifier station 1, u_{D1}, is larger in case 4 than that of cases 2 and 3. This suggests that the presence of an excitation control signal at machine 1 is working against the dc control at the same bus. This may be explained by the fact that the voltage drop at bus 1 is larger in case 4 than cases 2 and 3. It is also noticed that in general the dc control efforts at rectifier station 1 are much larger than the dc control efforts at rectifier station 3 since v_{t3} is constant and machine 1 is also closer to the fault location. The excitation control efforts are greatly reduced in the presence of dc controls.

6.2 Two Machine-Infinite Bus System with One Rectifier and Two Inverters

The study in this section is similar to that of section 6.1 except that converter station 3 is now operated as an inverter instead of a rectifier. So the only change in the cases listed before will be the fact that station 3 is an inverter. The operating point was given in Chapter 5 and the linearized system state equations are

$$
\begin{bmatrix}
\Delta\dot{\delta}_1 \\ \Delta\dot{\omega}_1 \\ \Delta\dot{\psi}_{fd1} \\ \Delta\dot{E}_{x1} \\ \Delta\dot{\cos\alpha}_{R1} \\ \Delta\dot{\delta}_2 \\ \Delta\dot{\omega}_2 \\ \Delta\dot{\psi}_{fd2} \\ \Delta\dot{E}_{x2} \\ \Delta\dot{\cos\alpha}_{I2} \\ \Delta\dot{\cos\alpha}_{I3}
\end{bmatrix}
=
\begin{bmatrix}
0.0 & 1.0 & 0.0 & 0.0 & 0.0 & 0.0 & 0.0 & 0.0 & 0.0 & 0.0 & 0.0 \\
-33 & 0.0 & -117.6 & 0.0 & -140.6 & 11.3 & 0.0 & 0.042 & 0.0 & -31.5 & -62.3 \\
-0.38 & 0.0 & -1.58 & 0.46 & -1.36 & 0.16 & 0.0 & 0.17 & 0.0 & -0.38 & -0.84 \\
0.056 & 0.0 & -6.51 & -0.5 & -1.33 & -0.2 & 0.0 & -1.01 & 0.0 & 0.14 & 0.82 \\
-286 & 0.0 & -19722 & 0.0 & -36163 & -291 & 0.0 & 4652 & 0.0 & -11241 & -16153 \\
0.0 & 0.0 & 0.0 & 0.0 & 0.0 & 0.0 & 1.0 & 0.0 & 0.0 & 0.0 & 0.0 \\
19.4 & 0.0 & 22.1 & 0.0 & 20.1 & -50 & 0.0 & -139 & 0.0 & 0.7 & -67.9 \\
0.09 & 0.0 & 0.36 & 0.0 & 0.41 & -0.28 & 0.0 & -1.78 & 0.45 & 1.01 & -0.7 \\
0.37 & 0.0 & -0.8 & 0.0 & -1.14 & -0.74 & 0.0 & -6.24 & -0.5 & -1.91 & 0.49 \\
12.6 & 0.0 & 77.9 & 0.0 & 152.4 & -23.9 & 0.0 & -212.3 & 0.0 & -46.8 & 4.45 \\
726 & 0.0 & -13434 & 0.0 & -23864 & -1633 & 0.0 & -12456 & 0.0 & 15930 & -35443
\end{bmatrix}
\begin{bmatrix}
\Delta\delta_1 \\ \Delta\omega_1 \\ \Delta\psi_{fd1} \\ \Delta E_{x1} \\ \Delta\cos\alpha_{R1} \\ \Delta\delta_2 \\ \Delta\omega_2 \\ \Delta\psi_{fd2} \\ \Delta E_{x2} \\ \Delta\cos\alpha_{I2} \\ \Delta\cos\alpha_{I3}
\end{bmatrix}
+ BU
$$

(6.4)

The weighing matrices Q and the corresponding nonzero elements of matrices B are

u_{E1} and u_{E2} : Q = diag. {100, 10, 1, 1, 1, 100, 10, 1, 1, 1, 1}

$b_{4,1} = 10, \quad b_{9,2} = 10$

u_{D1} and u_{D3} : Q = diag. {100, 10, 1000, 1, 1, 100, 10, 1000, 1, 1, 1}

$b_{5,1} = 10383.8, \quad b_{11,2} = 10799.1$ (6.5)

u_{D1}, u_{E2} and u_{D3} : Q = diag. {100, 10, 1, 1, 1, 100, 10, 1, 1, 1, 1}

$b_{5,1} = 10383.8, \quad b_{9,2} = 10, \quad b_{11,3} = 10799.1$

u_{E1}, u_{D1}, u_{E2} and u_{D3} : Q = diag. {10, 1, 10, 1, 1, 10, 1, 10, 1, 1, 1}

$b_{4,1} = 10, \quad b_{5,2} = 10383.8, \quad b_{9,3} = 10, \quad b_{11,4} = 10799.1$

The control laws are given in equation (6.6) and the system's eigenvalues are listed in Table VII.

The same disturbance described in section 6.1 is applied to this system for the nonlinear tests. The system responses are summarized in Figures 6.8 to 6.14.

Figures 6.8 and 6.9 show the angle and speed deviations respectively. The system is more stable without optimal control, case 0, than with excitation control, case 1. Cases 2 and 3 give the smallest angular deviations and it is also close for case 4.

The terminal voltage variations at bus 1, Figure 6.10, are largest in case 1 followed by cases 4, 0, 2 and 3 in that order. At bus 2 all the voltage deviations are small.

In Figures 6.12 (a, b, c) the variations of power transmitted over the dc network are shown. In cases 0 and 1 with the dc network operating on constant current control the dc power goes back to original values immediately after the faulted line is isolated and then decreases

$$
\begin{bmatrix} u_{E1} \\ u_{E2} \\ \hline u_{D1} \\ u_{D3} \\ \hline u_{D1} \\ u_{E2} \\ u_{D3} \\ \hline u_{E1} \\ u_{D1} \\ u_{E2} \\ u_{D3} \end{bmatrix} = \begin{bmatrix} -13 & 1.6 & -25.6 & -1.75 & -0.004 & 12.15 & -0.66 & -12 & -0.34 & 0.52 & 0.0013 \\ -4.4 & 2.74 & -14.7 & -0.34 & -0.01 & -12 & 1.11 & -23.3 & -1.67 & -0.36 & -0.0016 \\ \hline 10.8 & 3.1 & -0.63 & 1.99 & -0.22 & -3.25 & -0.25 & -11.6 & 0.27 & -0.12 & 0.102 \\ 0.17 & 0.57 & 1.28 & -2.81 & 0.11 & 10.4 & 3.1 & 7.76 & -0.49 & -0.93 & -0.2 \\ \hline 9.04 & 3.21 & -1.39 & 0.06 & -0.21 & -1.17 & -0.45 & -0.72 & 0.0003 & -0.025 & 0.102 \\ 0.21 & 0.02 & -1.08 & 0.21 & 0.3\times10^{-6} & -0.41 & 0.01 & -1.3 & -1.0 & 0.0026 & -0.8\times10^{-5} \\ 1.73 & 0.48 & 0.42 & -0.08 & 0.11 & 8.48 & 3.24 & -1.75 & -0.009 & -1.0 & -0.2 \\ \hline -0.15 & 0.03 & -2.16 & -1.05 & -0.5\times10^{-6} & 0.18 & -0.003 & -0.006 & -0.005 & -0.005 & -0.15\times10^{-4} \\ 2.43 & 1.06 & -1.07 & -0.0005 & -0.21 & -0.08 & -0.04 & -1.01 & 0.005 & -0.12 & 0.1 \\ 0.09 & 0.009 & -0.24 & -0.005 & 0.5\times10^{-5} & -0.2 & 0.01 & -1.32 & -1.01 & -0.0014 & -0.2\times10^{-4} \\ 0.52 & 0.07 & 0.49 & -0.02 & 0.11 & 1.94 & 1.07 & -0.72 & -0.02 & -0.48 & -0.19 \end{bmatrix}
$$

$$
\cdot[\Delta\delta_1 \quad \Delta\omega_1 \quad \Delta\psi_{fd1} \quad \Delta Ex_1 \quad \Delta\cos\alpha_{R1} \quad \Delta\delta_2 \quad \Delta\omega_2 \quad \Delta\psi_{fd2} \quad \Delta E_{x2} \quad \Delta\cos\alpha_{I2} \quad \Delta\cos\alpha_{I3}]^t \qquad (6.6)
$$

Table VII Eigenvalues for 2 Machine-Infinite Bus, 2 Inverters System

Control used	Eigenvalues
no control	-55443, -16056, -155, -0.785±j1.49, -0.405±j1.82, -0.201±j4.76, -0.168±j6.52
u_{E1} and u_{E2}	-55443, -16056, -155, -10.75,-9.91, -3.66±j7.91, -2.92, 2.15 ± j6.23, -2.11
u_{D1} and u_{D3}	-56428, -19286, -191, -94.45,-48.4, -3.16, -1.82 ± j2.2, -1.81, -0.78 ± j1.41
u_{D1}, u_{E2} & u_{D3}	-56428, -19286, -191, -93.9,-46.8, -9.64, -3.26, -3.18, -1.59, -0.874±j1.68
u_{E1}, u_{D1}, u_{E2} and u_{D3}	-56428, -19286, -149, -32.3, -14.38, -9.55, -9.49, -4.18, -3.39, -2.66, -2.17

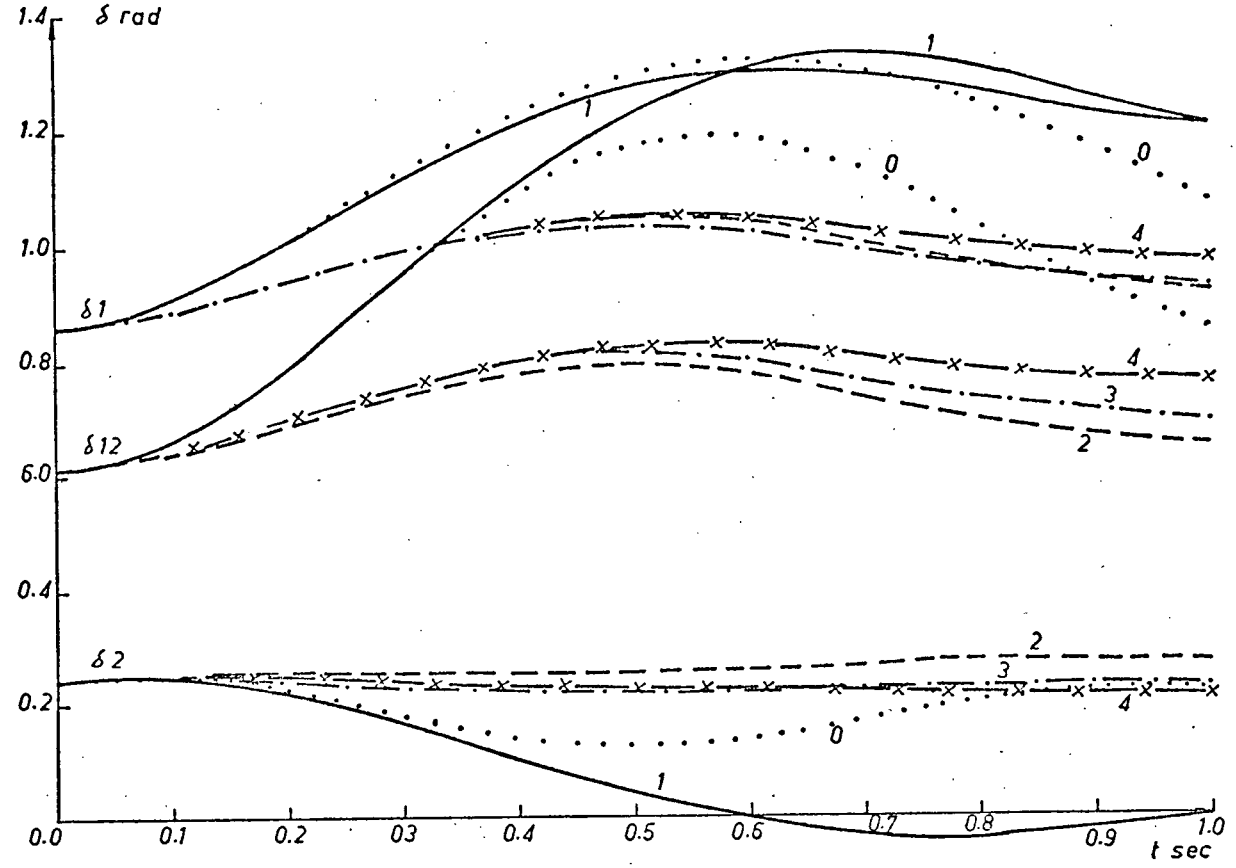

Fig. 6.8 Swing Curves for 2 Machine, 2 Inverter System

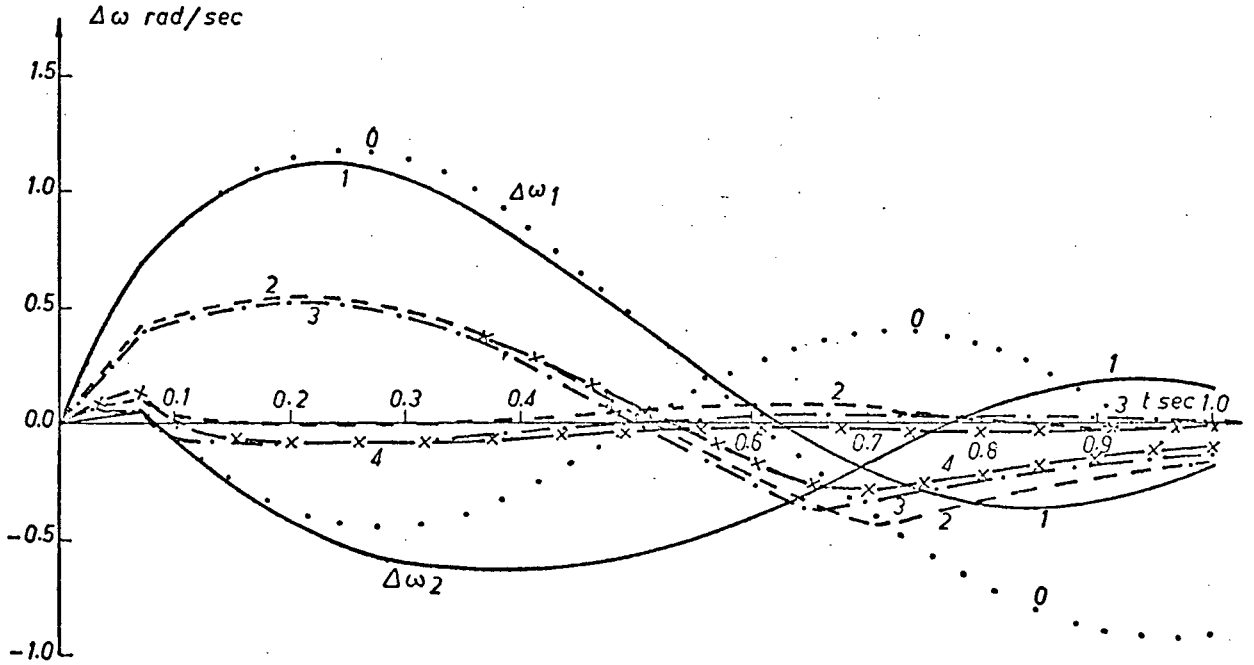

Fig. 6.9 Speed Deviation for 2 Machine, 2 Inverter System

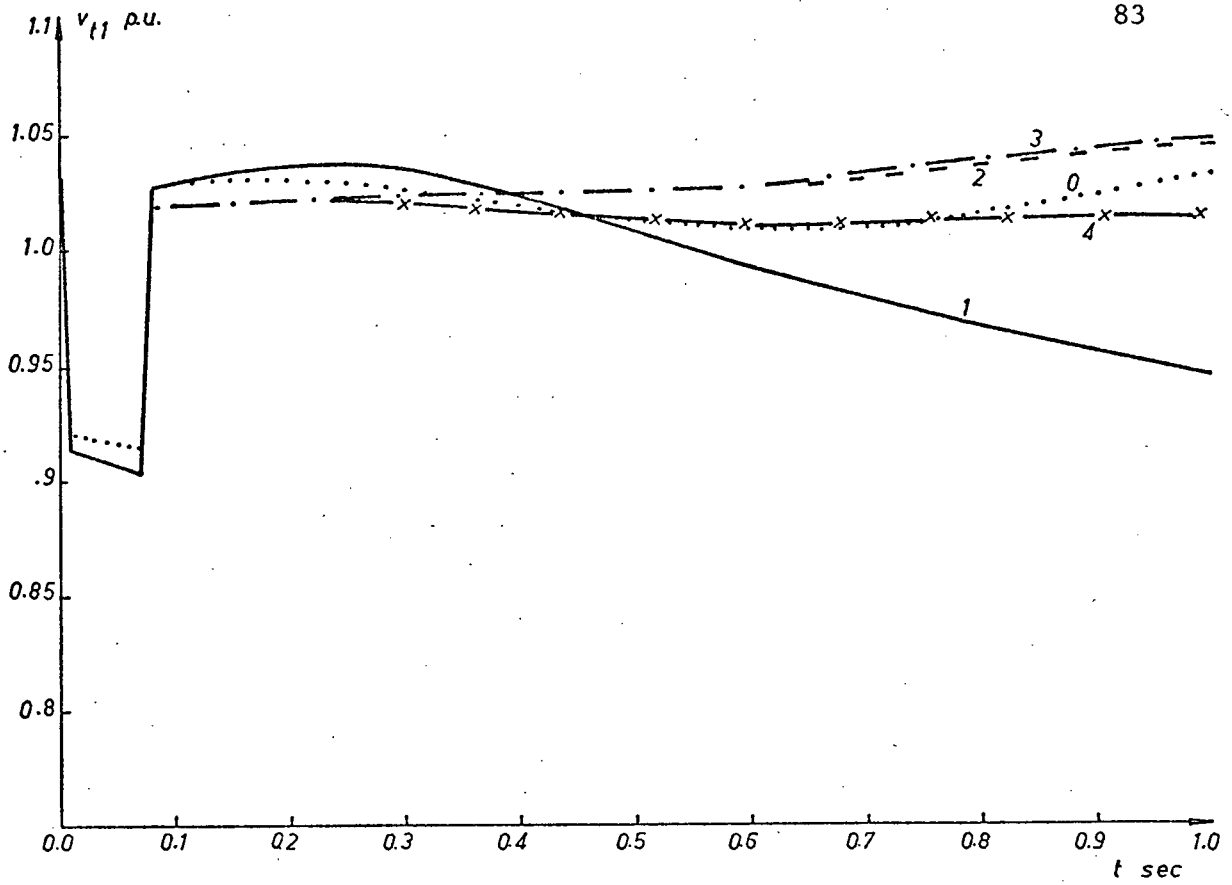

Fig. 6.10 Terminal Voltage Variations at Bus 1 for 2 Machine, 2 Inverter System

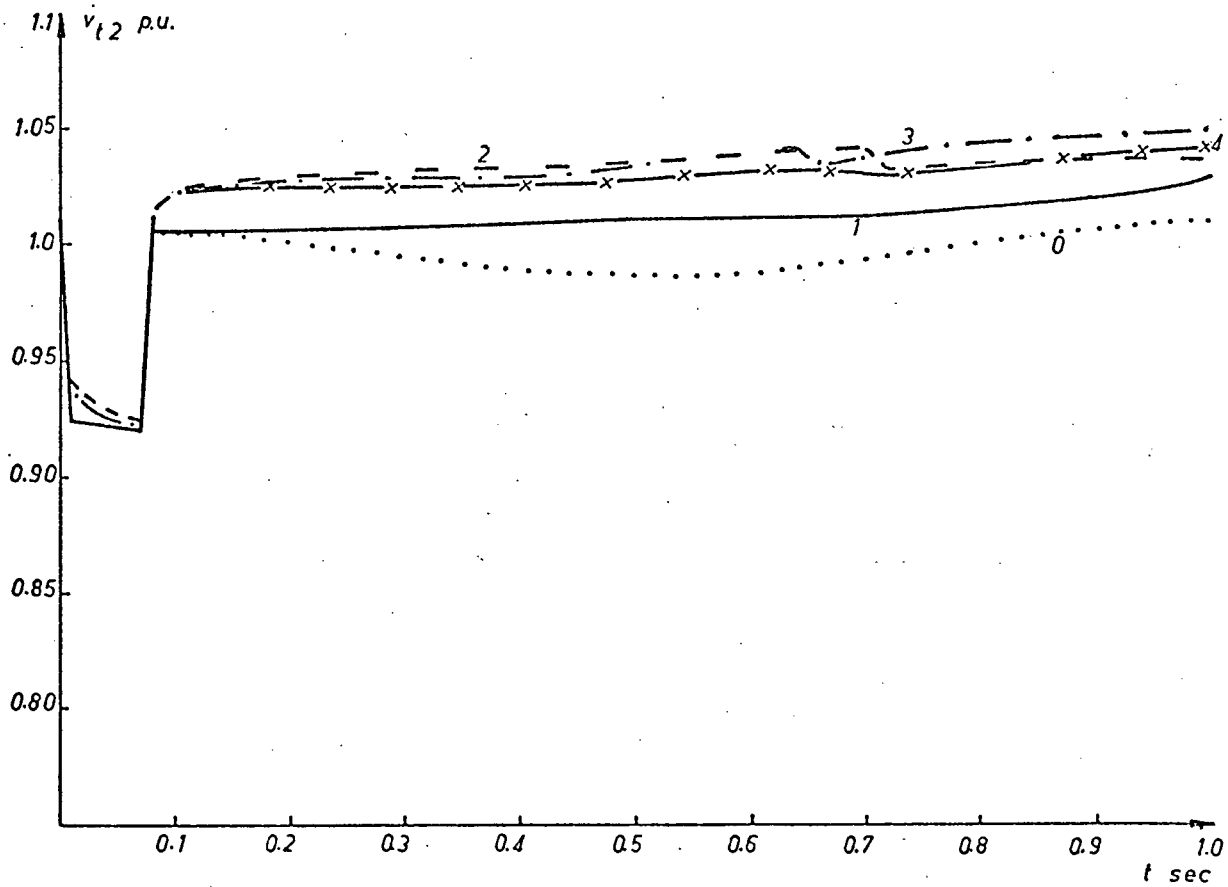

Fig. 6.11 Terminal Voltage Variations at Bus 2 for 2 Machine, 2 Inverter System

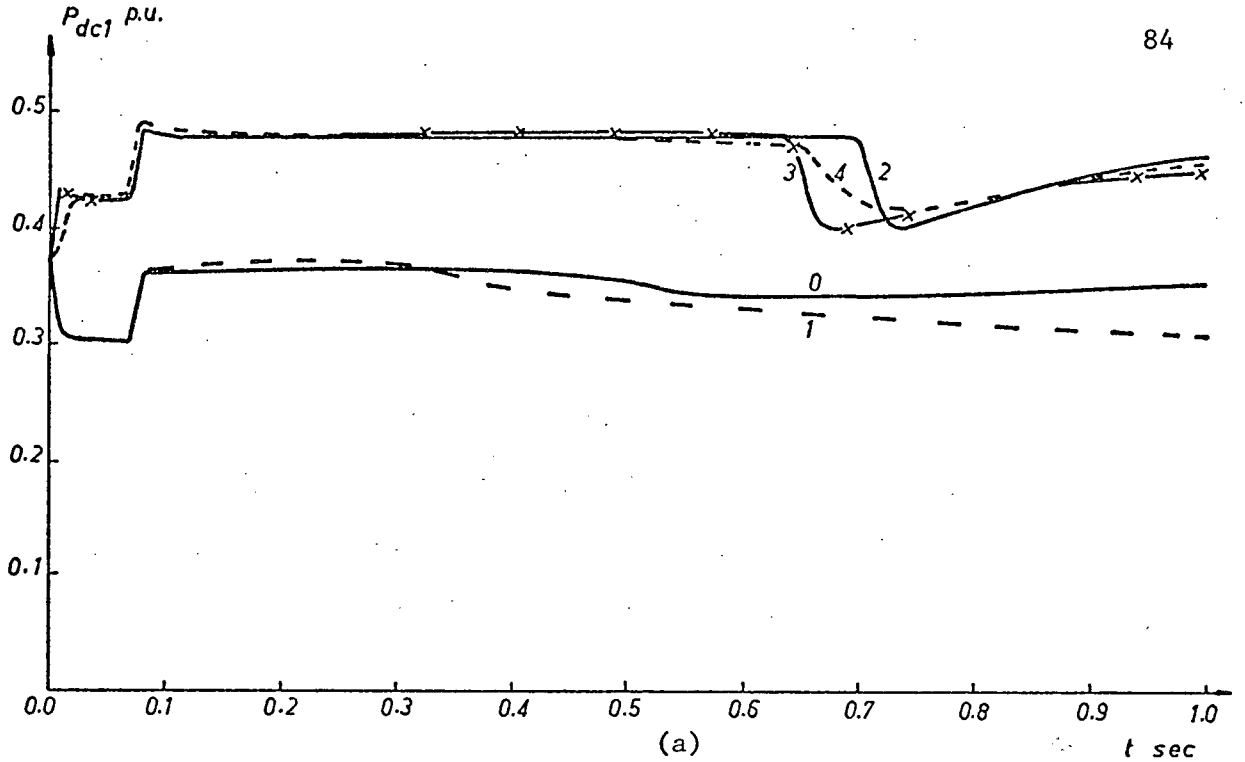

(a)

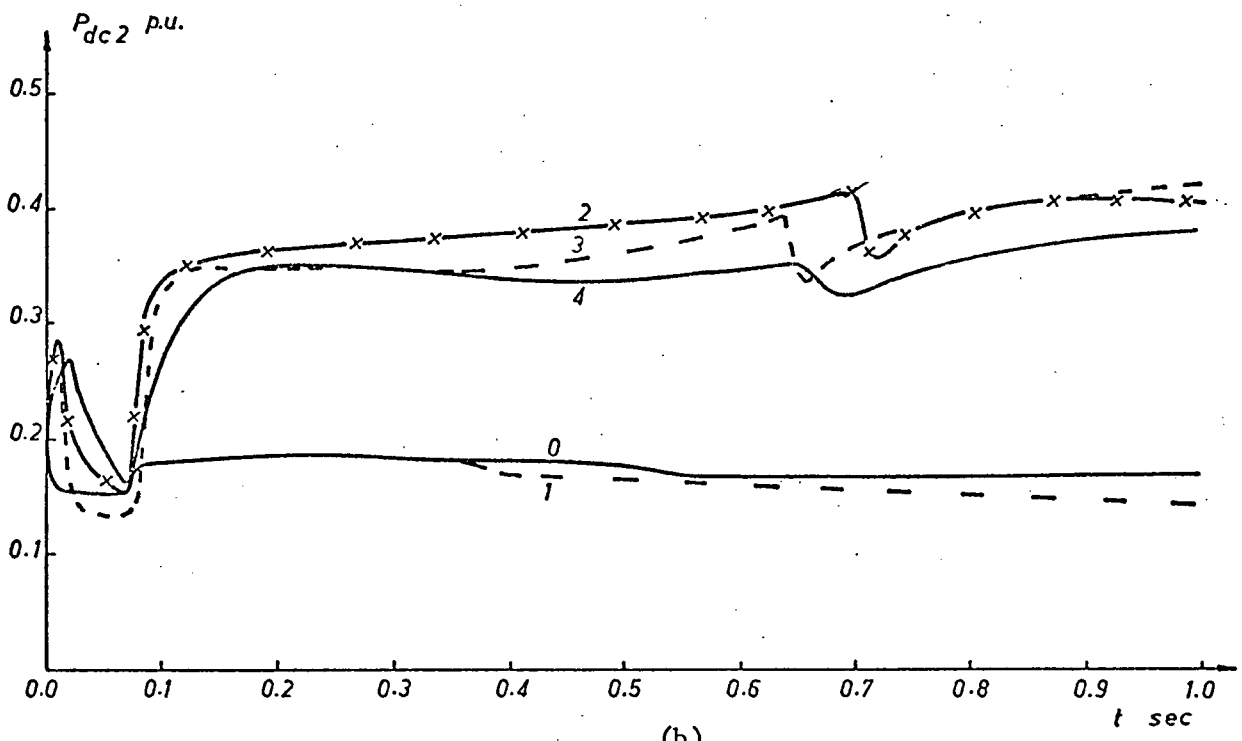

(b)

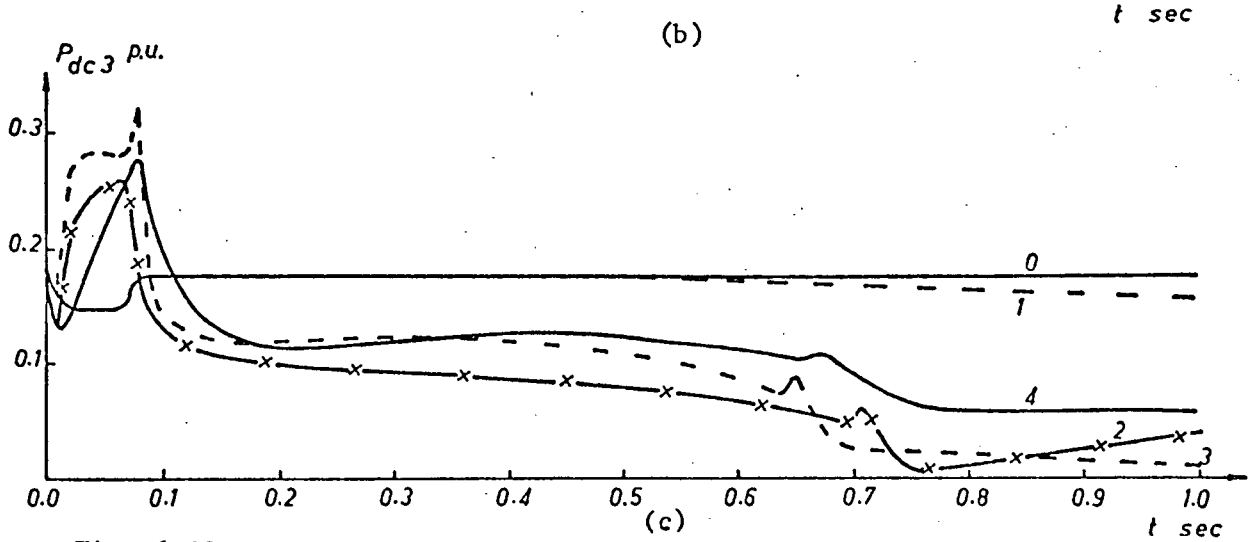

(c)

Fig. 6.12 DC Power Variations for 2 Machine, 2 Inverter System

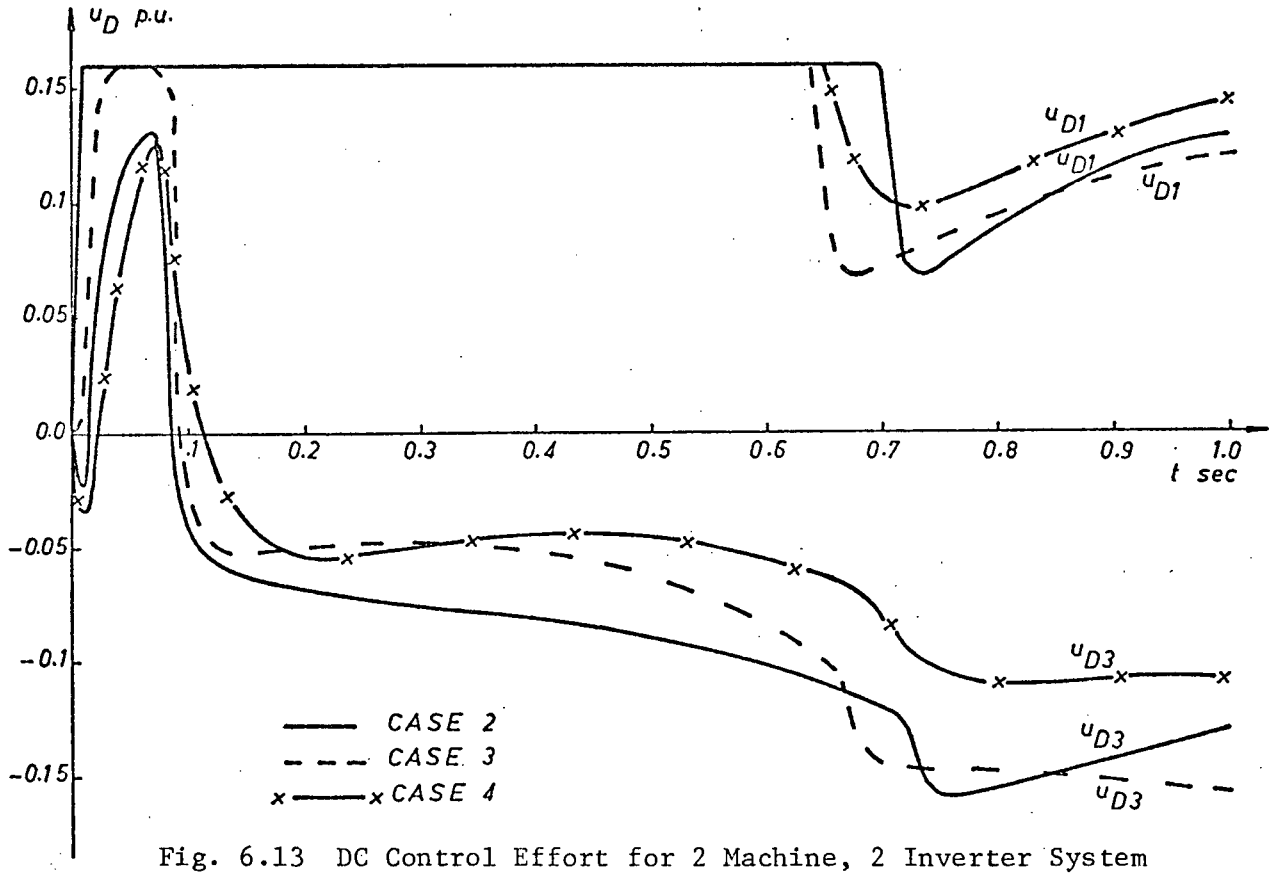

Fig. 6.13 DC Control Effort for 2 Machine, 2 Inverter System

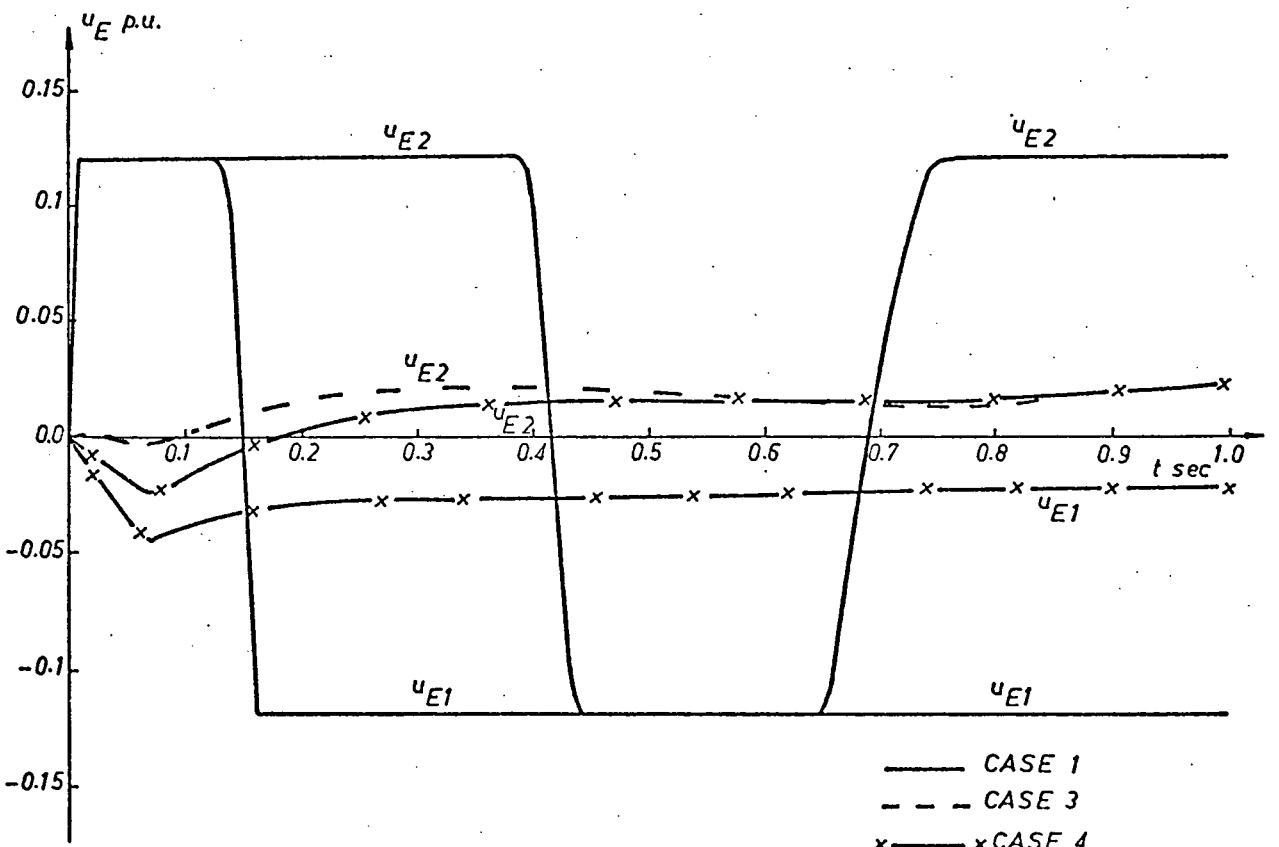

Fig. 6.14 Excitation Control Effort
for 2 Machine, 2 Inverter System

because of the ac voltage drop at the rectifier bus. In cases 2, 3 and 4 where the dc reference currents are modified by optimal control signals, the rectifier power is increased even with the fault on. The power is even increased further after the fault is removed and stays almost constant at about 0.48 p.u. then starts to go down at 0.7 sec.

The control efforts are shown in Figures 6.13 and 6.14. Again it is seen that the excitation control efforts, Figure 6.14, are greatly reduced in the presence of dc controls. It is also noticed that the dc control at converter station 3 jumps to high positive values for the fault duration and then changes sign after the faulted line is isolated. The reason for this is that during the fault inverter 3 draws more dc power since inverter 2 is incapable of absorbing this power due to the ac voltage drop. After the faulted line is removed inverter 2 starts to pick up more dc power to compensate for the ac line power loss.

6.3 Three Machine System with Two Rectifiers and One Inverter

The system studied here is the same as that of section 6.1 except that the infinite bus 3 is replaced by a small synchronous machine having one third the rating of either machines 1 or 2. The system's operating point is the same as section 6.1. The system's linearized state equations are given in eqn. (6.7).

$$
\begin{bmatrix}
\Delta\dot{\delta}_1 \\ \Delta\dot{\omega}_1 \\ \Delta\dot{\psi}_{fd1} \\ \Delta\dot{E}_{x1} \\ \Delta\dot{\cos\alpha}_{R1} \\ \Delta\dot{\delta}_2 \\ \Delta\dot{\omega}_2 \\ \Delta\dot{\psi}_{fd2} \\ \Delta\dot{E}_{x2} \\ \Delta\dot{\cos\alpha}_{I2} \\ \Delta\dot{\delta}_3 \\ \Delta\dot{\omega}_3 \\ \Delta\dot{\psi}_{fd3} \\ \Delta\dot{E}_{x3} \\ \Delta\dot{\cos\alpha}_{R3}
\end{bmatrix}
=
\begin{bmatrix}
0.0 & 1.0 & 0.0 & 0.0 & 0.0 & 0.0 & 0.0 & 0.0 & 0.0 & 0.0 & 0.0 & 0.0 & 0.0 & 0.0 & 0.0 \\
-23.2 & 0.0 & -99 & 0.0 & -105 & 13.4 & 0.0 & 7.85 & 0.0 & -52.6 & 9.77 & 0.0 & 10.7 & 0.0 & 31.2 \\
-0.36 & 0.0 & -1.23 & 0.45 & -0.9 & 0.24 & 0.0 & 0.35 & 0.0 & -0.57 & 0.125 & 0.0 & 0.21 & 0.0 & 0.35 \\
0.63 & 0.0 & -7.19 & -0.5 & -1.28 & -0.52 & 0.0 & -1.5 & 0.0 & 0.03 & -0.11 & 0.0 & -0.55 & 0.0 & -0.1 \\
-14690 & 0.0 & -14935 & 0.0 & -27366 & 1069 & 0.0 & 9644 & 0.0 & -11826 & 400 & 0.0 & 3849 & 0.0 & 13269 \\
0.0 & 0.0 & 0.0 & 0.0 & 0.0 & 0.0 & 1.0 & 0.0 & 0.0 & 0.0 & 0.0 & 0.0 & 0.0 & 0.0 & 0.0 \\
27.6 & 0.0 & 44.4 & 0.0 & 43.9 & -44.1 & 0.0 & -141 & 0.0 & 20.7 & 16.4 & 0.0 & 14.75 & 0.0 & 15.8 \\
0.11 & 0.0 & 0.7 & 0.0 & 0.82 & -0.26 & 0.0 & -1.67 & 0.48 & 0.77 & 0.15 & 0.0 & 0.24 & 0.0 & 0.25 \\
1.03 & 0.0 & -1.28 & 0.0 & -1.95 & -1.14 & 0.0 & -7.21 & -0.5 & -3.03 & 0.11 & 0.0 & -0.49 & 0.0 & -0.46 \\
2.0 & 0.0 & 129 & 0.0 & 211 & -18.45 & 0.0 & -175 & 0.0 & -103 & 16.45 & 0.0 & 49.3 & 0.0 & 140 \\
0.0 & 0.0 & 0.0 & 0.0 & 0.0 & 0.0 & 0.0 & 0.0 & 0.0 & 0.0 & 0.0 & 1.0 & 0.0 & 0.0 & 0.0 \\
49.6 & 0.0 & 42.8 & 0.0 & 42.3 & 29.8 & 0.0 & -9.89 & 0.0 & -86 & -79.4 & 0.0 & -129 & 0.0 & -170 \\
0.52 & 0.0 & 0.97 & 0.0 & 1.12 & 0.5 & 0.0 & 0.27 & 0.0 & -1.27 & -1.02 & 0.0 & -2.25 & 0.49 & -2.73 \\
1.27 & 0.0 & -3.13 & 0.0 & -4.45 & -0.76 & 0.0 & -3.33 & 0.0 & 0.82 & -0.51 & 0.0 & -2.89 & -0.5 & -3.3 \\
1718 & 0.0 & 3593 & 0.0 & 8926 & 36.9 & 0.0 & 2264 & 0.0 & -11034 & -17554 & 0.0 & -8268 & 0.0 & -25443
\end{bmatrix}
\begin{bmatrix}
\Delta\delta_1 \\ \Delta\omega_1 \\ \Delta\psi_{fd1} \\ \Delta E_{x1} \\ \Delta\cos\alpha_{R1} \\ \Delta\delta_2 \\ \Delta\omega_2 \\ \Delta\psi_{fd2} \\ \Delta E_{x2} \\ \Delta\cos\alpha_{I2} \\ \Delta\delta_3 \\ \Delta\omega_3 \\ \Delta\psi_{fd3} \\ \Delta E_{x3} \\ \Delta\cos\alpha_{R3}
\end{bmatrix}
+ BU
\tag{6.7}
$$

The matrices Q and the nonzero elements of B are given by

u_{E1}, u_{E2}, u_{E3} : Q = diag {10, 100, 1, 1, 1, 10, 100, 1, 1, 1, 10, 100, 1, 1,1}

$b_{4,1} = 10,\ b_{9,2} = 10,\ b_{14,3} = 10$

u_{D1}, u_{D3} : Q = diag {10, 1, 100, 1, 1, 10, 1, 100, 1, 1, 10, 1, 100, 1, 1}

$b_{5,1} = 10484.6, \quad b_{15,2} = 10587.4$ (6.8)

u_{D1}, u_{E2}, u_{D3} : Q = diag {10, 1, 100, 1, 1, 10, 1, 100, 1, 1, 10, 1, 100, 1, 1}

$b_{5,1} = 10484.6,\ b_{9,2} = 10,\ b_{15,3} = 10587.4$

$u_{E1}, u_{D1}, u_{E2}, u_{E3}, u_{D3}$: Q = diag {10, 10, 10, 1, 1, 10, 10, 10, 1, 1, 10, 10, 10, 1, 1}

$b_{4,1} = 10,\ b_{5,2} = 10484.6,\ b_{9,3} = 10,\ b_{14,4} = 10,\ b_{15,5} = 10587.4$

The corresponding control laws are given in (6.9). The system's eigenvalues for different controls are listed in Table VIII.

The same disturbance applied to the nonlinear tests of section 6.1 is applied to this three machine system. Figures 6.15 to 6.22 show the system responses for different control schemes. Again four cases are studied as listed in section 6.1 except that in cases land 4 excitation controls are applied to all three machines in this case. Since this three machine system is unstable without optimal controls as indicated by the eigenvalues in Table VIII, the nonlinear response for this case is not shown.

The angle and speed deviation curves, Figures 6.15 and 6.16 respectively, show that in case 1 machine 1 is unstable and that in general the variations in angle and speed deviations are the largest in this case. Case 2 results in the smallest deviations followed by cases 3 and 4 in that order.

Figures 6.17, 6.18 and 6.19 show the ac terminal voltages variations. At bus 1, Figure 6.17, the voltage changes most in case 1

$$
\begin{bmatrix} u_{E1} \\ u_{E2} \\ u_{E3} \\ \hline u_{D1} \\ u_{D3} \\ \hline u_{D1} \\ u_{E2} \\ u_{D3} \\ \hline u_{E1} \\ u_{D1} \\ u_{E2} \\ u_{E3} \\ u_{D3} \end{bmatrix} =
\left[\begin{array}{ccccccccccccccc}
-37.4 & 6.37 & -63.4 & -2.53 & -0.023 & 21.3 & -1.04 & -0.26 & -0.002 & 0.19 & 17.3 & -1.19 & 10.7 & 0.17 & 0.002 \\
26.3 & 5.24 & 0.69 & -0.002 & -0.016 & -23.9 & 7.81 & -129 & -3.49 & -0.4 & 2.26 & 2.36 & -9.19 & -0.19 & -0.015 \\
25 & 2.88 & 8.5 & 0.17 & -0.015 & 40 & 0.6 & -16.5 & -0.19 & 0.06 & -62.5 & 4.89 & -69.7 & -2.74 & -0.03 \\
\hline
7.14 & 1.26 & 0.47 & 0.19 & -0.21 & -3.94 & 0.64 & -21.6 & -0.61 & -0.14 & 1.08 & 0.05 & -0.54 & 1.09 & -0.09 \\
1.26 & 0.13 & 0.65 & -0.34 & -0.09 & -1.67 & 0.31 & -8.73 & -0.17 & -0.12 & 3.82 & 1.03 & 0.3 & -1.62 & -0.25 \\
\hline
6.24 & 1.23 & -0.001 & 0.19 & -0.21 & -2.77 & 0.49 & -15.2 & -0.32 & -0.13 & 0.69 & 0.05 & -0.62 & 1.1 & -0.09 \\
2.83 & 0.13 & 1.88 & 0.03 & -0.0003 & -2.91 & 0.61 & -20.6 & -1.6 & -0.03 & 1.11 & 0.03 & 0.25 & 0.13 & -0.0001 \\
0.89 & 0.12 & 0.44 & -0.3 & -0.09 & -1.11 & 0.25 & -6.05 & -0.13 & -0.12 & 3.64 & 1.03 & 0.22 & -1.61 & -0.25 \\
\hline
-0.73 & 0.007 & -2.41 & -1.05 & 0.2×10^{-4} & 0.78 & -0.12 & 2.92 & 0.08 & 0.005 & -0.14 & -0.006 & 0.04 & 0.001 & 0.8×10^{-5} \\
6.99 & 3.37 & 0.17 & 0.03 & -0.22 & -5.32 & 0.48 & -21.3 & -0.43 & -0.16 & 1.93 & 0.001 & 0.27 & 0.008 & -0.09 \\
9.87 & 0.44 & 3.16 & 0.08 & -0.0004 & -11.8 & 2.17 & -48.3 & -2.21 & -0.13 & 4.13 & 0.1 & 0.9 & 0.02 & -0.0002 \\
0.13 & 0.02 & -0.01 & 0.001 & 0.8×10^{-5} & 0.34 & -0.001 & 0.69 & 0.02 & -0.003 & -0.43 & 0.02 & -2.48 & -1.07 & 0.3×10^{-5} \\
2.32 & 0.14 & 0.92 & 0.01 & -0.09 & -1.92 & 0.28 & -9.06 & -0.18 & -0.16 & 3.1 & 3.19 & -0.63 & 0.004 & -0.26
\end{array}\right]
$$

$$
\cdot[\Delta\delta_1 \quad \Delta\omega_1 \quad \Delta\psi_{fd1} \quad \Delta Ex_1 \quad \Delta\cos\alpha_{R1} \quad \Delta\delta_2 \quad \Delta\omega_2 \quad \Delta\psi_{fd2} \quad \Delta E_{x2} \quad \Delta\cos\alpha_{I2} \quad \Delta\delta_3 \quad \Delta\omega_3 \quad \Delta\psi_{fd3} \quad \Delta E'_{x3} \quad \Delta\cos\alpha_{R3}]^t \tag{6.9}
$$

Table VIII Eigenvalues for 3 Machine, 2 Rectifier System.

Control used	Eigenvalues
no control	$-37332, -15211, -372, -0.585 \pm j1.95, -0.526 \pm j1.16, -0.501 \pm j1.58, -0.483 \pm j8.92, -0.314 \pm j6.88, \pm 0.88 \times 10^{-3}$
u_{E1}, u_{E2}, u_{E3}	$-37332, -15211, -372, -18.5, -15.4, -13.26, -0.9 \pm j14.9, -7.05 \pm j14.2, -6.1 \pm j10.26, -0.35, -0.34, -0.32$
u_{D1}, u_{D3}	$-38764, -18557, -342, -70.25, -38.24, -3.28, -3.18, -2.8 \pm j5.82, -1.44, -1.2 \pm j1.98, -0.526, -0.4 \pm j1.68$
u_{D1}, u_{E2}, u_{D3}	$-38764, -18557, -342, -70.2, -38.2, -9.57, -4.27, -4.19 \pm j6.88, -3.25, -3.2, -1.19 \pm j1.97, -0.41 \pm j1.67$
$u_{E1}, u_{D1} \cdot u_{E2}$, u_{E3}, u_{D3}	$-38764, -18556, -341, -225, -122, -13.06, -9.6, -9.57, -6.1 \pm j9.89, -1.73 \pm j0.07, -1.13, -1.1, -1.0$

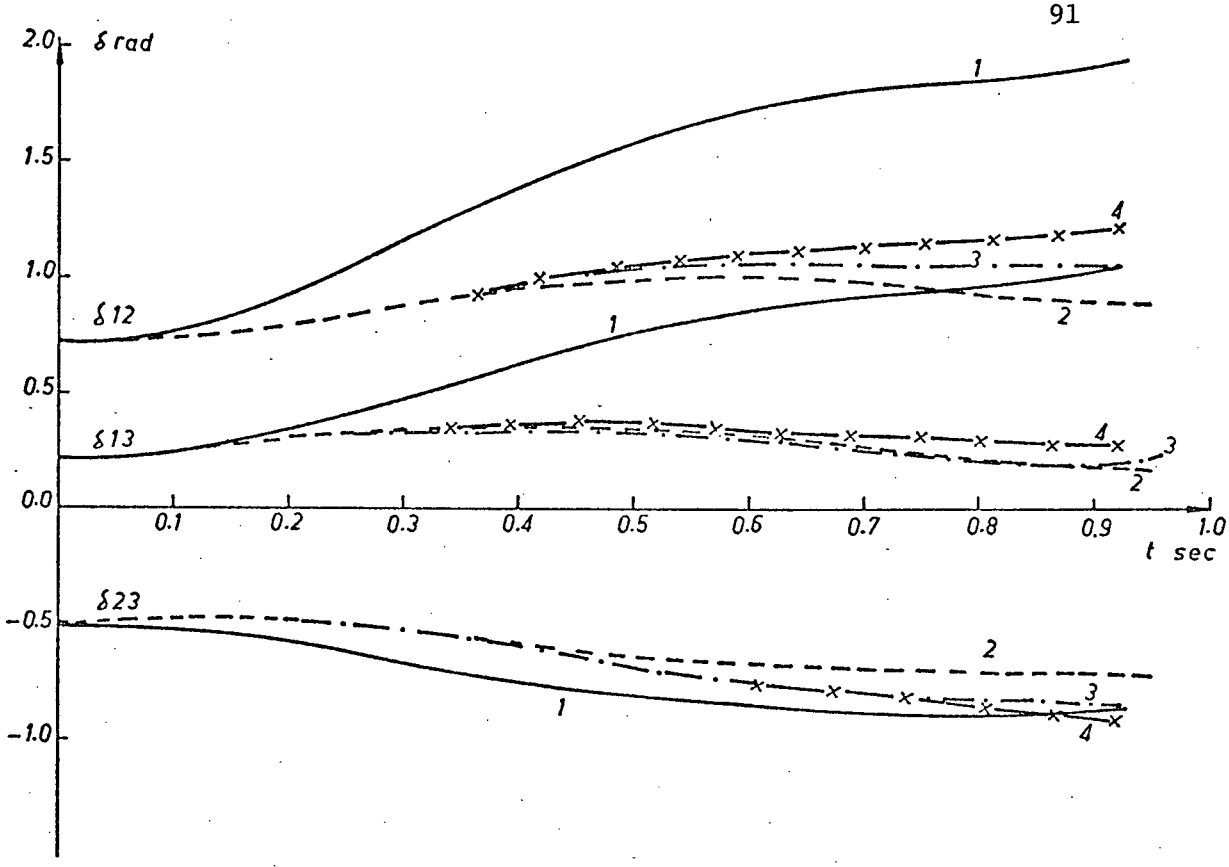

Fig. 6.15 Swing Curves for 3 Machine, 2 Rectifier System

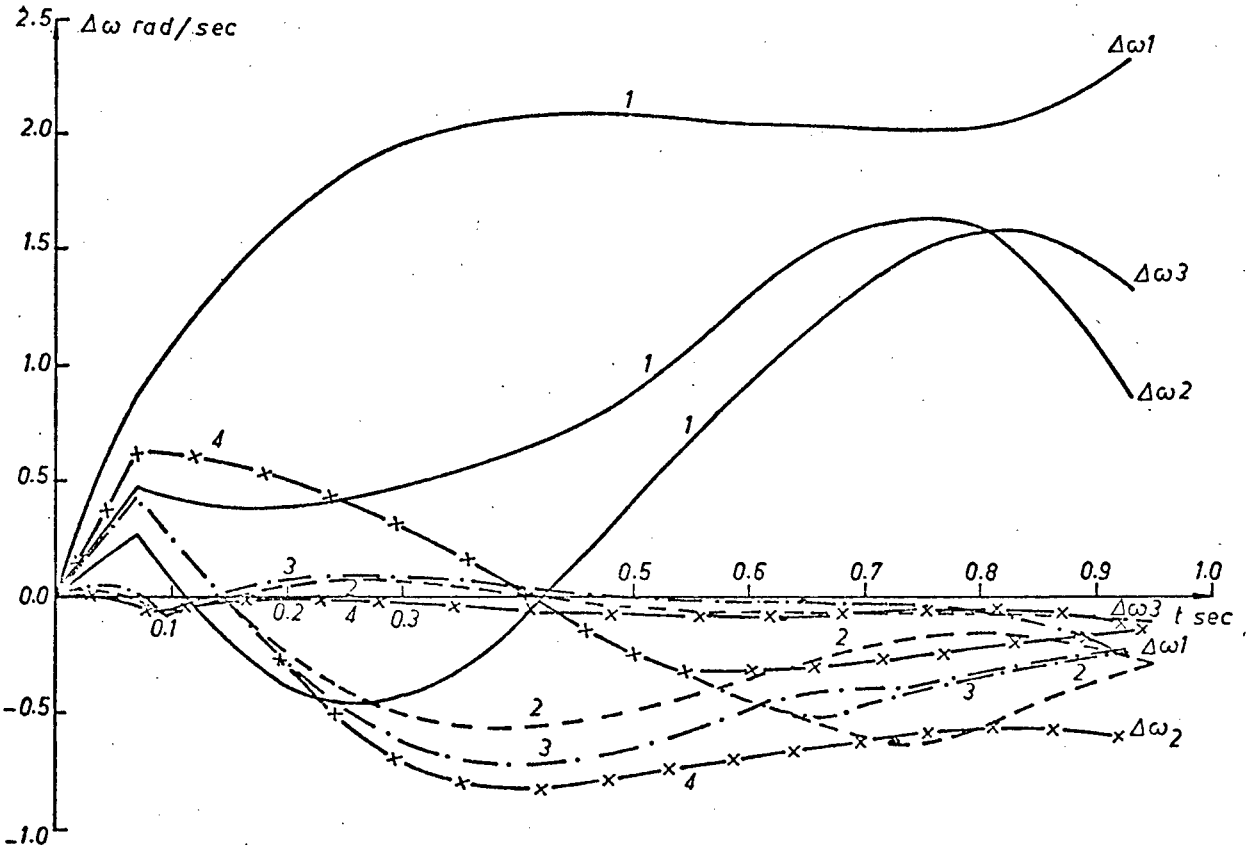

Fig. 6.16 Speed Deviation for 3 Machine, 2 Rectifier System

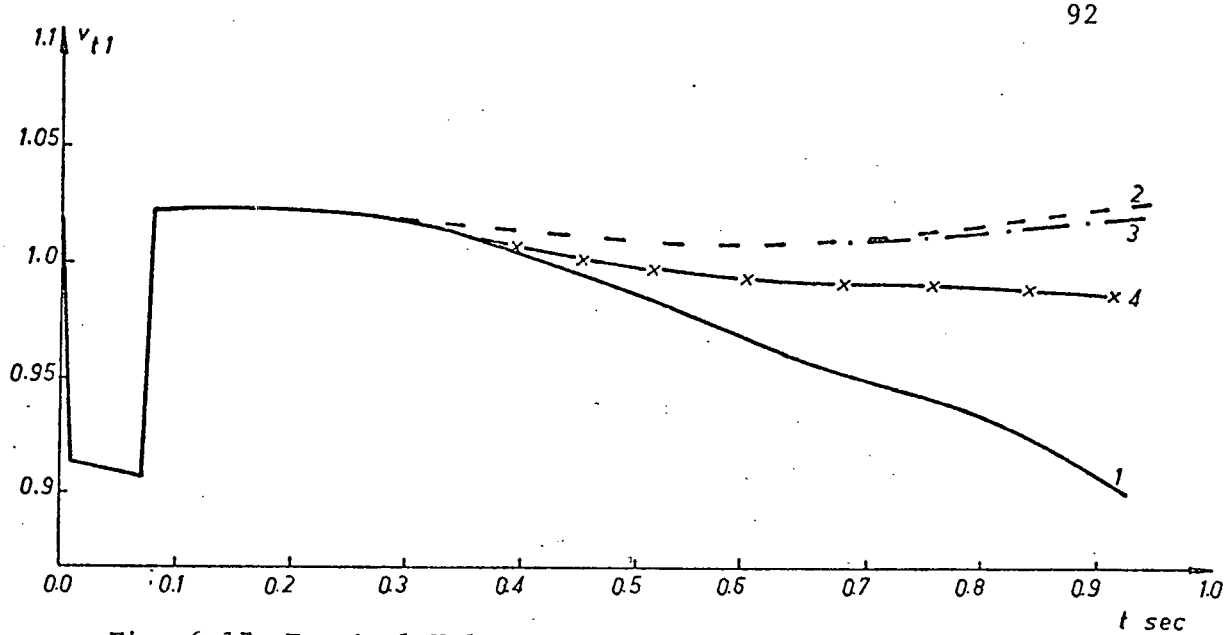

Fig. 6.17 Terminal Voltage Variations at Bus 1 for 3 Machine, 2 Rectifier System

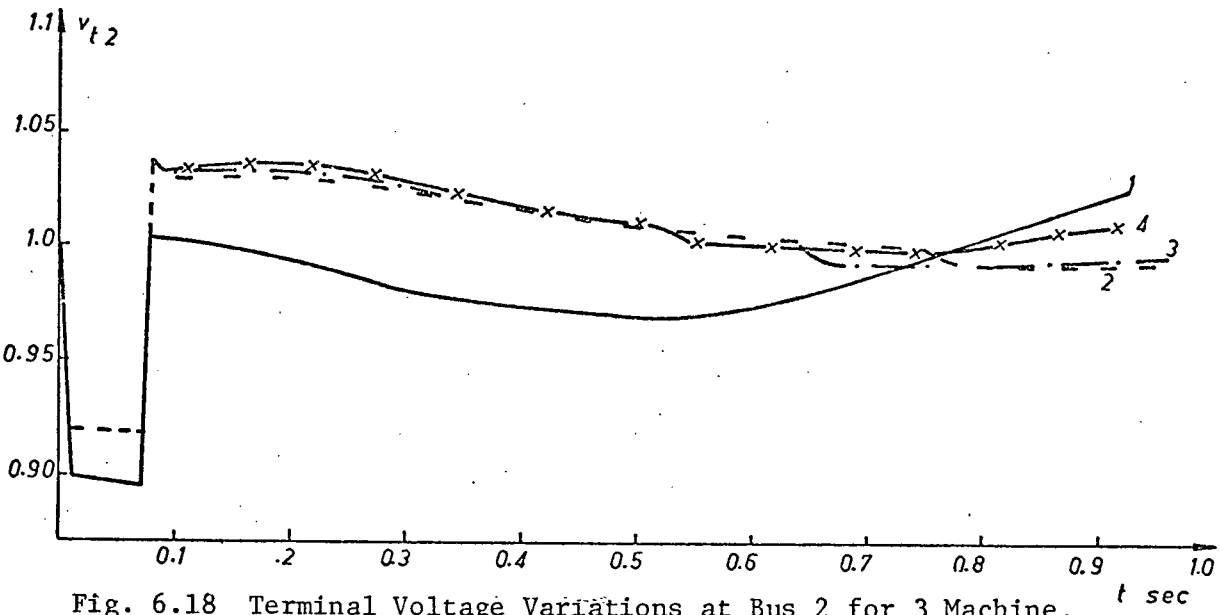

Fig. 6.18 Terminal Voltage Variations at Bus 2 for 3 Machine, 2 Rectifier System

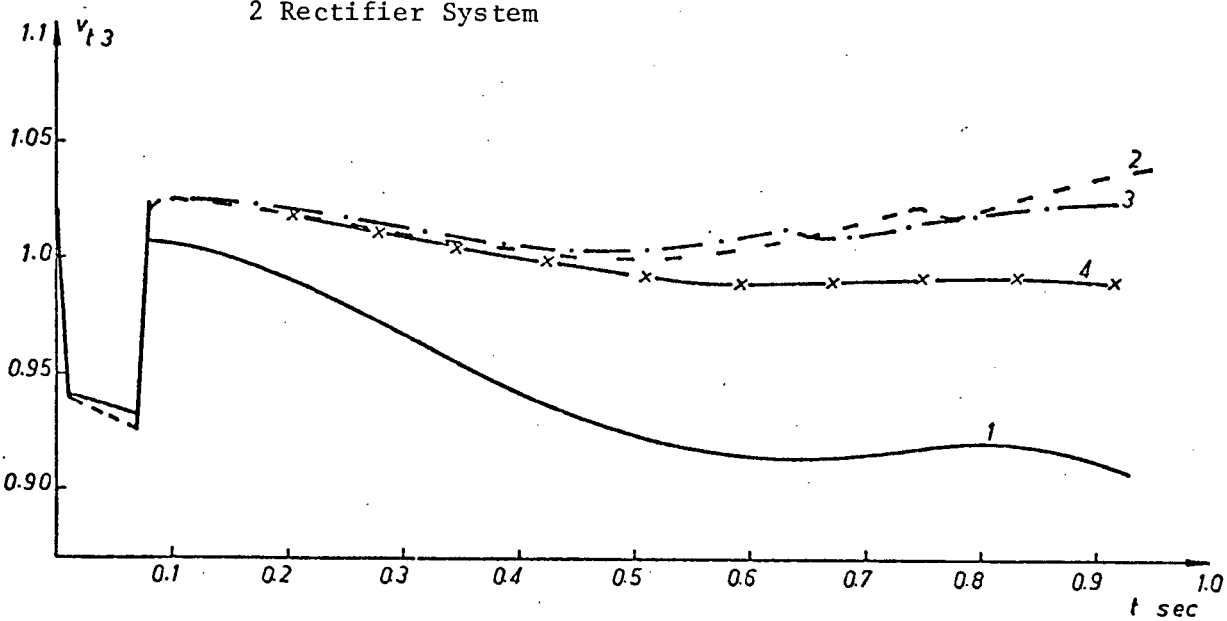

Fig. 6.19 Terminal Voltage Variations at Bus 3 for 3 Machine, 2 Rectifier System

followed by cases 4, 3 and 2 respectively. The largest changes in terminal voltage at bus 2, Figure 6.18, are also observed in case 1 followed by cases 2, 3 and 4 respectively. At bus 3, Figure 6.19, the order is changed to 1, 4, 2 and 3.

The dc power changes are shown in Figure 6.20 (a, b, c). In case 1, where no dc controls are applied, the dc power returns to pre-fault values after fault removal because of the constant current control and then starts to deteriorate after 0.45 sec. because of ac voltage drops. In cases 2, 3 and 4 the dc power transmitted over line 1 reaches its maximum value after fault removal and stays there for 0.75, 0.63 and 0.52 sec. for cases 2, 3 and 4 respectively. Then they all go down rapidly at first and then gradually. The total energy transmitted over the dc network is maximum in case 2 followed by cases 4 and 3 respectively.

The control efforts are shown in Figure 6.21 and 6.22. The required excitation control efforts are maximum in case 1 and are greatly reduced in case 4. The dc control signal u_{D1} is largest in case 2 followed by cases 3 and 4 while u_{D3} is largest in case 3 followed by cases 4 and 2.

6.4 Three Machine System with One Rectifier and Two Inverters

Similar to section 6.3 again four cases are studied with the exception that converter station 3 is operated as an inverter instead of a rectifier for all cases. Converter station 1 is operated as a rectifier and is controlling the dc current. Inverter station 2 is controlling the dc voltage while station 3 is operated under constant current control. The system's operating point is the same as that of section 6.2. The linearized state equations are given by (6.10). The weighing matrices Q and control laws for different control schemes are

$$
\begin{bmatrix}
\Delta\dot{\delta}_1 \\ \Delta\dot{\omega}_1 \\ \Delta\dot{\psi}_{fd1} \\ \Delta\dot{E}_{x1} \\ \Delta\dot{\cos\alpha}_{R1} \\ \Delta\dot{\delta}_2 \\ \Delta\dot{\omega}_2 \\ \Delta\dot{\psi}_{fd2} \\ \Delta\dot{E}_{x2} \\ \Delta\dot{\cos\alpha}_{I2} \\ \Delta\dot{\delta}_3 \\ \Delta\dot{\omega}_3 \\ \Delta\dot{\psi}_{fd3} \\ \Delta\dot{E}_{x3} \\ \Delta\dot{\cos\alpha}_{I3}
\end{bmatrix}
=
\begin{bmatrix}
0.0 & 1.0 & 0.0 & 0.0 & 0.0 & 0.0 & 0.0 & 0.0 & 0.0 & 0.0 & 0.0 & 0.0 & 0.0 & 0.0 & 0.0 \\
-28.2 & 0.0 & -101 & 0.0 & -119 & 18 & 0.0 & 9.58 & 0.0 & -48.1 & 10.1 & 0.0 & 8.91 & 0.0 & -31.4 \\
-0.36 & 0.0 & -1.29 & 0.45 & -1 & 0.24 & 0.0 & 0.37 & 0.0 & -0.54 & 0.12 & 0.0 & 0.22 & 0.0 & -0.34 \\
0.28 & 0.0 & -6.94 & -0.5 & -1.88 & -0.24 & 0.0 & -1.56 & 0.0 & 0.08 & -0.04 & 0.0 & -0.73 & 0.0 & -0.04 \\
-1381 & 0.0 & -16638 & 0.0 & -32176 & 747 & 0.0 & 8155 & 0.0 & -11526 & 635 & 0.0 & 4497 & 0.0 & -10085 \\
0.0 & 0.0 & 0.0 & 0.0 & 0.0 & 0.0 & 1.0 & 0.0 & 0.0 & 0.0 & 0.0 & 0.0 & 0.0 & 0.0 & 0.0 \\
26.3 & 0.0 & 44.1 & 0.0 & 49.9 & -40.4 & 0.0 & -126 & 0.0 & 46.6 & 14.1 & 0.0 & 11.7 & 0.0 & -25.7 \\
0.1 & 0.0 & 0.61 & 0.0 & 0.74 & -0.21 & 0.0 & -1.58 & 0.45 & 0.85 & 0.11 & 0.0 & 0.24 & 0.0 & -0.21 \\
0.64 & 0.0 & -1.06 & 0.0 & -1.47 & -0.71 & 0.0 & -6.69 & -0.5 & -2.14 & 0.06 & 0.0 & -0.64 & 0.0 & -0.05 \\
1.66 & 0.0 & 124 & 0.0 & 213 & -14.8 & 0.0 & -164 & 0.0 & -59.1 & 13.1 & 0.0 & 59.8 & 0.0 & -121 \\
0.0 & 0.0 & 0.0 & 0.0 & 0.0 & 0.0 & 0.0 & 0.0 & 0.0 & 0.0 & 0.0 & 1.0 & 0.0 & 0.0 & 0.0 \\
45.9 & 0.0 & 52.3 & 0.0 & 73.4 & 34.3 & 0.0 & 5.76 & 0.0 & -97.6 & -80.3 & 0.0 & -148 & 0.0 & 98.1 \\
0.49 & 0.0 & 1.03 & 0.0 & 1.41 & 0.51 & 0.0 & 0.46 & 0.0 & -1.33 & -1 & 0.0 & -2.51 & 0.49 & 1.97 \\
0.87 & 0.0 & -2.45 & 0.0 & -3.17 & -0.36 & 0.0 & -2.79 & 0.0 & 0.23 & -0.51 & 0.0 & -3.58 & -0.5 & -4.83 \\
-1400 & 0.0 & -6195 & 0.0 & -14464 & -379 & 0.0 & -4604 & 0.0 & 14619 & 1778 & 0.0 & 9940 & 0.0 & -21231
\end{bmatrix}
\begin{bmatrix}
\Delta\delta_1 \\ \Delta\omega_1 \\ \Delta\psi_{fd1} \\ \Delta E_{x1} \\ \Delta\cos\alpha_{R1} \\ \Delta\delta_2 \\ \Delta\omega_2 \\ \Delta\psi_{fd2} \\ \Delta E_{x2} \\ \Delta\cos\alpha_{I2} \\ \Delta\delta_3 \\ \Delta\omega_3 \\ \Delta\psi_{fd3} \\ \Delta E_{x3} \\ \Delta\cos\alpha_{I3}
\end{bmatrix}
+ BU
$$

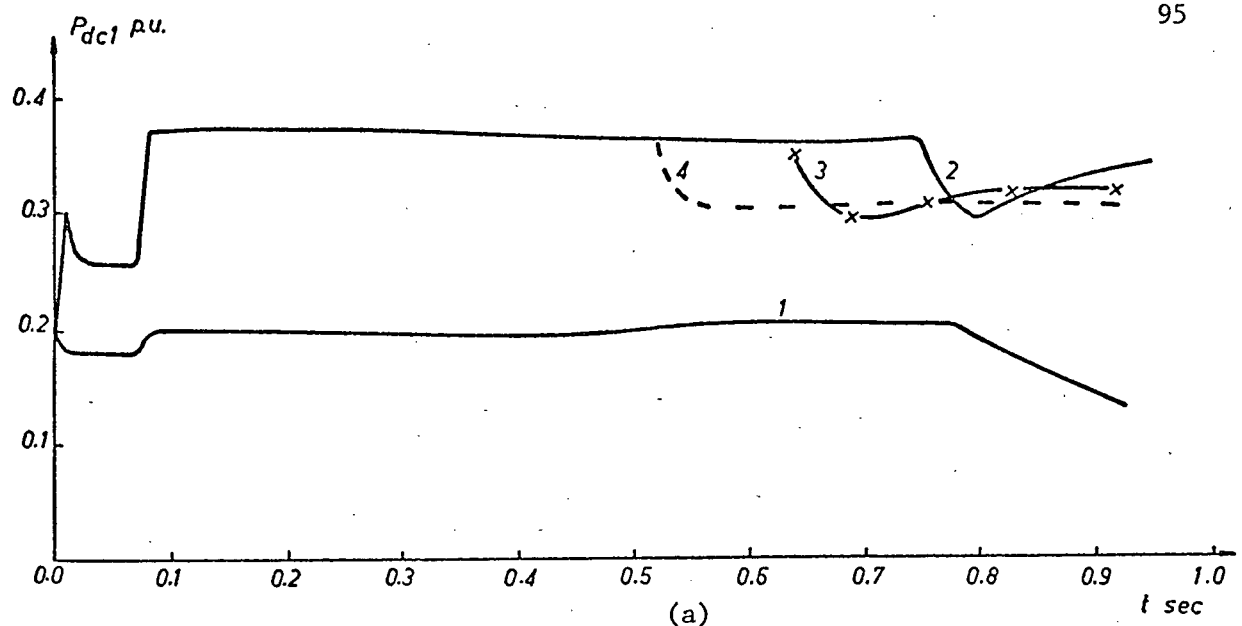

(a)

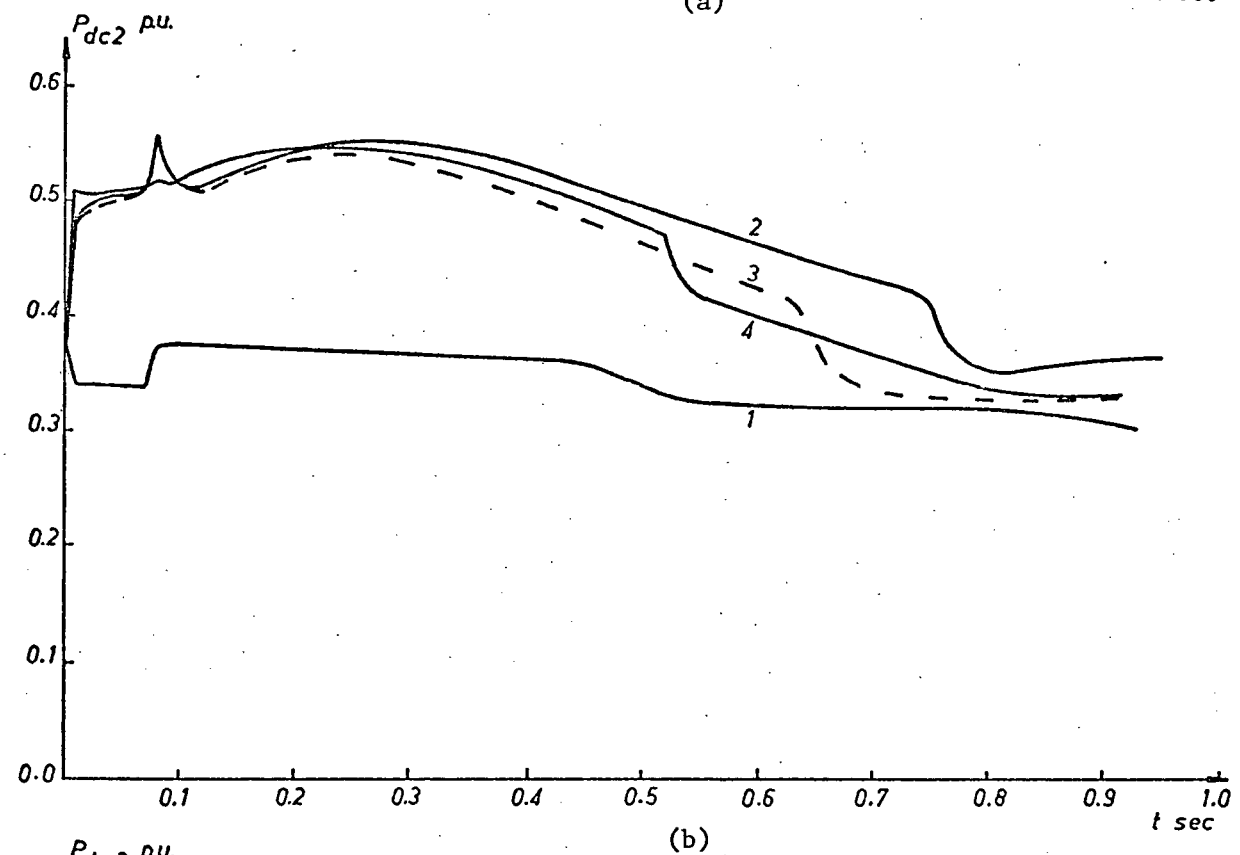

(b)

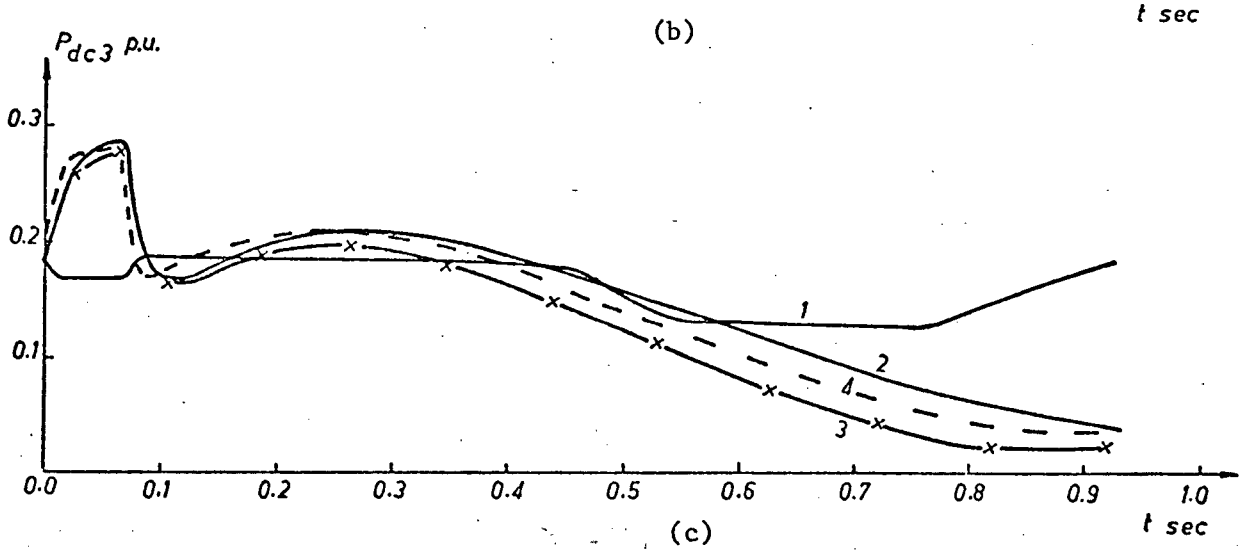

(c)

Fig. 6.20 DC Power Variations for 3 Machine, 2 Rectifier System

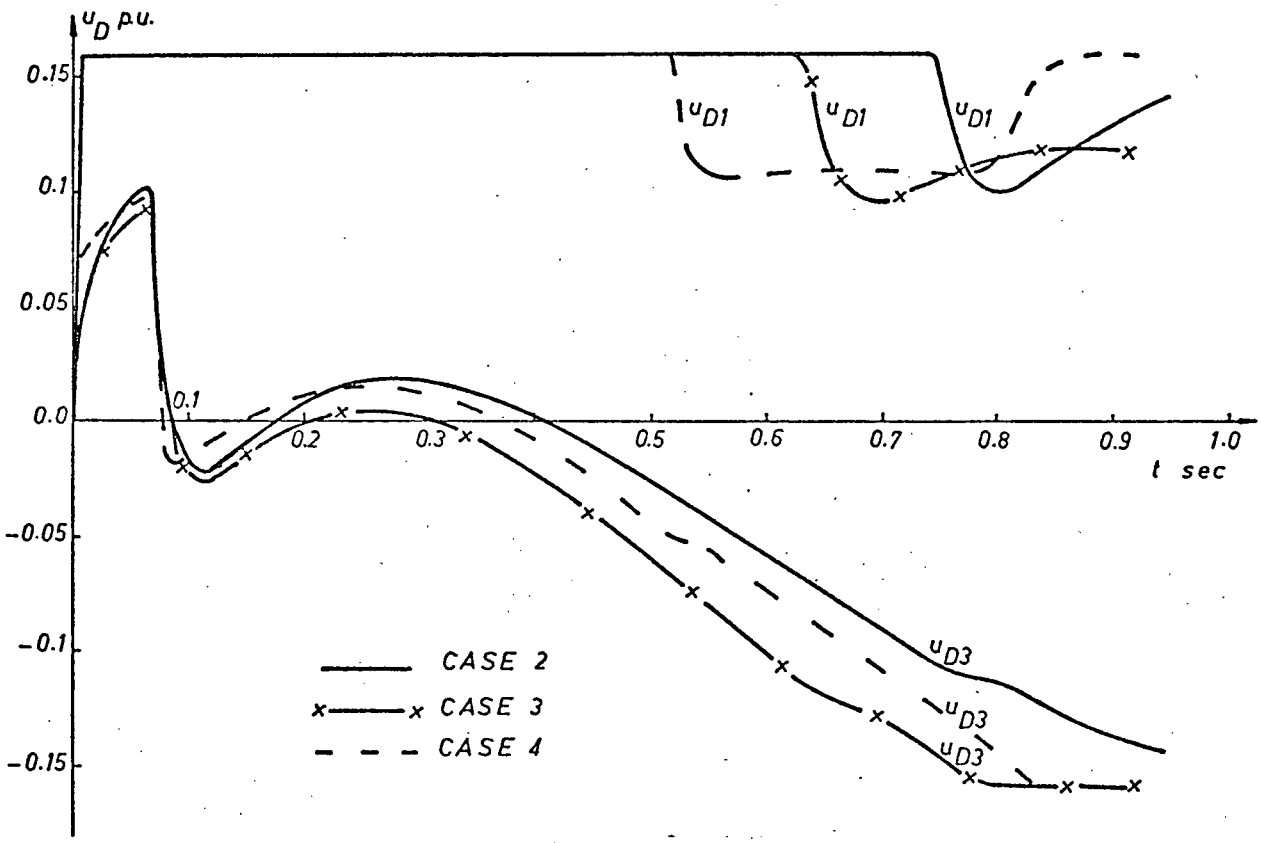

Fig. 6.21 DC Control Effort for 3 Machine, 2 Rectifier System

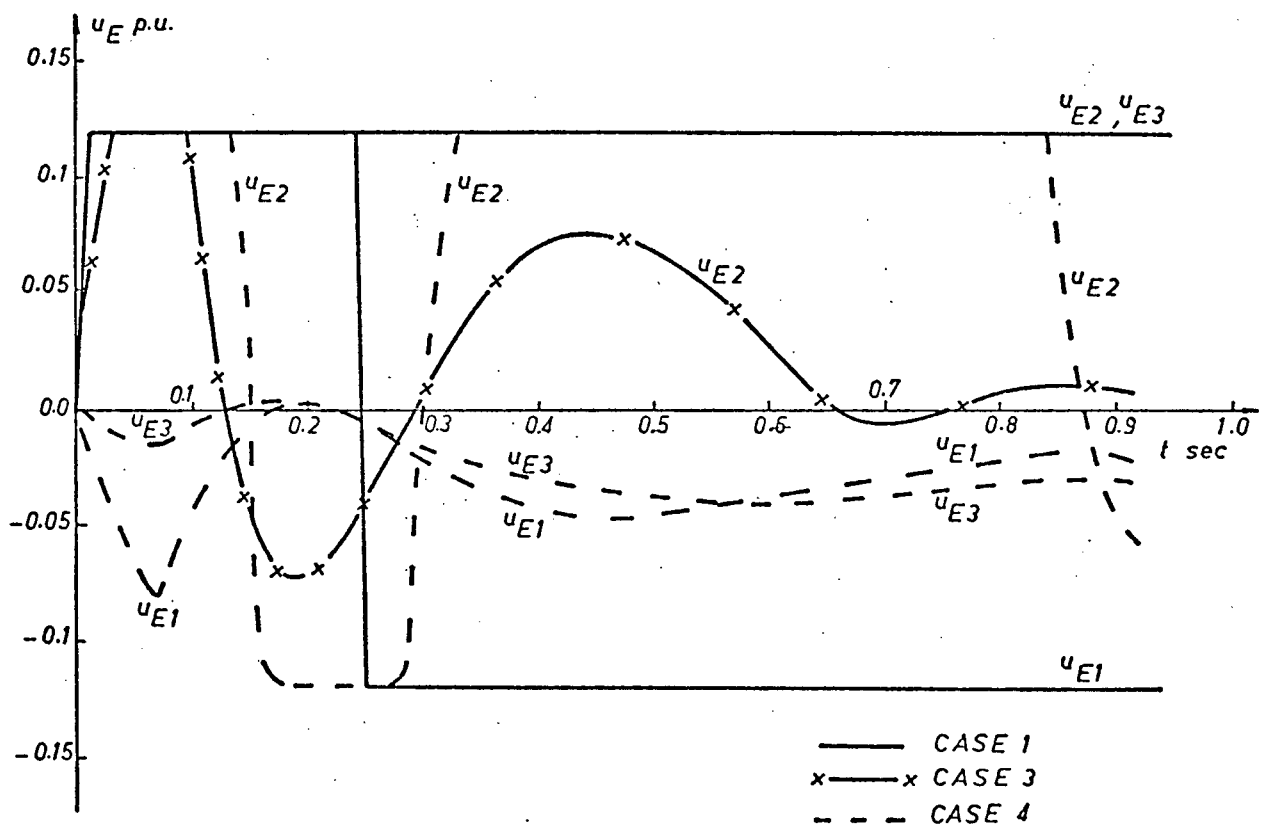

Fig. 6.22 Excitation Control Effort for 3 Machine, 2 Rectifier System

given in equations (6.11) and (6.12) respectively. The system's eigenvalues are listed in Table IX and it is seen that without optimal controls the system is nearly unstable.

u_{E1}, u_{E2}, u_{E3} : Q = diag {10, 100, 1, 1, 1, 10, 100, 1, 1, 1, 10, 100, 1, 1, 1}

$b_{4,1} = 10, \quad b_{9,2} = 10, \quad b_{14,3} = 10$

u_{D1}, u_{D3} : Q = diag {10, 1, 100, 1, 1, 10, 1, 100, 1, 1, 10, 1, 100, 1, 1}

$b_{5,1} = 10384, \quad b_{15,2} = 10799$

u_{D1}, u_{E2}, u_{D3} : Q = diag {10, 1, 100, 1, 1, 10, 1, 100, 1, 1, 10, 1, 100, 1, 1}

$b_{5,1} = 10384, \quad b_{9,2} = 10, \quad b_{15,3} = 10799$ (6.11)

u_{E1}, u_{D1}, u_{E2}, u_{E3}, u_{D3} : Q = diag {10, 1, 100, 1, 1, 10, 1, 100, 1, 1, 10, 1, 100, 1, 1}

$b_{4,1} = 10, \quad b_{5,2} = 10384, \quad b_{9,3} = 10, \quad b_{14,4} = 10,$

$b_{15,5} = 10799$

The test results of nonlinear system responses to the same disturbance used for the three previous systems are summarized in Figures 6.23 to 6.30.

Again case 2 is the most stable, as indicated by angle and speed deviations shown in Figures 6.23 and 6.24, followed closely by cases 3 and 4 respectively. Case 1 is the least stable case proving once more that excitation control signals by themselves are not sufficient to effectively stabilize such a system.

Figures 6.25 to 6.27 show that ac terminal voltages variations are largest in case 1 and smallest in case 2 with cases 3 and 4 in between.

$$
\begin{bmatrix} u_{E1} \\ u_{E2} \\ u_{E3} \\ u_{D1} \\ u_{D3} \\ u_{D1} \\ u_{E2} \\ u_{D3} \\ u_{E1} \\ u_{D1} \\ u_{E2} \\ u_{E3} \\ u_{D3} \end{bmatrix} =
\begin{bmatrix}
-40.4 & 6.06 & -57.7 & -2.43 & -0.02 & 26.2 & -0.4 & -3.92 & -0.05 & 0.13 & 15.8 & -0.49 & 5.33 & 0.08 & 0.4\times10^{-4} \\
20.8 & 4.35 & -2.18 & -0.05 & -0.006 & -28.2 & 7.81 & -107 & -3.19 & -0.55 & 11.5 & 1.24 & -10.7 & -0.19 & -0.004 \\
29.2 & 3.22 & 4.59 & 0.08 & -0.01 & 35.5 & 1.82 & -15.7 & -0.19 & -0.64 & -61.4 & 5.87 & -93.5 & -3.14 & 0.02 \\
8.72 & 1.51 & 0.04 & -0.03 & -0.2 & -2.76 & 0.87 & -24 & -0.91 & -0.27 & -0.57 & 0.4 & -8.8 & -0.24 & 0.1 \\
1.12 & 0.13 & 0.02 & 0.09 & 0.11 & 1.01 & 0.38 & 1.67 & 0.2 & 0.15 & -3.13 & -0.89 & -1.78 & 1.74 & -0.29 \\
7.37 & 1.41 & -0.13 & -0.04 & -0.2 & -1.76 & 0.62 & -15.6 & -0.36 & -0.25 & -0.61 & 0.34 & -7.17 & 0.19 & 0.1 \\
3.52 & 0.31 & 0.41 & 0.05 & -0.0003 & -1.74 & 0.77 & -20.2 & -1.59 & -0.05 & 0.11 & 0.2 & -3.95 & -0.83 & 0.7\times10^{-5} \\
1.16 & 0.11 & 0.12 & 0.13 & 0.11 & 0.66 & 0.35 & -0.4 & 0.007 & 0.15 & -3.02 & -0.91 & -1.66 & 1.65 & -0.29 \\
-0.06 & 0.07 & -8.43 & -1.27 & 0.4\times10^{-5} & 0.04 & -0.05 & 0.5 & 0.01 & 0.005 & 0.03 & -0.01 & 0.19 & 0.005 & 0.2\times10^{-5} \\
6.94 & 1.42 & -0.33 & 0.004 & -0.2 & -1.88 & 0.61 & -15.6 & -0.36 & -0.24 & -0.21 & 0.31 & -5.38 & -0.12 & 0.1 \\
3.64 & 0.29 & 0.26 & 0.01 & -0.0003 & -1.55 & 0.74 & -19.5 & -1.56 & -0.06 & -0.19 & 0.19 & -3.24 & -0.09 & -0.3\times10^{-4} \\
1.63 & 0.11 & 0.14 & 0.005 & -0.0001 & -0.25 & 0.25 & -3.8 & -0.09 & -0.02 & -0.43 & 0.2 & -10.4 & -1.37 & -0.5\times10^{-5} \\
0.43 & 0.17 & -0.25 & 0.002 & 0.11 & 0.23 & 0.39 & -1.48 & -0.03 & 0.16 & -2.07 & -0.93 & -0.88 & -0.005 & -0.29
\end{bmatrix}
$$

$$
\cdot[\Delta\delta_1 \;\; \Delta\omega_1 \;\; \Delta\psi_{fd1} \;\; \Delta E_{x1} \;\; \Delta\cos\alpha_{R1} \;\; \Delta\delta_2 \;\; \Delta\omega_2 \;\; \Delta\psi_{fd2} \;\; \Delta E_{x2} \;\; \Delta\cos\alpha_{I2} \;\; \Delta\delta_3 \;\; \Delta\omega_3 \;\; \Delta\psi_{fd3} \;\; \Delta E_{x3} \;\; \Delta\cos\alpha_{I3}]^t \qquad (6.12)
$$

Table IX Eigenvalues for 3 Machine, 2 Inverter System

Control used	Eigenvalues
no control	$-39956, -13146, -366, -0.641 \pm j1.52, -0.608 \pm j1.93, -0.564 \pm j9.05, -0.458 \pm j1.38, -0.245 \pm j7.1, -0.527 \times 10^{-7} \pm j0.68 \times 10^{-3}$
u_{E1}, u_{E2}, u_{E3}	$-39956, -13146, -366, -17.74, -16.21, -13.26, -8.12 \pm j13.8, -8.03 \pm j15.26, -6.07 \pm j10.48, -0.355, -0.343, -0.316$
u_{D1}, u_{D3}	$-41301, -16972, -317, -60.7, -38.85, -3.29, -3.21, -3.03 \pm j4.59, -1.72, -1.1 \pm j2.2, -0.478, -0.443 \pm j1.59$
u_{D1}, u_{E2}, u_{D3}	$-41301, -16972, -317, -607, -36.86, -9.32, -4.32 \pm j5.65, -4.19, -3.26 \pm j0.054, -1.25 \pm j2.11, -0.442 \pm j1.59$
$u_{E1}, u_{D1}, u_{E2}, u_{E3}, u_{D3}$	$-41301, -16972, -317, -60.7, -36.86, -9.39, -7.93, -6.55 \pm j0.9, -5.71, -4.43 \pm j5.73, -4.42, -4.11, -3.19$

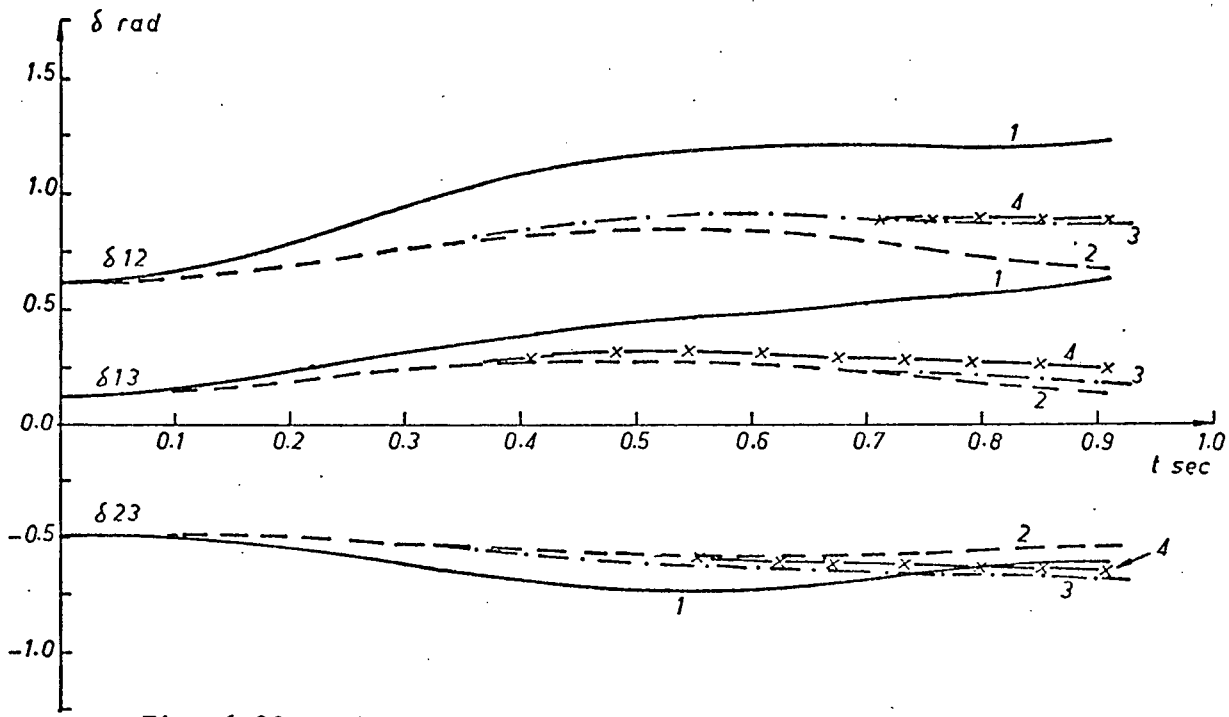

Fig. 6.23 Swing Curves for 3 Machine, 2 Inverter System

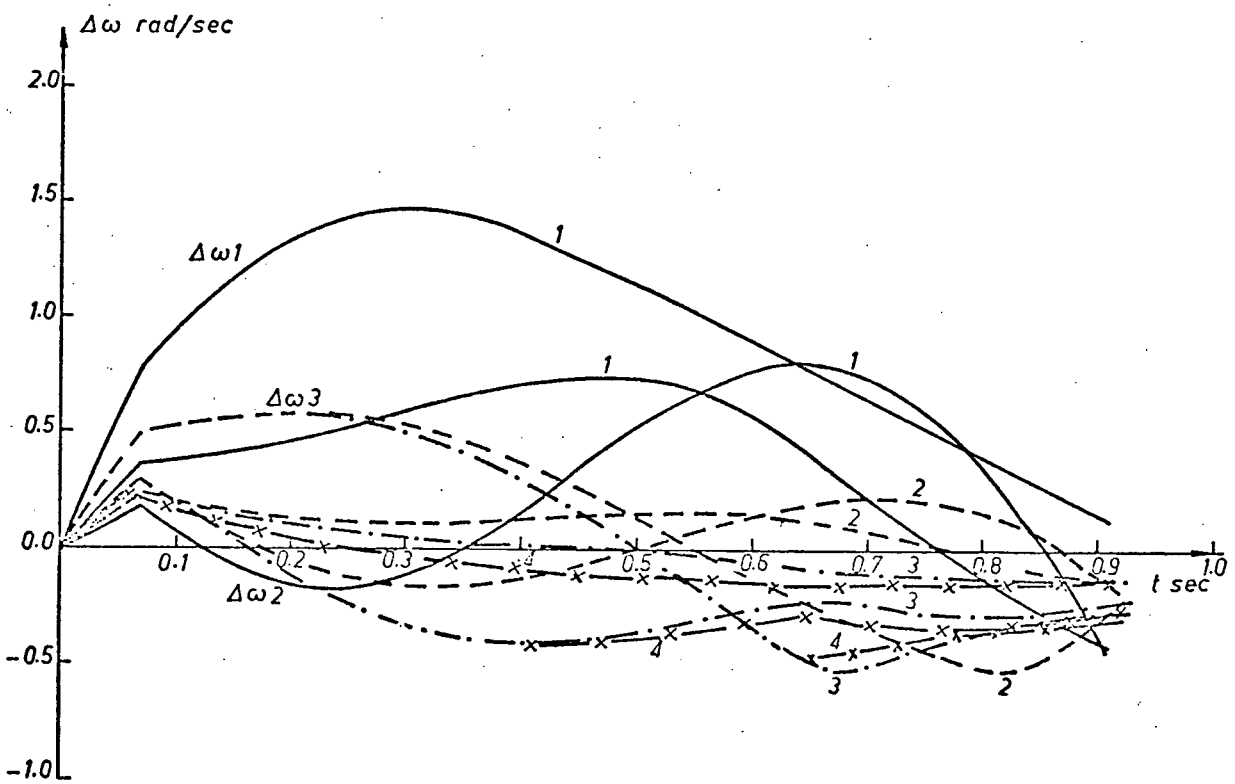

Fig. 6.24 Speed Deviation for 3 Machine, 2 Inverter System

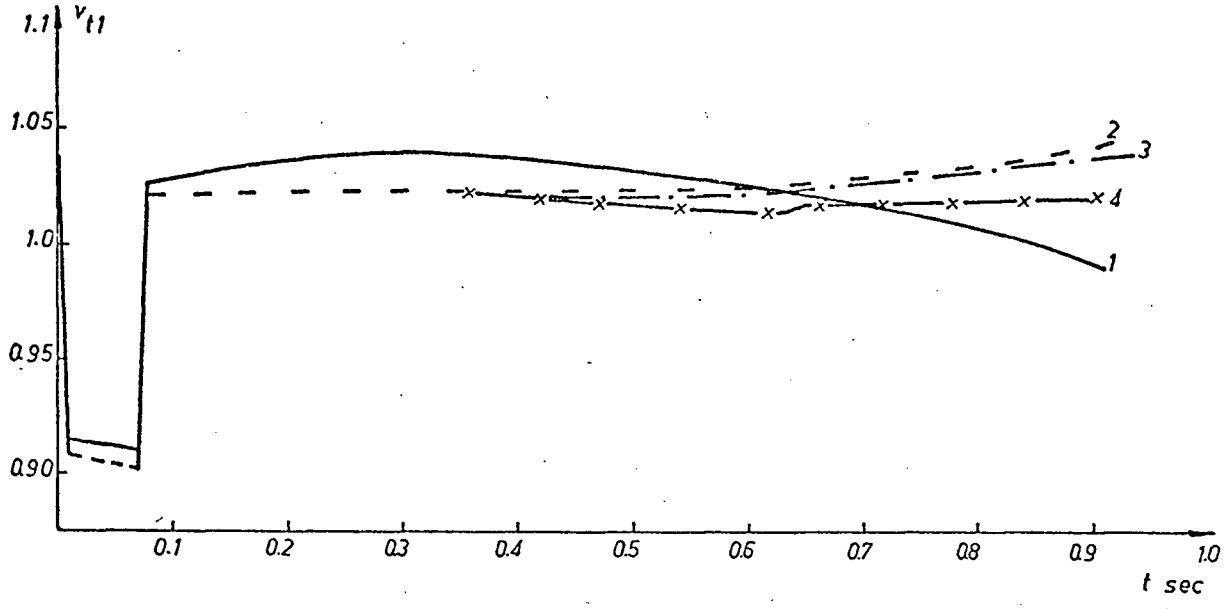

Fig. 6.25 Terminal Voltage Variations at Bus 1 for 3 Machine, 2 Inverter System

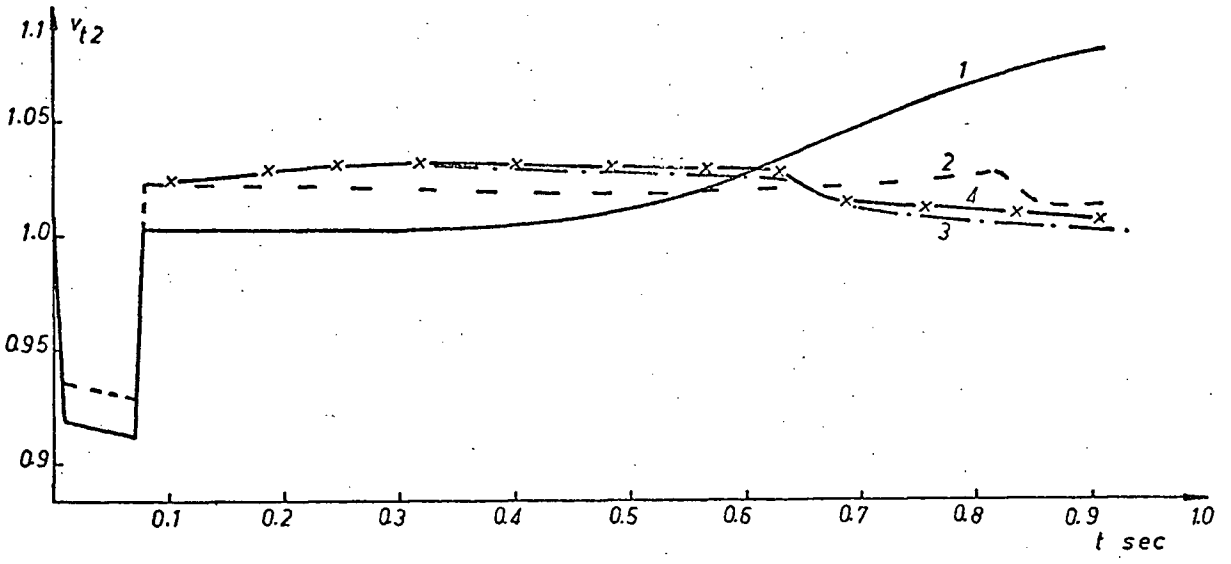

Fig. 6.26 Terminal Voltage Variations at Bus 2 for 3 Machine, 2 Inverter System

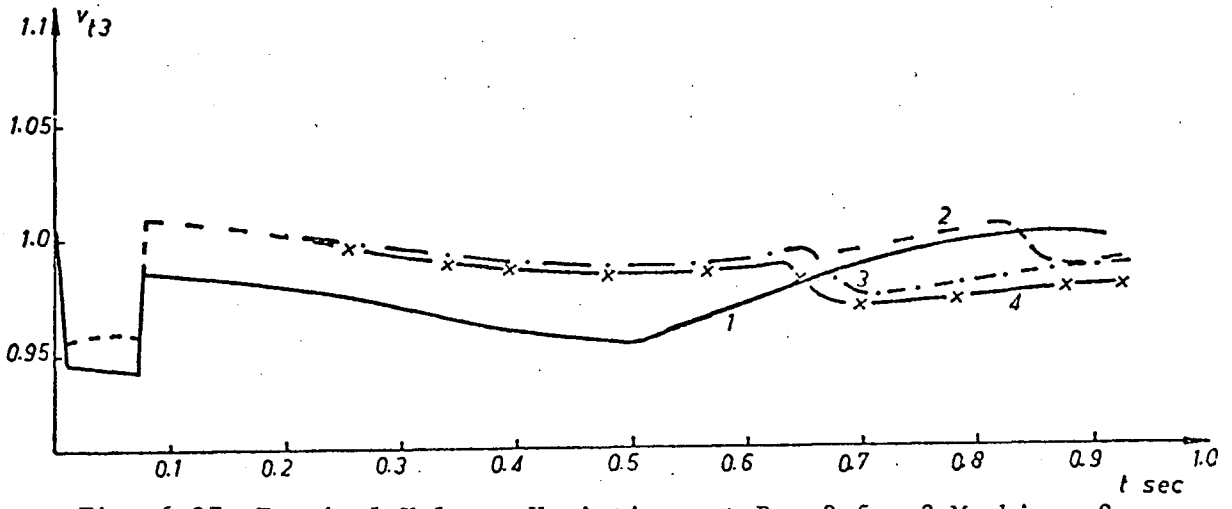

Fig. 6.27 Terminal Voltage Variations at Bus 3 for 3 Machine, 2 Inverter System

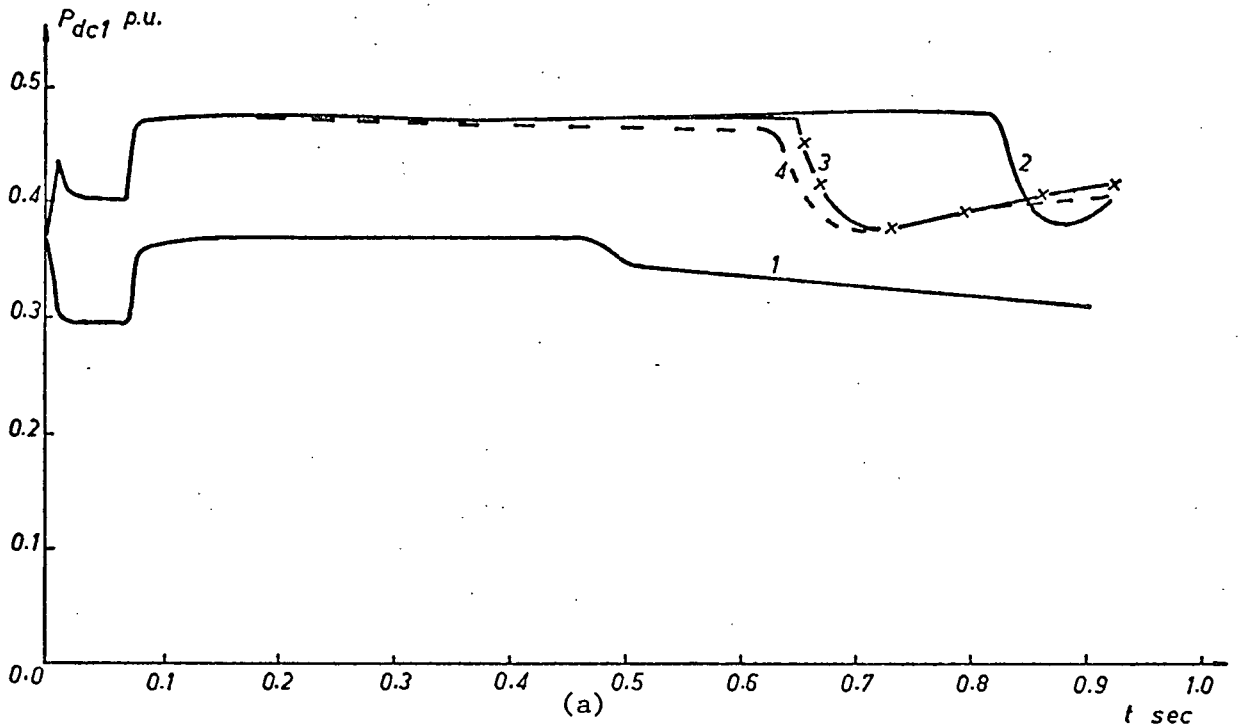

(a)

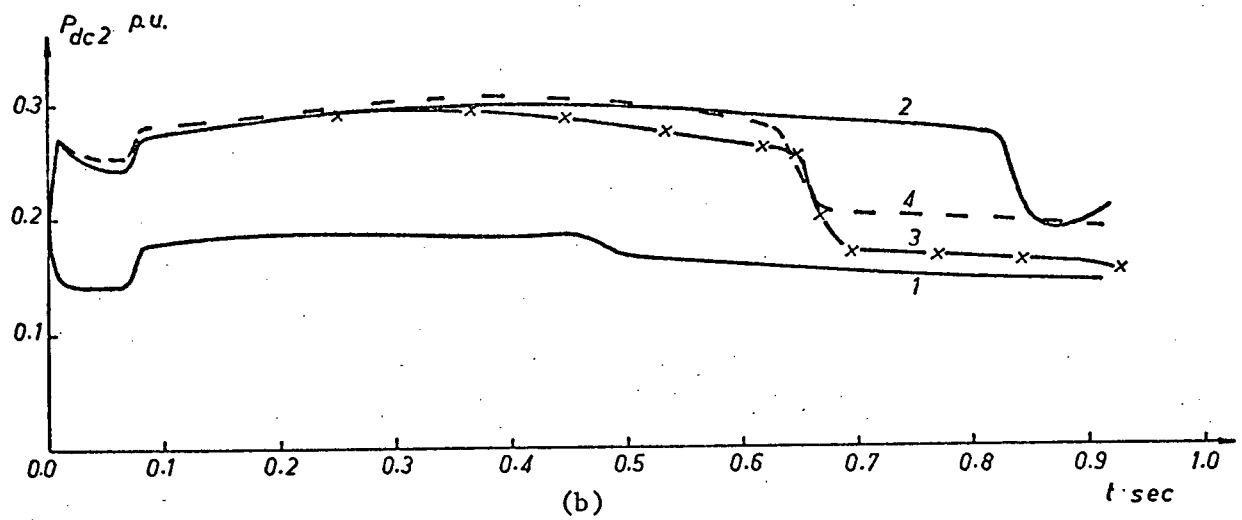

(b)

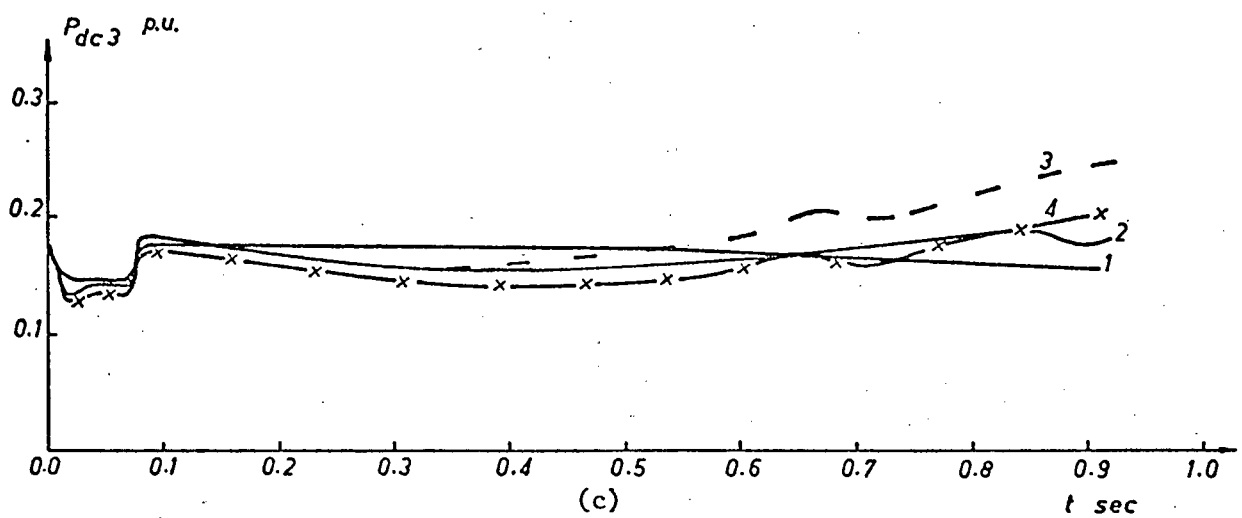

(c)

Fig. 6.28 DC Power Variations for 3 Machine, 2 Inverter System

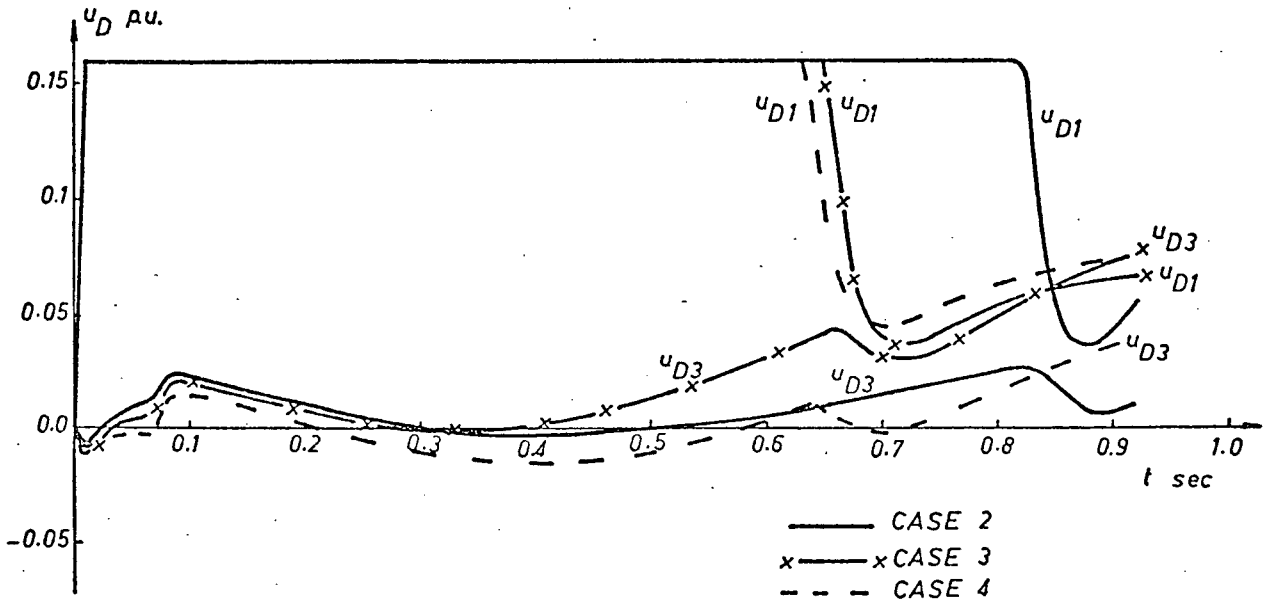

Fig. 6.29 DC Control Effort for 3 Machine, 2 Inverter System

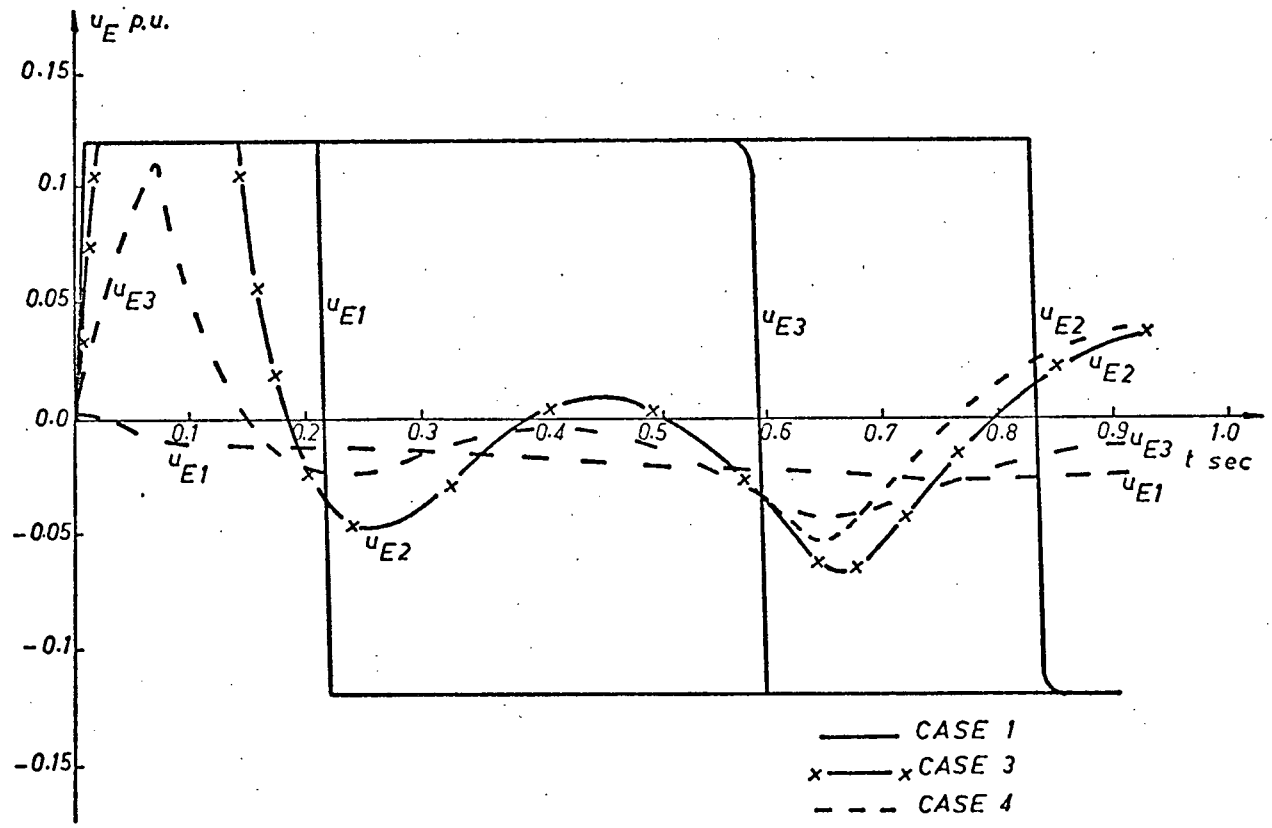

Fig. 6.30 Excitation Control Effort for 3 Machine, 2 Inverter System

Figure 6.28 shows the dc power variations. In case 1 the power returns to rated values immediately after fault removal and starts to go down at 0.45 sec. Cases 2, 3 and 4 are very similar. In all three cases the power transmitted over the dc network is greatly increased after fault removal and stays at a value of about 0.47 p.u. then goes down. The dc energy transmission is maximum in case 2 followed by cases 3 and 4 respectively.

Control efforts are shown in Figures 6.29 and 6.30. The control changes have a pattern similar to previous systems.

For the four systems studied in this chapter the nonlinear test results indicate strongly that optimizing the dc reference currents is the most suitable for controlling the dc/ac parallel systems. The dc network in such cases acts as a variable load at the machine terminals with the ability to adjust itself according to the system stability requirements. Optimal excitation controls, on the other hand, are slower and hence far less effective than dc controls. In certain cases where the excitation control signals cause the ac terminal voltages to drop, the power transmitted over the dc network is reduced accordingly, since the dc system is operating under constant current control, and the system is less stable. It is noted that applying combinations of optimal dc and excitation controls also yield stable systems with responses close to the case with dc optimal control alone.

7. CONCLUDING REMARKS

The hvdc system dynamics are described in Chapter 2. For a simple two-terminal dc/ac parallel system it takes a 39th order model to describe the system dynamics in detail including filters, reactive power condensers, ac tie lines, dc tie line and controls, synchronous machine and control loops.

Dynamic models for the stability and control studies are developed in Chapter 3. Despite the accuracy of the 39th order model it is practically impossible for digital computation due to the tremendous time required because of the small step size. Several reduced models are found in this thesis which are accurate enough for practical purposes. The most suitable one seems to be the 6th order model consisting of a 3rd order synchronous machine, a 1st order voltage regulator, and two dc firing circuit controls.

In Chapter 4 linear optimal controls are designed for two different single machine-infinite bus systems. It is found that a control signal modifying the dc reference current is the most effective one in stabilizing a strong dc system. As for the excitation control it is found that there is very limited effect on system stabilization. When the two controls, excitation and dc, are applied simultaneously an increase of dc control effort is noted. For a weak ac system, by adding a parallel dc link in expansion, it is found that the best results are achieved by using a dc control signal in addition to the existing excitation control designed for the ac system, but the system response still can be improved slightly by modifying the excitation control signal with the system expansion.

The investigation of optimal control for multi-terminal dc

systems begins in Chapter 5. The system equations for a tapped three-terminal dc line superimposed on a three bus ac system are derived.

In Chapter 6 two multi-terminal systems are investigated, each with two different modes of operation. The two machine-infinite bus system was stable but the three machine system was unstable when there were no controls. Four different control schemes are tested for each system and it is found that the application of optimal control signals to modify dc reference currents at the current controlling converter stations is the most effective scheme for all systems studied. On the other hand the application of optimal excitation controls is the least effective scheme and in some cases it was even worse than not having controls. A combination of dc and excitation controls does stabilize the systems studied but is less effective than the dc control by itself. It is also evidenced that the dc control effort is increased rather than decreased in the presence of excitation control signals, suggesting that the two kinds of controls may work against each other.

There are a few points deserving special discussion. In choosing the weighing matrix Q for the linear optimal control design for an ac system more emphasis must be placed on speed deviation[51]. This result is also confirmed in this thesis when designing excitation controls alone. But when dc controls were being designed for a dc/ac parallel system it is found that more emphasis should be placed on the field flux linkage. This can be explained as follows. Since the basic function of the dc control is to pick up some power from the ac system which may cause large acceleration of the synchronous machines in order to achieve stability and since the dc control is regulating dc current, then it is preferable to keep the change in ac terminal voltages, which are directly related to

field flux linkages, to a minimum and hence a larger weighing factor must be assigned to field flux linkage deviations.

Another reason for high computer costs, in addition to small step size because of the large eigenvalues, is the iterative solution of the system's auxilliary nonlinear algebraic equations four times for each integration step. One way of overcoming this difficulty is linearization of these algebraic equations but the effect of this linearization on the accuracy of results has to be investigated.

As for future work the present study may be extended to the cases of dc line disturbances such as loss of one pole in a bipolar system, and the possibility of using suboptimal controls by neglecting the smaller gains in the control laws. The switching transients over transmission lines might have some effect on the control performance of dc/ac parallel systems with small time constants in the control loop. Finally, the implementation of such optimal controls in actual systems is of course a challenging problem to utilities.

REFERENCES

1. E.W. Kimbark, "Direct Current Transmission, Vol. I", Wiley-Interscience, N.Y., 1971.

2. C. Adamson and N.G. Hingorani, "High Voltage Direct Current Power Transmission", Garraway Limited, London, England, 1960.

3. C. Adamson, "The Basis of HVDC Transmission", Manitoba Power Conference on EHV-DC, Winnipeg, Manitoba, June 1971.

4. Y. Yoshida, T. Machida and N.G. Hingorani, "Analog Computer Study of Automatic Frequency Ratio Control on an HVDC Transmission System", IEEE Trans. on Power Apparatus and Systems, Vol. PAS-87, No. 3, March 1968, pp. 796.

5. C.M. Stairs, "Development of an HVDC Solid State Back to Back Asynchronous Tie", Manitoba Power Converence on EHV-DC Winnipeg, Manitoba, June 1971.

6. R.W. Haywood and K.J. Ralls, "Use of HVDC for Improving AC System Stability and Speed Control", ibid.

7. N.G.Hingorani, J.L. Hay and R.E. Crosbie, "Dynamic Simulation of HVDC Transmission Systems on Digital Computers", Proc. IEE, Vol. 113, No. 5, May 1966, pp. 793.

8. N.G. Hingorani and J.L. Hay, "Representation of Faults in the Dynamic Simultation of HVDC Systems by Digital Computers", ibid., Vol. 114, No. 5, May 1967, pp. 629.

9. N.G. Hingorani, R.H. Kitchen and J.L. Hay, "Dynamic Simulation of HVDC Power Transmission Systems on Digital Computers - Generalized Mesh Analysis Approach", IEEE Trans. on Power Apparatus and Systems, Vol. PAS-87, No. 4, April 1968, pp. 989.

10. J.L. Hay and N.G. Hingorani, "Dynamic Simulation of Multiconverter HVDC Systems by Digital Computers, Part I: Mathematical Model", ibid., Vol. PAS-89, No. 2, February 1970, pp. 218.

11. P.G. O'Regan and C.T.G. Dillon, "Digital Computer Simulation of Transients in HVDC Converters with Harmonic Filters", Proc. IEE, Vol. 117, No. 2, February 1970, pp. 421.

12. D.B. Giesner and J. Arrillaga, "Behaviour of HVDC Links Under Balanced AC Fault Conditions", ibid., Vol. 118, No. 3/4, March/April 1971, pp. 591.

13. N.G. Hingorani and M.F. Burbery, "Simulation of AC System Impedance in HVDC Studies", IEEE Trans. on Power Apparatus and Systems, Vol. PAS-89, No. 5, May/June 1970, pp. 820.

14. J.P. Bowels, "AC System and Transformer Representation for HVDC Transmission Studies", ibid. Vol. PAS-89, No. 7, September/October 1970, pp. 1607.

15. P.C. Krause and D.P. Carroll, "A Hybrid Computer Study of a DC Power System", ibid., Vol. PAS-87, No. 4, April 1968, pp. 970.

16. J.E. Hudson, E.M. Hunter and D.D. Wilson, "EHV-DC Simulator", ibid., Vol. PAS-85, No. 11, November 1966, pp. 1101.

17. N.G. Hingorani and D.J. Mountford, "Simulation of HVDC Systems in AC Load-Flow Analysis by Digital Computers", Proc. IEE, Vol. 113, No. 9, September 1966, pp. 1541.

18. G.D. Breuer, J.F. Luini and C.C. Young, "Studies of Large AC/DC Systems on the Digital Computer", IEEE Trans. on Power Apparatus and Systems, Vol. PAS-85, No. 11, November 1966, pp. 1107.

19. N. Sato and J. Arrillaga, "Improved Load Flow Techniques for Integrated AC/DC Systems", Proc. IEE, Vol. 116, No. 4, April 1969, pp. 525.

20. H.A. Peterson and P.C. Krause Jr., "A Direct- and Quadrature-Axis Representation of a Parallel AC and DC Power System", IEEE Trans. on Power Apparatus and Systems, Vol. PAS-85, No. 3, March 1966, pp. 210.

21. J.L. Hay, J.S. Bhatti and N.G. Hingorani, "Simplified Dynamic Simulation of HVDC Systems by Digital Computers", ibid., Vol. PAS-90, No. 2, March/April 1971, pp. 859.

22. E. Uhlman, "Stabilization of an AC Link by a Parallel DC Link", Direct Current, August 1964, pp. 89.

23. T. Machida, "Improving Transient Stability of AC Systems by Joint Usage of DC Systems", IEEE Trans. on Power Apparatus and Systems, Vol. PAS-85, No. 3, March 1966, pp. 226.

24. H.A. Peterson and P.C. Krause Jr., "Damping of Power Swings in a Parallel AC and DC System", ibid., Vol. PAS-85, No. 12, December 1966, pp. 1231.

25. J.J. Dougherty and T. Hillesland Jr., "Power System Stability Considerations with Dynamically Responsive DC Transmission Lines", ibid., Vol. PAS-89, No. 1, January 1970, pp. 34.

26. D.B. Goudie, "Steady-State Stability of Parallel HV DC-AC Power Transmission Systems", Proc. IEE, Vol. 119, No. 2, February 1972, pp. 216.

27. M.S. Sachdev, R.J. Fleming and J. Chand, "Optimal Control of A HVDC Transmission Link", IEEE-PES Winter Meeting, New York, N.Y. January 28 - February 2, 1973.

28. W.F. Long, "HVDC Breaker/System Interactions - A Simulator Study", IEEE-PES Winter Meeting, New York, N.Y., January 30 - February 4, 1972.

29. A.N. Greenwood and T.H. Lee, "Theory and Application of the Commutation Principle for HVDC Circuit Breakers", ibid.

30. G.A. Hofmann, W.F. Long and W. Knauer, "Inductive Test Circuit for a Fast Acting HVDC Interrupter", IEEE-PES Winter Meeting, New York, N.Y., January 28 - February 2, 1973.

31. W.F. Long, "Means of DC Circuit Breaking in a Three Terminal HVDC System", IEEE-PES Summer Meeting, Vancouver, B.C., July 15-20, 1973.

32. B. Hammerlund, "Telecommunications for HVDC Transmission", IEEE Trans. on Power Apparatus and Systems, Vol. PAS-87, No. 3, March 1968, pp. 690.

33. J.P. Norton and B.J. Cory, "Digital Simulation Program for Multiterminal HVDC Systems", Proc. IEE, Vol. 115, No. 3, March 1968, pp. 397.

34. C. Adamson and J. Arrillaga, "Behaviour of Multiterminal AC-DC Interconnections with Series Connected Stations", ibid., Vol. 115, No. 11, November 1968, pp. 1685.

35. J.P. Norton and B.J. Cory, "Control System Stability in Multiterminal HVDC Systems", ibid., Vol. 115, No. 12, December 1968, pp. 1828.

36. R. Foerst, G. Heyner, K.W. Kangeisser and H. Weldmann, "Multiterminal Operation of HVDC Converter Stations", IEEE Trans. on Power Apparatus and Systems, Vol. PAS-88, No. 7, July 1969, pp. 1042.

37. J.J. Dougherty, "Operating Characteristics of a Three-Terminal DC Transmission Line", ibid., Vol. PAS-89, No. 5, May/June 1970, pp. 775.

38. D.P. Carroll, "Hybrid Computer Simulation of Multiterminal DC Power Transmission Systems", ibid., Vol. PAS-89, No. 6, July/August 1970, pp. 1126.

39. J.J. Dougherty and H. Kirkham, "System Aspects of a Tapped DC Line with Dynamic Controls", ibid., Vol. PAS-89, No. 8, November/December 1970, pp. 2066.

40. D.P. Carroll and J.E. Scheiderich, "Inverter Control in Multiterminal HVDC Power Systems", IEEE-PES Winter Meeting, New York, N.Y., January 28 - February 2, 1973.

41. J. Reeve, "Control Strategy and Performance Expectations for Multiterminal HVDC Power Systems", CEA Spring Meeting, Mountreal, Que., March 1973.

42. J. Reeve and S.C. Kapoor, "Dynamic Fault Analysis for HVDC Systems with AC System Representation", IEEE Trans. on Power Apparatus and Systems, Vol. PAS-91, No. 2, March/April 1972, pp. 688.

43. J.P. Bowels, "Control Systems for HVDC Transmission", CEA Spring Meeting, Vancouver, B.C. March 1971.

44. R.H. Park, "Two Reaction Theory of Synchronous Machines: I - Generalized Method of Analysis", AIEE Trans., Vol. 48, July 1929, pp. 716.

45. E.J. Davison, "A Method of Simplifying Linear Dynamic Systems", IEEE Trans. on Automatic Control, Vol. AC-11, No. 1, January 1966, pp. 93.

46. A. Kuppurajulu and S. Elangovan, "System Analysis by Simplified Models", ibid., Vol. AC-15, No. 2, April 1970, pp. 234.

47. A. Kuppurajulu and S. Elangovan, "Simplified Power System Models for Dynamic Stability Studies", IEEE Trans. on Power Apparatus and Systems, Vol. PAS-90, No. 1, January/February 1971, pp. 11.

48. M. Athans and P.L. Falb, "Optimal Control", McGraw Hill, New York, 1966.

49. J.E. Potter, "Matrix Quadratic Solutions", SIAM, Journal of Applied Math., Vol. 14, No. 3, May 1966, pp. 496.

50. C.E. Fosha Jr. and O.I. Elgard, "Optimum Linear Control of the Multi-Variable Megawatt-Frequency Control Problem", JAAC 1969, pp. 471.

51. F.P. DeMello and C. Concordia, "Concepts of Synchronous Machine Stability as Affected by Excitation Control", IEEE Trans. on Power Apparatus and Systems, Vol. PAS-88, No. 4, April 1969, pp. 316.

52. H.A.M. Moussa and Y.N. Yu, "Optimal Power System Stabilization Through Excitation and/or Governor Control", ibid., Vol. PAS-91, No. 3, May/June 1972, pp. 1166.

53. Y.N. Yu and H.A.M. Moussa, "Optimal Stabilization of a Multi-Machine System", ibid., Vol. PAS-91, No. 3, May/June 1972, pp. 1174.